

Ứng dụng WebGIS trong quản lý thông tin giá đất trên địa bàn thành phố Tuy Hòa, tỉnh Phú Yên

Trương Quang Hiến*, Ngô Anh Tú, Phan Văn Thơ, Bùi Thị Diệu Hiền

Khoa Khoa học Tự nhiên, Trường Đại học Quy Nhơn, Việt Nam

Ngày nhận bài: 26/11/2021; Ngày nhận đăng: 25/01/2022; Ngày xuất bản: 28/10/2022

TÓM TẮT

Hiện nay, việc ứng dụng GIS (Geographic Information System) trong quản lý giá đất hiện nay còn ít được quan tâm; việc xác định giá đất Nhà nước chủ yếu dựa vào bảng giá đất hàng năm do Ủy ban nhân dân cấp tỉnh ban hành, dẫn đến việc truy vấn thông tin giá đất rất khó khăn cho người quản lý và người dân. Do đó, việc ứng dụng GIS và nền tảng internet trực tuyến để người dân có thể dễ dàng tiếp cận được thông tin về giá đất và giúp cho nhà quản lý tìm kiếm thông tin giá đất nhanh chóng, đây là một việc cần thiết và thực tiễn trong công tác quản lý Nhà nước về đất đai trong thời điểm hiện nay. Trong nghiên cứu này, đã ứng dụng GIS xây dựng cơ sở dữ liệu giá đất cho thành phố Tuy Hòa, tỉnh Phú Yên dựa vào nền bản đồ địa chính theo hệ số giá đất do tỉnh Phú Yên ban hành theo vị trí tuyến đường, sau đó nghiên cứu thực hiện xây dựng website tích hợp cơ sở dữ liệu giá đất lên nền tảng trực tuyến. Kết quả nghiên cứu đã xây dựng được trang WebGIS quản lý thông tin giá đất trên địa bàn thành phố Tuy Hòa, tỉnh Phú Yên với các dữ liệu không gian và thuộc tính, chương trình này giúp cho người quản lý và người sử dụng có thể tìm kiếm trực tuyến thông tin giá đất chính xác tới từng vị trí thửa đất và tạo điều kiện thuận lợi cho công tác quản lý dữ liệu giá đất.

Từ khóa: *Giá đất, GIS, Tuy Hòa, WebGIS.*

* Tác giả liên hệ chính.

Email: truongquanghien@qnu.edu.vn

Application of WebGIS for management of land price information in Tuy Hoa City, Phu Yen Province

Truong Quang Hien*, Ngo Anh Tu, Phan Van Tho, Bui Thi Dieu Hien

Faculty of Natural Sciences, Quy Nhon University, Vietnam

Received: 26/11/2021; Accepted: 25/01/2022; Published: 28/10/2022

ABSTRACT

Nowadays, the application of GIS (Geographic Information System) in land price management does not draw much attention. The determination of the current State land price is based on the annual land price list issued by the Provincial People's Committee, leading to the fact that the query of land price information is very difficult for everyone, especially the managers. Therefore, the application of GIS and an online internet platform that people can easily access the information on land prices, and help the managers find the information about land prices quickly is a necessary and practical issue in the state management of land. In this study, GIS was applied to build a land price database for Tuy Hoa City, Phu Yen Province, based on the cadastral map following the land price. It was coefficient issued by Phu Yen Province according to the route location. Then we researched and built a website to integrate the land price database on the online platform. The research results have built a WebGIS program to manage land price information in Tuy Hoa City, Phu Yen Province with the spatial data and attributes. This program helps the managers and users search online for accurate land price information to each land plot location and facilitate the management of land price data conveniently.

Keywords: *Land price, GIS, Tuy Hoa, WebGIS.*

1. INTRODUCTION

In-State management, the application of GIS technology to build a land price database will be an effective tool to support the management of land prices according to each land plot, location of the land plot, and street name. It is the basis to serve the specific land valuation in a favorable way. At the same time, it makes the addition and adjustment of the land price list and the construction of the annual land price adjustment more convenient and consistent with reality.^{1,2} The spatial information management system and land price attributes integrated into the database help to look up land price information more

conveniently, especially information about land prices such as surface location, area and street name. In addition, GIS technology also helps managers easily update annual land price data for each route if there is an annual land price adjustment easily and conveniently.³

Research and application of GIS technology in the state management of land and other fields have been carried out in Vietnam recently. The subjects have exploited the features and utilities of software tools for database management, meeting the needs for information technology development in the new era. Especially, research projects on the application of new technologies

* Corresponding author.

Email: truongquanghien@qnu.edu.vn

in land price management are interesting and have been deployed in a number of provinces in the country such as Dong Nai, Thua Thien Hue, Quang Binh, etc.

Phu Yen is a coastal province in the South-Central Coast of Vietnam with a natural area of 5,045 km² and a coastline of 189 km. These days, Phu Yen province is promoting and attracting investment in Tuy Hoa city in order to build Tuy Hoa city into a modern and dynamic urban area, and land price is one of the key factors. The first thing that investors pay attention to is to choose an investment location. Therefore, the construction of a land price map will help investors be more proactive in collecting information on land prices and choosing a suitable location, thus facilitating investment attraction.⁴

For the above reasons, it is necessary to apply WebGIS to management of land price information in Tuy Hoa city, Phu Yen province. It will solve many economic problems, apply practical applications in local land price management, help land price management in Tuy Hoa city become more effective, and meet the requirements in the current financial management of land.

2. RESEARCH PROCEDURES AND METHODS

2.1. Research process

The development of WebGIS website is based on the provisions of Circular No. 26/2014/TT-BTNMT dated May 28, 2014 of the Ministry of Natural Resources and Environment.²

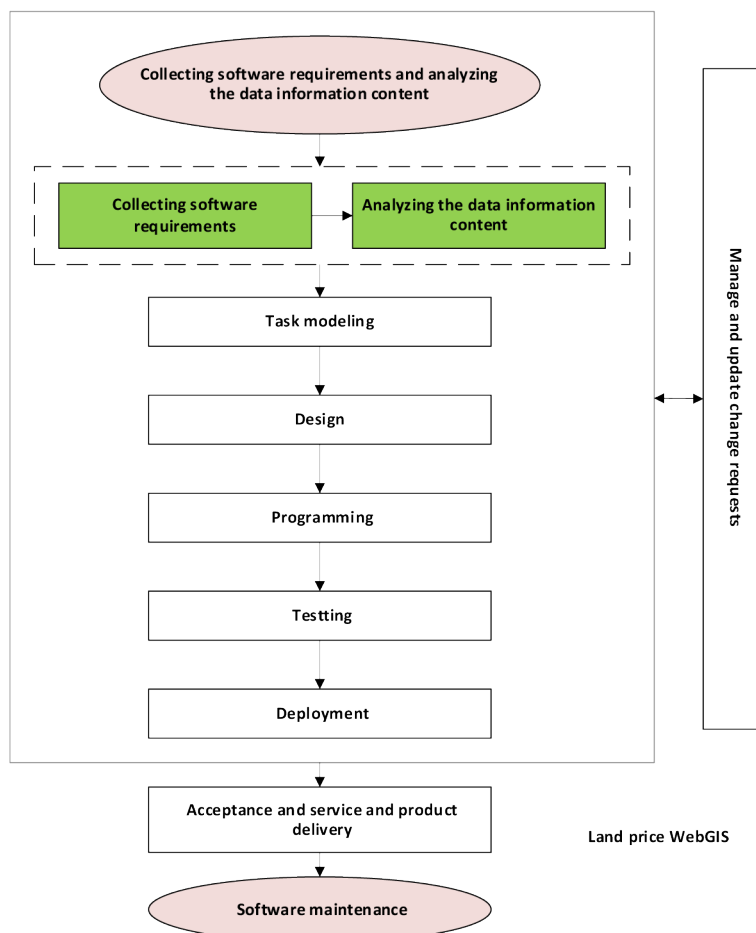


Figure 1. Overview of the process of building a WebGIS website for land prices

2.2. Research methods

To accomplish the above content, the study used the following methods:

+ Methods of data collection and field investigation: Collecting data, including geographic background data, cadastral maps, current land use maps, satellite image data and land price data survey market from the study area.

+ Methods of synthesizing, analyzing and editing data: Data are collected directly in the field and collected through secondary information channels in departments, in-depth research groups, data related to land price list in Tuy Hoa city, natural and socio-economic conditions. From the analysis and processing, the collected data is the input data for the construction of WebGIS. The most important and most accurate document is the cadastral map and land price data according to different types of land prices along with routes and each parcel of land.⁵

+ Methods of applying GIS technology: The method presented research results and research contents on graphic space with a unified mathematical basis and standard spatial and attribute databases.

This is an important method in building land price maps. Research and use ArcGIS technology to build a GIS database of residential land prices to create a map of residential land prices in Tuy Hoa city, Phu Yen province includes the following contents:

+ Organizing a GIS database on residential land prices and using algorithms to analyze, synthesize and process data.

+ Setting up traffic system data, residential area according to the traffic system.

+ Setting detailed residential land prices according to the State land price bracket according to the main street route and the location of alleys in the study area.

+ Building a map of land prices in Tuy Hoa city, Phu Yen province.

+ Method of application of WebGIS technology: It allows the design of the WebGIS structure diagram, design of WebGIS user interface, test operation of WebGIS system: installation on the server (Server) and test operation with the source name address is installed on the server, the website accesses the land price system: <http://giadattuyhoa.com/>. At the same time, it allows users to view information, and management agencies can log in to the database management system and view land price information for each land parcel, update the map data system and other information. information on regulations on land prices.

3. RESEARCH RESULTS AND DISCUSSION

3.1. Introduction of the study area

Tuy Hoa city is the economic and cultural center of Phu Yen province, with a natural area of about 107.3 km², a population of over 202 thousand people (by 2020) with 16 administrative units (including 12 wards and 4 communes). Tuy Hoa city is located adjacent to Phu Hoa district, Tuy An district, Dong Hoa district, Son Hoa district and to the East by the East Sea.

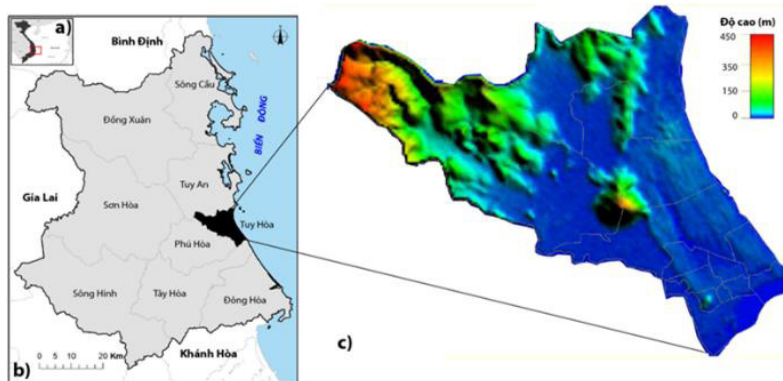


Figure 2. Map of study area Tuy Hoa city, Phu Yen province

Tuy Hoa city has a fairly flat topography with little division. The city has a humid tropical monsoon climate typical of the South-Central region. However, because it is located close to the sea, the climate is quite moderate. The east of the city borders the sea with a coastline of more than 30 km extending from Xuan Hai Bay to Vung Ro. The coast has many beautiful landscapes and beaches alternating both coastal and inland, such as Tuy Hoa beach, Nhan tower, Chop Chai Mountain and nearby scenic spots such as Long Thuy beach, Ganh Da Dia, O Loan lagoon, Doi Thom tourist area, etc. These are very convenient for tourism development and aquaculture. Tuy Hoa is also the crossroads and convergence of many important traffic routes, such as National Highway 1A, Highway 25 to Gia Lai, Highway 29 to Dak Lak, North-South railway, Tuy Hoa airport, Vung Ro seaport, etc.

In short, the advantages of natural, socio-economic conditions and infrastructure have created favorable conditions for the city to develop in a variety of fields, especially the marine economy. This is an outstanding strength for the city to become a major administrative and economic center not only of Phu Yen province but also of the region and a place of East - West and North - South economic exchanges of the whole country.

3.2. Building a database of land prices in Tuy Hoa city, Phu Yen province

3.2.1. Spatial data construction

In order to build a database of land prices for each location of the land plot, the study proceeds to build spatial information layers such as Land plot and traffic objects along routes, which are divided into main roads associated with the names of roads and alleys according to levels affecting land prices. The process of building a database in accordance with the provisions of Circular 02/2012/TT-BTNMT dated March 19, 2012, of the Minister of Natural Resources and Environment on basic geographic information

standards; Circular 17/2010/BTNMT dated October 4, 2010, providing technical regulations on cadastral data standards; Official Dispatch 1159/TCQLĐD-CDKTK dated September 21, 2011, providing guidance on building cadastral database.^{1,6}

The spatial land price database is built on the VN-2000 coordinate system, spatially normalized data for each parcel of land along with traffic data for the streets. Then, the topology to correct spatial errors and build spatial linkages for land parcels is standardized, meeting the requirements of current database standards.

3.2.2. Building a database of land price attributes

In this study, we used land price table data issued by the People's Committee of Phu Yen province and applied for 5 years for the period 2020 - 2024, which was collected from the Department of Natural Resources and Environment of Phu Yen province. The information in the form of tabular attributes is filtered through the land price information according to the location of the routes and arranged to link with spatial data through the attribute fields by route, in which the data Traffic has been normalized from the cadastral map.^{5,6}

After obtaining land price information according to the research routes, we have built land prices for each location of the land plot based on the location of the route and the width of the alley. To do this, we used tools to query land plot information by the main route to assign land prices to roads. Then, the land plots in the alley are queried in turn according to the width of the alley which is specified in the issued land price list.

After obtaining land prices for the roads and alleys, we performed the location of the frontage to calculate the land value for these locations increasing by 10%. After that, we used GIS tools to build a land price map for Tuy Hoa city in the period of 2020 - 2024.

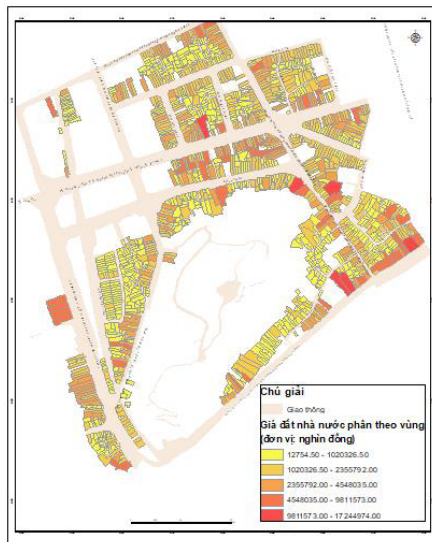


Figure 3. State land price database by streets in Tuy Hoa city

3.3. Designing the interface of the WebGIS to manage land prices in Tuy Hoa city

3.3.1. Setting up the graphical interface

The graphical interface is designed based on the WebGIS platform, consisting of two contents.

The first is the data content interface, specifically spatial data (map). The second is the graphical interface of the WebGIS, which is designed for users to control directly on devices connected to the Internet.

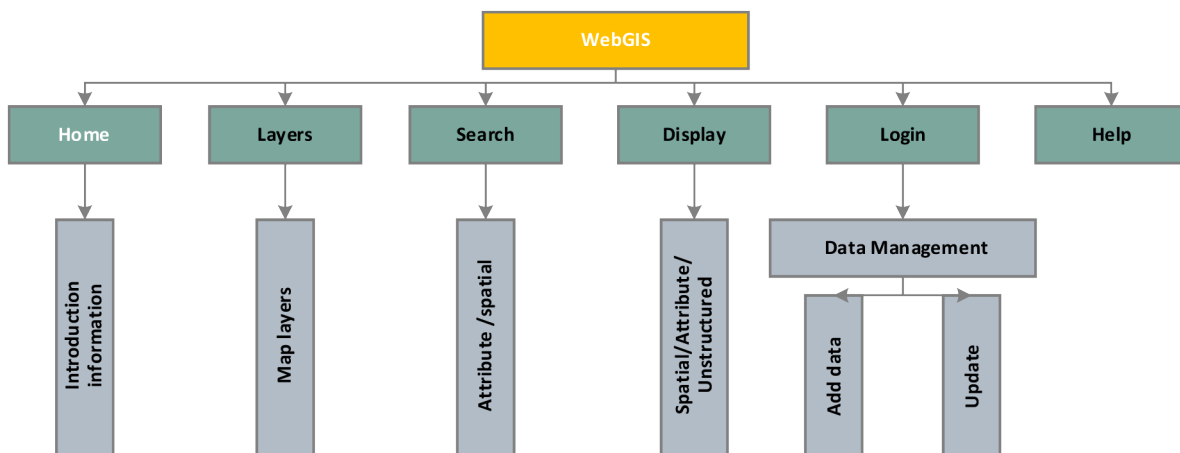


Figure 4. WebGIS organization chart Tuy Hoa city land price

WebGIS includes homepage, layers, search, display, login and assistance:

+ Home page (Menu): Showing general information.

+ Layers: Representing spatial data layers related to geographic background data and land prices.

+ Search: Helping users search for information on the map by keywords, searching

for information related to land prices by location of routes and each parcel of land.

+ Display function: The area has the function of displaying spatial information and data. This is a very important content that represents most of the information of a WebGIS site.

+ Login: The searcher logs in to his/her personal account (username, password). This content is for site administrators.... After

logging in, and going to the management pages, the manager can add new information about land prices and update, including the features of adding, deleting, and editing information of geographic background data and land prices...

+ Assistance: WebGIS manual page, contacting information.

3.3.2. Guidelines for general and detailed interface design WebGIS

- The general interface of the user page includes the homepage, search, and introduction pages (see information designed as shown in Figure 5).

- System login page interface: It helps managers to log in to the WebGIS system to serve more users, change login information, etc.

HEADER	
MENU	
Tool and search	Layer
Map Display information	
FOOTER	

Figure 5. WebGIS general design interface for land price management

- Map management interface: Users can add information to the geographic base database and land prices to periodically update the data for WebGIS.

HEADER	
MENU	
Geodata background group	Add data
	Save
Land price data group	Add data
	Save
FOOTER	

Figure 6. Map management design interface

3.3.3. Programming WebGIS web page components

The Web uses Leaflet's method of connecting libraries to display information, mainly by JavaScript. The interconnected JavaScripts connect the GeoJSON data and display them on the map, including the map background data and the attribute data. The detailed code is to develop the function of displaying the map, searching for information, moving the map, zooming in, out, etc. WebGIS are programmed, developed and shared on the homepage giadattuyhoa.com help people view GIS-based land price information online.

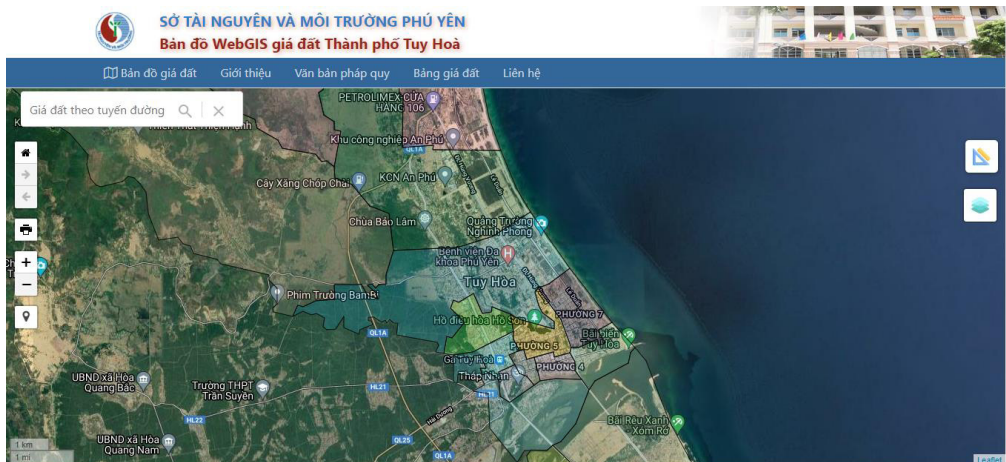


Figure 7. WebGIS interface to manage land prices in Tuy Hoa city

- The main tools of WebGIS, which are frequently used to meet the main functions of WebGIS, are displayed by default in the vertical toolbars on the right: For example, tools to zoom in and out, move the map, search for land price

information according to the location of the routes, printing, etc.

- Data layer management framework is a list of online map data layers that can be added to help identify and display available landmarks

on Google map, OpenStreet Map and distance measurement functions directly on the WebGIS platform.

- The area of legal documents and land price list is placed on the above horizontal bar so that users can view legal documents and contact the land price data management agency in Tuy Hoa city.^{9,10}

- The status bar shows the scale of the map.
- The main area of Web-based GIS data.





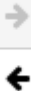


3.4. Building tools, utilities and manipulating functions on the WebGIS program to manage land prices in Tuy Hoa city

These tools help users customize the display of information layers used on the display and data processing frames.

3.4.1. The tool group is displayed on the left in the WebGIS interface

The main tools shown above are detailed in the following table:

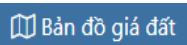
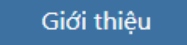
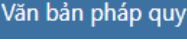

Table 1. Tool group on the left side of WebGIS interface

Image	Tool name	Main function
	Zoom in	Zoom in on the map display area in the selected area by dragging the mouse.
	Zoom out	Minimize the visible area on the main canvas by dragging the mouse.
	Positioning	Finding your current location - GPS.
	Full screen	Displaying all information layers and data processing frame.
	Moving	Moving the map information layers that have been opened in the Main Data Processing and Display Frame.
	Printing	Printing map, printing according to the selected area, printing the whole map area, printing vertically, printing horizontally on the screen, etc.
	Searching for land sales	Searching for land price information by the route.

3.4.2. Framework to manage data layers, search, measure, information menu

In the upper frame of the WebGIS interface, there are the following main items:



Table 2. Main functions on the right of WebGIS

Illustration	Tool name	Main function
	Land price map	Display of the entire land price map of the whole city, helping users locate the wards
	Introduction	A brief introduction to the online land price map
	Legal documents	Legal documents related to the current land price bracket
	Land price list	Land price list for the city in text form

On the right of the WebGIS interface, there are functional toolbars that measure the

distance between points on the map, switch on map data layers, specifically as follows:

Table 3. Tool group on the right of the WebGIS interface

Illustration	Tool name	Main function
	Measurements	Measure and calculate distance, area in square meters and hectares.
	Data layers	Manage the switch data layers on WebGIS.

3.4.3. Working with main features on WebGIS

Users can exploit the main features on WebGIS to manage land price databases such as View land price maps online; Displaying attribute

information; Looking for information; Print maps online; Positioning; logging in and updating data (for managers). Viewing the land price map is done through the function of zooming in and out of the map, displaying data layers.



Figure 8. Area for managing data layers

Displaying road property information

The purpose is to display detailed information on the selected data background to help show data more intuitively. In the WebGIS interface, the function of displaying street names by streets has been implemented, helping people to easily search for the location of the land plot and land price quickly and conveniently,

by zooming in to the search area, the road information will be displayed visually.

Finding information on the map



Purpose: Helping users easily find information about land prices quickly and intuitively; electing the icon  then typing the street name and clicking the search button .



Figure 9. Illustrated image of searching for information by a parcel of land

Bảng giá đất

Năm:
 Phường/xã:

Bảng giá đất Phường 8, Thành phố Tuy Hòa DVT: 1.000 đồng/m²

STT	Tên đường	VT1	VT2	VT3	VT4
1	Lê Thành Phương - Đoạn từ đường Trần Phú đến đại lộ Nguyễn Tất Thành	14.000	9.000	6.000	4.000
2	Nguyễn Trung Trực - Đoạn từ đường Trần Phú đến Nguyễn Bình Khiêm	8.000	5.500	4.000	2.500
3	Nguyễn Tất Thành - Đoạn từ đường Trần Hưng Đạo đến ranh giới phường 8 và phường 9	16.000	11.000	8.000	5.000
4	Nguyễn Tất Thành - Đoạn từ ranh giới phường 8 và phường 9 đến ranh giới phường 9 và xã Bình Kiến	13.000	10.000	7.000	5.000

Figure 10. Illustrative image of looking up land price information attributes by administrative unit

Attribute information search

Not only does design information search according to spatial data, but the program also designs a window to search for land price information by year and by administrative units, thereby helping users to easily access information about desired land prices and can know land prices according to locations on a route.

Printing map online

It is an operation to extract information in an image format for printing. This function is intended to help users print data online. To print the map, we select the icon and print.



Figure 11. Illustration for online map printing

Reallocation locator - GPS

Purpose: Helping the user determine the current location, this function helps the user in finding the route conveniently. We select the positioning function to determine the actual location. If we use a smartphone, we must turn on the location function to use it.

3.4.4. Program management and security

The program manager's job is only granted to the top manager, and this person has the right to create accounts for other managers. The authorization on WebGIS is divided into 2 levels as follows:

Admin (supreme administrator) of WebGIS site: admin has all rights such as login account, adding, editing account, adding a user account, changing website blog appearance, changing status menu, website banner, etc. Admin is a technical officer involved in the management of land price information of agencies Department of Natural Resources and Environment of Phu Yen province, Department of Natural Resources and Environment of Tuy Hoa city.

The administrator is the person who manages the land price data catalog. He can exploit the information and has the right to use other functions of the system provided by the

administrator. Administrators can select “Login” on the WebGIS Menu to log in to the system. After entering the username and password, log in for the following results: In the System section, the administrator can change the login information or add a username. Users who access the system's portal have the right to look up, share and exploit land price information of Tuy Hoa city. However, people who are not administrators are not provided with the system login name and password.

4. CONCLUSION

The article has built a WebGIS website which supports the management of land prices in Tuy Hoa city, Phu Yen province. The results of the article on building a WebGIS program for integrating land prices on an online platform will help people and land managers to quickly search for land price information at land plot locations within a specific area and to each parcel of land. The WebGIS program on land prices in Tuy Hoa city is built according to the land price list prescribed by the State. Therefore, it helps to provide transparent information to the people, so that people can know information about the land area and land price according to regulations easily. On the other hand, the system supports searching for land price information by routes through the web environment and

online base map, which is convenient for people and managers in using and querying. Research results are an important tool in land management and use, creating favorable conditions for people and managers in querying information about land prices and the location of land plots in Tuy Hoa as well as throughout the province in the years to come.

REFERENCES

1. Ministry of Natural Resources and Environment, Circular No. 02/2012/TT-BTNMT stipulating the National Technical Regulation on basic geographic information standards, 2012.
2. Ministry of Natural Resources and Environment, Circular No. 26/2014/TT-BTNMT on economic-technical processes and norms for building a resource and environment database, 2014.
3. Nguyen Thanh Phi, Tran Van Son. Building a geographic information system for urban planning management and land valuation in Soc Trang city, *Can Tho University Scientific Journal*, **2018**, 54(3A), 12-20.
4. Department of Natural Resources and Environment of Phu Yen province. Report on statistical results of land inventory in Tuy Hoa city, 2019.
5. People's Committee of Phu Yen province. Decision No. 53/2019/QD-UBND on the price list of state land in Phu Yen province in the period of 2020 - 2024, 2020.
6. Ministry of Natural Resources and Environment, Circular No. 17/2010/TT-BTNMT technical regulations on cadastral data standards, 2010.
7. Truong Quang Hien, Bui Thi Dieu Hien. The actual situation of land prices in the market in Bong Son town, Hoai Nhon district, Binh Dinh province, *Science Journal of Natural Resources and Environment*, **2018**, 20, 86-98.
8. Truong Quang Hien, Ngo Anh Tu. GIS application to establish land price map in Nhon Phu ward, Quy Nhon City, Binh Dinh province, *Journal of Science, Ho Chi Minh City University of Education*, **2018**, 15(11b), 185-192.
9. Phu Yen Provincial People's Committee. Decision No. 07/2016/QD-UBND dated April 1, 2016, on amending and supplementing Decision No. 56/2014/QD-UBND dated December 29, 2014, of the Provincial People's Committee on promulgating the price list of all types of land in the province for 5 years (2016 - 2019), 2016.
10. Phu Yen Provincial People's Committee. Decision No. 07/2019/QD-UBND dated March 25, 2019, promulgating the Regulation on land price adjustment coefficient in Phu Yen province, 2019.
11. Phu Yen Provincial People's Committee. Decision No. 2572/QD-UBND dated December 29, 2017, on promulgating the Decision Promulgating the e-Government Architecture of Phu Yen province, version 1.0, 2017.

Tập tính ăn và lượng vi nhựa ăn vào của một số loài cá bống phân bố ở đầm Thị Nại, tỉnh Bình Định

Trình Thị Thúy Hằng^{1,2}, Võ Văn Chí^{1,*}

¹Khoa Khoa học Tự nhiên, Trường Đại học Quy Nhơn, Việt Nam

²Trường THPT Nguyễn Diêu, huyện Tuy Phước, tỉnh Bình Định, Việt Nam

Ngày nhận bài: 14/06/2022; Ngày nhận đăng: 25/07/2022; Ngày xuất bản: 28/10/2022

TÓM TẮT

Nghiên cứu này nhằm đánh giá tập tính ăn và lượng vi nhựa ăn vào của 3 loài cá bống phân bố ở đầm Thị Nại, tỉnh Bình Định. Mỗi loài được thu 30 cá thể từ ngư dân để nghiên cứu. Trong đó, 20 cá thể của mỗi loài được giải phẫu để xác định thức ăn tự nhiên và 10 cá thể còn lại được tách lấy ống tiêu hóa và phân tích sự tích tụ vi nhựa. Kết quả cho thấy, mặc dù tính ăn của 3 loài cá là khác nhau nhưng tần suất xuất hiện của mùn bã hữu cơ trong dạ dày của các loài đều cao hơn so với các loại thức ăn khác. Lượng vi nhựa ăn vào không khác nhau có ý nghĩa thống kê giữa 3 loài, dao động từ 6,50 đến 9,20 vi nhựa/cá thể; từ 0,58 đến 1,16 vi nhựa/g khối lượng cơ thể; và từ 31,47 đến 57,55 vi nhựa/g khối lượng ống tiêu hóa. Cả 3 loài cá đều ăn vào phần lớn là vi nhựa dạng sợi (75,38 - 82,50%) có kích thước từ 500-2000 μm (59,09 – 65,75%). Từ những kết quả thu được có thể nhận định rằng, tập tính ăn khác nhau của 3 loài cá bống trong nghiên cứu này không ảnh hưởng đến lượng vi nhựa ăn vào và vi nhựa trong mùn bã hữu cơ là nguồn vi nhựa tích lũy chính trong hệ tiêu hóa của 3 loài này. Cần có nhiều nghiên cứu thêm để xác định rõ hơn các tác động sinh học và sinh thái của các vi nhựa đối với cá.

Từ khóa: Vi nhựa, đầm Thị Nại, loài cá bống, tập tính ăn, tích tụ vi nhựa.

*Tác giả liên hệ chính.

Email: vovanchi@qnu.edu.vn

Feeding habits and quantity of ingested microplastics of some goby species distributed in Thi Nai lagoon, Binh Dinh province

Trinh Thi Thuy Hang^{1,2}, Vo Van Chi^{1,*}

¹Faculty of Natural Sciences, Quy Nhon University, Vietnam

²Nguyen Dieu high school, Tuy Phuoc district, Binh Dinh province, Vietnam

Received: 14/06/2022; Accepted: 25/07/2022; Published: 28/10/2022

ABSTRACT

This study aimed to evaluate feeding habits and microplastic ingestion of three goby species distributed in Thi Nai lagoon, Binh Dinh province. Thirty individuals of each species from fishermen for study. Twenty were dissected to identify natural food and the other ten were used to determine microplastic accumulation in digestive system. The results showed that feeding habits of these three fish species were different, but the occurrence frequency of organic matter in the digestive system of fish was higher than that of other natural food. The concentration of ingested microplastics was from 6.50 to 9.20 particles/fish, from 0.58 to 1.16 particles/g wet body weight and from 31.47 to 57.55 particles/g digestive tract weight and did not significantly differ among these fish species. These three fish species mostly ingested microplastic fibers (75.38 – 82.50%) with most size of 500-2000 μm (59.09 – 65.75%). Our findings indicate that the different feeding habits of the three goby species in this study do not affect the amount of ingested microplastics and the microplastics in organic matter are the main source of microplastics accumulated in the digestive system of these three species. Three studies are needed to better characterize the biological and ecological impacts of microplastics on fish.

Keywords: *Microplastic, Thi Nai lagoon, goby species, feeding habits, microplastic accumulation.*

1. INTRODUCTION

Plastic pollution has been paid attention to worldwide. Human awareness and concerns about microplastic pollution are increasing, especially microplastic pollution in aquatic environment. Microplastic accumulation in aquatic organisms has been reported by many researchers around the world for a long time as well as recently by scientists in Vietnam. Microplastics has been found in many organisms at different nutritional levels such as zooplankton,¹ invertebrates,^{1,3} fish.⁴ There are many studies conducted and

found microplastics in aquatic animals such as in clam *Mytilus galloprovincialis* inhabiting in estuaries of Tagus, Portugal and Po river, Italy,⁵ crab *Neohelice granulata* in estuaries in Southwest Atlantic Ocean,⁶ or in 24 fish species in estuaries in Brazil,⁷ oyster *Crassostrea virginica* and crab *Panopeus herbstii* in estuaries in Florida.⁸ In Vietnam, some researchers have recorded microplastic contamination in molluscs such as *Anadara granosa*, *Anadara subcrenata* in Thi Nai lagoon, Binh Dinh province,^{9,10} *Macra grandis*, *Callista lilacina*,

*Corresponding author.

Email: vovanchi@qnu.edu.vn

Marcia hiantina in Cu Mong lagoon, Phu Yen province,^{11,12} small fish species in coastal areas of Binh Dinh province¹³ or *Meretrix lyrata* in Ho Chi Minh city.¹⁴ In general, these authors mostly focused on determining microplastic contamination in studied animals, but did not assess relationships between feeding habits and microplastics ingestion of these animals. Therefore, understanding of such relationships is still limited.

A large amount of plastics and microplastics discharged from human activities in both lands and seas are accumulated in coastal areas in the world.¹⁴ In the same situation, coastal areas or lagoons (including Thi Nai) in Vietnam are also accumulated microplastics with different concentrations.^{9,15}

Thi Nai in Binh Dinh province is the second largest lagoon in Vietnam after Tam Giang – Cau Hai, Thua Thien Hue province. Thi Nai has a diversity of ecosystems such as mangroves, seagrass, etc., where many organisms including fish inhabit, feed and reproduce. Fish species composition in this lagoon recently increase, but they diverse relatively, with 95 species including 7 goby species (Vo and Nguyen).¹⁶ Among goby species in Thi Nai lagoon, tropical sand goby (*Acentrogobius caninus*), maned goby (*Oxyurichthys microlepis*) and redspot arrowfin goby (*Oxyurichthys tentacularis*) are 3 species that commonly appear and are collected to supply local consumers. This study focused on assessing feeding habits and microplastic ingestion, and examined microplastic characteristics accumulated in the digestive tracts of these 3 goby species to contribute to microplastic source identification.

2. METHODS

2.1. Fish collection and treatment

Tropical sand goby (*Acentrogobius caninus*), maned goby (*Oxyurichthys microlepis*) and redspot arrowfin goby (*Oxyurichthys tentacularis*) were collected from fishermen in Thi Nai lagoon, with 20 individuals of each

species to be examined for feeding habits and 10 for microplastic accumulation.

Fish were frozen at the collection sites and brought to lab. In the laboratory, fish used for microplastic examination (10 individuals/species) were treated within the day or frozen in the fridge for later analysis. Fish for examination of feeding habits (20 individuals/species) were treated within the day or fixed in 5% formal for later analysis.

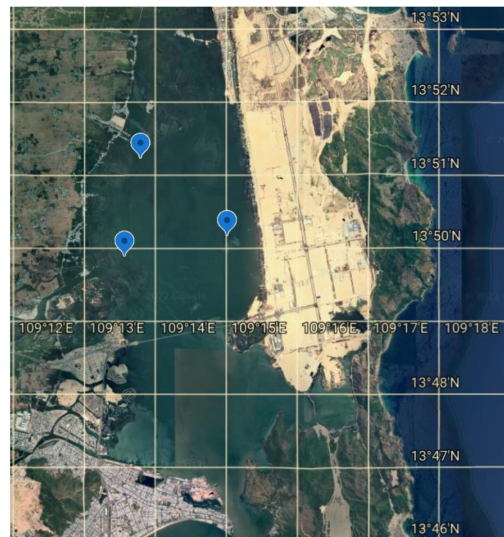


Figure 1. Sample collection sites in Thi Nai lagoon

2.2. Feeding habit examination

Fish individuals were dissected to examine natural food in their digestive tracts. Stereomicroscope Meiji EMTR-3 and binocular microscope Olympus CX21 were used to analyse and identify the food. Based on the analysis results, occurrence frequency of food items ($O_i\%$) in the digestive tracts of fish was calculated according to the method of Hyslop.¹⁸

$$O_i\% = \left(\frac{\text{Number of digestive tracts containing food item } i}{\text{Total number of digestive tracts containing food}} \right) \times 100.$$

2.3. Microplastic contamination examination

Each fish individual was weighed, measured and washed using water filtered through the glass fiber filters GF/A with pore sizes of 1.6 μm , then dissected to remove the digestive tract. Next, the digestive tract was put into a glass

beaker containing 20 ml 10% KOH, covered by aluminum foil and placed in an incubator at 60 °C for 24 hours according to the method of Alexandre et al.¹⁸ The samples after incubated were filtered through 1 mm mesh sieve to collect microplastic particles 1- 5 mm on the sieve (if any). The samples under the sieve were then filtered through a 250 µm mesh sieve, and the material on the sieve was rinsed into a beaker to perform the overflow technique using a saturated NaCl solution with 3 replicates. Finally, the sample solution was filtered through a 1.6 µm GF/A filters according to the method of Emilie et al.¹⁵ to remove microplastics. The filters were stored in clean Petri dishes and put in room condition for later stereoscopic observation.

Put the filters under the Leica S9i stereomicroscope to observe and identify microplastics using LASX software. Microplastics were identified with 3 shapes as described by Emilie et al.¹⁵ such as fibers, fragments and pellets. Microplastics on the filters were measured and photographed.

Microplastic concentration was considered as number of microplastics per individual, number of microplastics per gram of wet body weight and number of microplastics per gram of digestive tract weight of fish.

To control microplastic contamination from the surrounding environment during sample treatment and observation, we followed to suggestions of GESAMP¹⁹ such as cleaning the working area with alcohol before observing and treating samples, wearing cotton clothes and rubber gloves, etc. In addition, at each period of sample observation and treatment, we placed a new filter in a Petri dish nearby the place we were working to check microplastic contamination. During the steps on sample, we did not find any microplastics on the control filter papers.

2.4. Data analysis

Microsoft Excel 2013 was used to calculate the necessary parameters and make diagrams.

Anova single factor in Microsoft Excel 2013 was applied to compare some parameters between studied fish species.

3. RESULTS AND DISCUSSION

3.1. Results

3.1.1. Feeding habits of fish

Feeding habits of tropical sand goby, maned goby and redspot arrowfin goby was different (Table 1). The food spectrum of tropical sand goby was most diverse, with 6 groups of prey found in the digestive tracts of fish, of which occurrence frequency of organic matters, fish, seaweeds and shrimps was higher than that of others. Natural food of maned goby only comprised two groups of prey which are organic matters and fish, with the dominance of organic matters (92.86% in occurrence frequency), and natural food of redspot arrowfin goby included 3 groups which are organic matters, fish and seaweeds with the predominance of organic matters. Thus, it can be seen that organic matters are dominant in the natural food spectrum of 3 studied goby species.

Table 1. Natural food of three goby species

Kinds of food	Occurrence frequency of food (%)		
	Maned goby (n=20)	Redspot arrowfin goby (n=20)	Tropical sand goby (n=20)
Organic matters	92.86	45.00	40.00
Fish	7.14	35.00	26.67
Seaweeds	0.00	20.00	26.67
Snails	0.00	0.00	6.67
Shrimps	0.00	0.00	20.00
Zooplanktons	0.00	0.00	6.67

3.1.2. Microplastic accumulation in fish

Microplastic concentration in 3 goby species is expressed as number of microplastics per individual, number of microplastics per gram of

wet body weight and number of microplastics per gram of digestive tract weight of fish (Table 2). The results showed that the concentration of microplastic ingested by 3 goby species varied from 6.50 to 9.20 microplastics/individual,

0.58 to 1.16 microplastics/g wet body weight and 31.47 to 57.55 microplastics/g weight of digestive tract. There was not significant difference of microplastic concentration between three goby species ($p > 0,05$).

Table 2. Concentration of ingested microplastic in three goby species

Fish species	Number of microplastics/ individual	Number of microplastics/g wet body weight	Number of microplastics/g digestive tract weight
Maned goby (n=10)	9.20 ± 3.44 ^a	0.87 ± 0.38 ^a	57.55 ± 29.45 ^a
Redspot arrowfin goby (n=10)	6.50 ± 3.12 ^a	1.16 ± 0.58 ^a	46.76 ± 27.77 ^a
Tropical sand goby (n=10)	8.00 ± 4.06 ^a	0.58 ± 0.29 ^a	31.47 ± 22.50 ^a

Note: The different letters indicate significant differences for each parameter ($p < 0.05$).

The weight of tropical sand goby was highest (13.79 g/fish), followed by maned goby (10.81 g/fish) and redspot arrowfin goby (5.70 g/fish) ($p < 0,05$) (Table 3). However, the amount of ingested microplastics per gram of wet body weight was not significantly different between three studied species (Table 2). Similarly, the weight of digestive tracts of tropical sand goby was different from others, but the amount of ingested microplastics per gram of weight of digestive tracts was not significantly different between three goby species. Therefore, it can be said that fish size and weight of digestive tract of fish are not the main factors governing amount

of microplastics ingested by fish. This is clearly indicated through the correlation between the number of microplastics ingested and wet body weight or digestive tract weight of fish (Table 3). Specifically, the correlation between the number of microplastics and wet body weight of fish was negative for maned goby and redspot arrowfin goby with the coefficient from -0.49 to -0.24 while there was no correlation between these two parameters for tropical sand goby ($r = 0.08$); the negative correlation was recorded between number of microplastics and weight of digestive tract of fish (coefficient from -0.40 to -0.27).

Table 3. The correlation between wet body weight, digestive tract weight of fish and amount of microplastics ingested in three goby species

Fish species	Wet body weight of fish (g)	Digestive tract weight of fish (g)	Correlation between number of microplastics and wet body weight of fish (r)	Correlation between number of microplastics and digestive tract weight of fish (r)
Maned goby (n=10)	10.81 ± 1.59 ^b	0.18 ± 0.07 ^b	-0.49	-0.27
Redspot arrowfin goby (n=10)	5.70 ± 0.74 ^c	0.15 ± 0.04 ^b	-0.24	-0.40
Tropical sand goby (n=10)	13.79 ± 1.86 ^a	0.28 ± 0.11 ^a	0.08	-0.33

Note: The different letters indicate significant differences for each parameter ($p < 0.05$).

The shape data of microplastics were pooled for 10 fish of each species. The results showed that there were two shapes of microplastics found in the digestive tracts of three studied fish species, that were fibers and fragments, of which fibers were dominant in all goby species (Figure 2). Specifically, microplastic fibers accounted for from 79.03% to 82.50% while the ratio of microplastic fragments was from 17.50% to 20.97%.

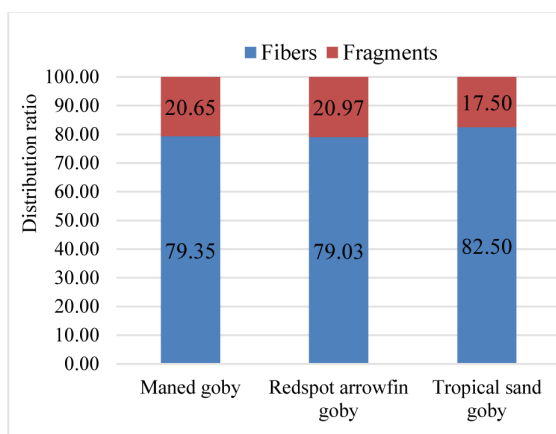


Figure 2. Shapes of microplastics found in three goby species

The fibers found in the digestive tracts of three studied fish species mostly had the length of 300 to 2500 μm , especially the size range of 500 to 2000 μm , excepting a high ratio of fibers with the length of 2500-3000 μm (13,64%) observed in tropical sand goby (Figure 3). Specifically, fibers with the length of 500-2000 μm accounted for 65.75% in maned goby, 63.27% in redspot arrowfin goby and 59.09% in tropical sand goby while other fibers only accounted for 34.25%, 36.73% and 40.49% in these three goby species, respectively (Figure 4). Fragments observed in the digestive tracts of three goby species had the area of 45000 to 600000 μm^2 but dominant in range of 45000 - 200000 μm^2 , with 77.78%, 69.23% and 71.43% in total in maned goby, redspot arrowfin goby and tropical sand goby, respectively (Figure 5). Thus, it can be seen that the studied fish species ingested microplastics in small size rather than big size range.

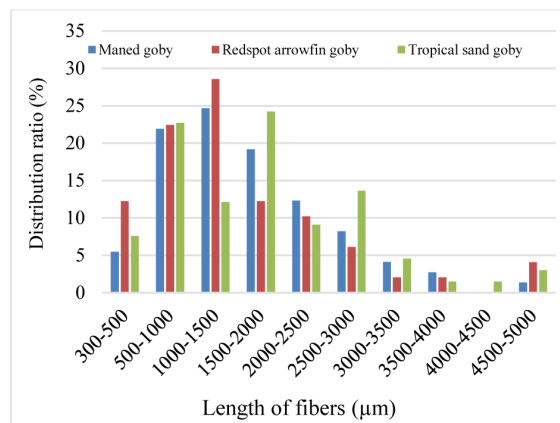


Figure 3. The length distribution of microplastic fibers

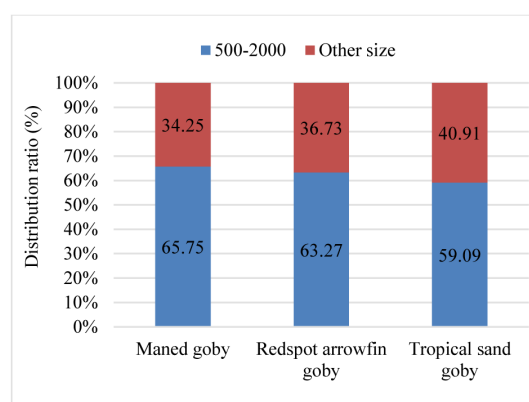


Figure 4. Percentage of microplastic fibers with length of 500-2000 μm compared to others

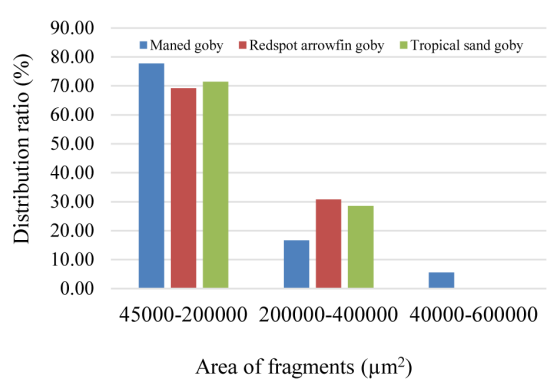


Figure 5. The area distribution of microplastic fragments

3.2. DISCUSSION

3.2.1. Feeding habits and microplastic ingestion of fish

Although the average microplastic concentration in each fish species is different, perhaps this difference is not large enough to lead to significant difference. Natural food spectrum of three studied

goby species is different, but organic matters are the dominant food of these species. Hence, it can be speculated that the main source of microplastics accumulated in the digestive tract of these goby species is from organic matters. It can be seen that occurrence frequency of organic matters in the digestive tracts of maned goby is highest (92,86%) and microplastic concentration in this species is high (9.20 microplastics/individual) while occurrence frequency of organic matters in the digestive tracts of tropical sand goby is just 40% but weight of digestive tract of this species 1.5 times significant higher than that maned goby, so the amount of organic matters ingested by tropical sand goby may be nearly similar to maned goby and results in a relatively high microplastic intake in tropical sand goby (8.0 microplastics/individual). The amount of microplastics accumulated in redspot arowfin goby is low (6.5 microplastics/individual) because occurrence frequency of organic matters in this species is just 45% while its digestive tract weight is not different from maned goby, that means the amount of organic matters ingested by redspot arowfin goby is less than maned goby. In addition to main source of microplastics from organic matters, fish can also indirectly ingest microplastics accumulated in their other foods such as fish, shrimps, snails, seaweeds. Walkinshaw et al.²¹ suggested that fish species having a narrow food spectrum would be more likely to directly ingest microplastics from environment than indirectly through prey such as in fish species with large food spectrum. This is somewhat reasonable with our results when comparing the food spectrum of maned goby and other 2 species in consideration of the corresponding amount of microplastic ingested. However, redspot arowfin goby also has a natural food spectrum narrower than that of tropical sand goby, but the concentration of microplastics ingested by this species is lower than that of maned goby. This may be due to the dominance of organic matters in the diet of fish as mentioned above.

3.2.2. Characteristics of microplastics accumulated in the digestive tracts of fish

Concentration of microplastics accumulated in fish species in our study varied from 6.50 to 9.20 microplastics/individual, 0.58 to 1.16 microplastics/g wet body weight and 31.47 to 57.55 microplastics/g digestive tract weight, that is much higher than records of Gopal et al.²² in 10 marine fish species in Bengal bay - Bangladesh (1.0-3.8 microplastics/individual, 0.02-0.15 microplastics/g wet body weight and 0.63-6.45 microplastics/g digestive tract weight) or the study results of Vendel et al.²³ in 69 fish species in estuaries in Northeast Brazil (vary 1 to 4 and 1.06 microplastics/individual in average), Wanlada and Suwaree²⁴ in 7 fish species in coastal areas of Thailand Gulf and Adaman sea (0 – 0.4 microplastics/individual), Sukree et al.²⁵ in *Rastrelliger brachysoma* in Thailand Gulf (2.70 ± 16.62 microplastics/individual). However, microplastic concentration in our study is lower than that reported by Ayu et al.²⁶ in 9 fish species in coastal areas of Pantai Indah Kapuk, Indonesia (varies from 4.9 to 20 and average of 12.21 microplastics/individual). Therefore, microplastic accumulation level in fish species mentioned in different studies is not similar and that can be due to different characteristics of these fish species but may be also governed by environment at study locations.

The dominance of fibers compared to fragments is also observed in our study. The similar results are reported by Gopal et al.²² (fibers accounted for 53.4%), Vendel et al.²³ (fibers accounted for 90%), Ayu et al.²⁶ (89.63% of fibers in total), or Wanlada and Suwaree²⁴ (fibers accounted for 57.14% in pelagic fish and 82.76% in benthic fish). Likewise, such tendency is also found in molluscs.^{26,28} Fish or aquatic animals ingesting amount of fibers higher than other shapes can be due to dominance of fibers in their environment compared to others. This is supported by the study results of Vo⁹ and Le¹¹ with predominance of fibers in surface waters and benthic sediments.

In this study, we found that the studied fish species mostly ingested microplastics in the small size range (500-2000 μm for fibers and 45000 - 200000 μm^2 for fragments). Similar results are also recorded by Vo and Vo¹⁰ in blood cockle distributed in Thi Nai lagoon, with most fibers long from 500 to 2100 μm . However, the area of fragments observed by these authors is bigger than that in our study. Gopal et al.²² found that 85% of microplastics obtained from 10 studied fish species had the size of less than 500 μm while ones from 500 – 5000 μm were found with low percentage. Thus, it can be seen that aquatic creatures often ingest a large proportion of microplastics in small size range. This may be due to accumulation concentration of small-sized microplastics in their habitats is higher than that of large-sized microplastics. The evidences of this can be found in the study results of Vo⁹ and Le¹¹. However, despite ingesting small-sized microplastics, size range together with corresponding percentage of microplastics accumulated in different fish species differ, which can be governed by their feeding habits.

4. CONCLUSION

Feeding habits of maned goby, redspot arrowfin goby and tropical sand goby are different but occurrence frequency of organic matters is higher than that of other food in the diets of these species.

The concentration of microplastics accumulated in three studied goby species is not significantly different and vary from 6.50 to 9.20 microplastics/individual, 0.58 to 1.16 microplastics/g wet body weight, and 31.47 to 57.55 microplastics/g digestive tract weight.

Three studied goby fish species ingest a large amount of 500 - 2000 μm fibers.

Feeding habits does not affect amount of ingested microplastics and the main source of microplastics accumulated in three studied goby species is mostly from organic matters.

REFERENCES

1. X. Sun, Q. Li, M. Zhu, J. Lian, S. Zheng, Y. Zhao. Ingestion of microplastics by natural zooplankton groups in the northern South China Sea, *Marine Pollution Bulletin*, **2017**, *115*, 217–224.
2. O. Setälä, J. Norkko, M. Lehtiniemi. Feeding type affects microplastic ingestion in coastal invertebrate community, *Marine Pollution Bulletin*, **2016**, *102*, 95–101.
3. L. Van Cauwenberghe, M. Claessens, M. Vandegehuchte, C. R. Janssen. Microplastics are taken up by mussels (*Mytilus edulis*) and lugworms (*Arenicola marina*) living in natural habitats, *Environmental Pollution*, **2015**, *199*, 10–17.
4. R. S. Pazos, T. Maiztegui, D. C. Colautti, A. H. Paracampo. Microplastics in gut contents of coastal freshwater fish from Río de la Plata estuary, *Marine Pollution Bulletin*, **2017**, *122*(1-2), 85-90.
5. G. Vandermeersch, L. V. Cauwenberghe, C. R. Janssen, A. Marques, K. Granby, G. Fait, M. J. J. Kotterman, J. Diogène, K. Bekaert, J. Robbens, and L. Devriese. A critical view on microplastic quantification in aquatic organisms, *Environmental Research*, **2015**, *143*, 46–55.
6. A. L. Vendel, F. Bessa, V. E. N. Alves, A. L. A. Amorim, J. Patrício, A. R. T. Palma. Widespread microplastic ingestion by fish assemblages in tropical estuaries subjected to anthropogenic pressures, *Marine Pollution Bulletin*, **2017**, *117*(1–2), 448–455.
7. D. M. Villagran, D. M. Truchet, N. S. Buzzi, A. D. F. Lopez, and M. D. F. Severini. A baseline study of microplastics in the burrowing crab (*Neohelice granulata*) from a temperate southwestern Atlantic estuary, *Marine Pollution Bulletin*, **2020**, *150*, 110686.
8. H. R. Waite, M. J. Donnelly, and L. J. Walters. Quantity and types of microplastics in the organic tissues of the eastern oyster *Crassostrea virginica* and Atlantic mud crab *Panopeus herbstii* from a Florida estuary, *Marine Pollution Bulletin*, **2018**, *129*(1), 179-185.

9. T. N. Q. Vo. *The microplastic contamination status in waters, sediments and digestive tracts of some molluscs in Thi Nai lagoon, Binh Dinh province*, Master thesis in Experimental Biology, Quy Nhon University (in Vietnamese), Vietnam, 2021.
10. V. C. Vo, and T. N. Q. Vo. Microplastic contamination in blood cockle (*Anadara granosa*) distributed in Thi Nai lagoon, Binh Dinh province. *Journal of Sciences and Technology, Da Nang University*, **2021**, 20(1), 21-25 (in Vietnamese).
11. Q. H. Le. *Assessing the microplastic contamination status in sediments and digestive tracts of some bivalves distributed in Cu Mong lagoon, Phu Yen province*, Master thesis in Experimental Biology, Quy Nhon University (in Vietnamese), 2021.
12. Q. H. Le, and V. C. Vo. Concentration and characteristics of microplastic in Big brown mactra clam (*Macra grandis*) distributed in Cu Mong lagoon, Phu Yen province, *Quy Nhon University Journal of Science*, **2022**, 16(1), 63-70.
13. V. H. Nguyen. *Examining status of microplastic contamination in some small marine fish species in the coastal areas of Binh Dinh province* (in Vietnamese), Master thesis in Experimental Biology, Quy Nhon University (in Vietnamese), 2021.
14. T. C. K. Le, Q. V. Tran, T. N. S. Truong, E. Strady. Anthropogenic fibres in white clams, *Meretrix lyrata*, cultivated downstream a developing megacity, Ho Chi Minh City, Viet Nam, *Marine Pollution Bulletin*, **2022**, 174, 113302.
15. P. G. Ryan, C. J. Moore, J. A. V. Franeker, C. L. Moloney. Monitoring the abundance of plastic debris in the marine environment, *Philosophical Transactions of the Royal Society B*, **2009**, 364(1526), 1999–2012.
16. E. Strady, T. H. Dang, T. D. Dao, H. N. Dinh, T. T. D. Do, T. N. Duong, T. T. Duong, D. A. Hoang, T. C. K. Le, T. P. Q. Le, H. Mai, D. M. Trinh, Q. H. Nguyen, Q. A. T. Nguyen, Q. V. Tran, T. N. S. Truong, V. H. Chu, V. C. Vo. Baseline assessment of microplastic concentrations in marine and freshwater environments of a developing Southeast Asian country, Viet Nam, *Marine Pollution Bulletin*, **2021**, 162, 111870.
17. V. C. Vo, T. P. H. Nguyen. The fish species composition diversity in Thi Nai lagoon, Binh Dinh province, *Quy Nhon University Journal of Science*, **2020**, 14(1), 87-94.
18. E. J. Hyslop. Stomach contents analysis: a review of methods and their application, *Journal of Fish Biology*, **1980**, 17, 411-429.
19. A. Dehaut, A.-L. Cassone, L. Frere, L. Hermabessiere, C. Himber, E. Rinnert, G. Riviere, C. Lambert, P. Soudant, A. Huvet, G. Duffos, I. Paul-Pont. Microplastics in seafood: Benchmark protocol for their extraction and characterization, *Environmental Pollution*, **2016**, 215, 223-233.
20. GESAMP, In: P. J. Kershaw, A. Turra, F. Galgani, (Eds.), *Guidelines for the Monitoring and Assessment of Plastic Litter and Microplastics in the Ocean*, GESAMP Joint Group of Experts on the Scientific Aspects of Marine Environmental Protection, London, UK, 2019.
21. C. Walkinshaw, P. K. Lindeque, R. Thompson, T. Tolhurst, M. Cole. Microplastics and seafood: lower trophic organisms at highest risk of contamination, *Ecotoxicology Environmental Safety*, **2020**, 190, 110066.
22. G. C. Ghosh, S. M. Akter, R. M. Islam, A. Habib, T. K. Chakraborty, S. Zaman, A. H. M. E. Kabir, O. V. Shipin, M. A. Wahid. Microplastics contamination in commercial marine fish from the Bay of Bengal, *Regional Studies in Marine Science*, **2021**, 44, 101728.
23. A. L. Vendel, F. Bessa, V. E. N. Alves, A. L. A. Amorim, J. Patrício, A. R. T. Palma. Widespread microplastic ingestion by fish assemblages in tropical estuaries subjected to anthropogenic pressures, *Marine Pollution Bulletin*, **2017**, 117, 448-455.
24. W. Klangnurak and S. Chunniyom. Screening for microplastics in marine fish of Thailand: the accumulation of microplastics in the gastrointestinal tract of different foraging preferences, *Environmental Science and Pollution Research*, **2020**, 27, 27161–27168.

25. S. Hajisamae, K. K. Soe, S. Pradit, J. Chaiyvareesajja, H. Fazrul. Feeding habits and microplastic ingestion of short mackerel, *Rastrelliger brachysoma*, in a tropical estuarine environment, *Environmental Biology of Fishes*, **2022**, *105*, 289–302.
26. A. R. Hastuti, D. T. F. Lumbanbatu, Y. Wardiatno. The presence of microplastics in the digestive tract of commercial fishes off Pantai Indah Kapuk coast, Jakarta, Indonesia, *Biodiversitas*, **2019**, *20*(5), 1233-1242.
27. S. Abidli, Y. Lahbib, N. T. E. Menif. Microplastics in commercial molluscs from the lagoon of Bizerte (Northern Tunisia), *Marine Pollution Bulletin*, **2019**, *142*, 243–252.
28. J. Li, D. Yang, L. Li, K. Jabeen, H. Shi. Microplastics in commercial bivalves from China, *Environmental Pollution*, **2015**, *207*, 190–195.

Một số bất đẳng thức kiểu Fejér cho hàm $(\mathcal{M}_\phi, \mathcal{M}_\psi)$ -lồi mạnh

Nguyễn Ngọc Huệ*

Khoa Khoa học Tự nhiên và Công nghệ, Đại học Tây Nguyên, Đắk Lắk, Việt Nam

Ngày nhận bài: 30/03/2022; Ngày nhận đăng: 07/06/2022; Ngày xuất bản: 28/10/2022

TÓM TẮT

Trong bài báo này, chúng tôi xem xét một lớp hàm lồi mạnh mở rộng liên quan đến một cặp tựa trung bình số học, được gọi là hàm $(\mathcal{M}_\phi, \mathcal{M}_\psi)$ -lồi mạnh từ đó thiết lập một số bất đẳng thức kiểu Fejér cho lớp hàm lồi mạnh này. Các bất đẳng thức mới này là sự mở rộng thực sự của các bất đẳng thức Hermite-Hadamard và bất đẳng thức Fejér được thiết lập gần đây đối với hàm lồi mạnh và một số dạng mở rộng của lớp hàm lồi mạnh. Hơn nữa, các bất đẳng thức mới còn đặc trưng cho lớp hàm $(\mathcal{M}_\phi, \mathcal{M}_\psi)$ -lồi mạnh.

Từ khóa: Hàm $(\mathcal{M}_\phi, \mathcal{M}_\psi)$ -lồi mạnh, tựa trung bình số học, hàm lồi, bất đẳng thức Hermite-Hadamard, bất đẳng thức Fejér.

*Tác giả liên hệ chính.
Email: nnhue@ttn.edu.vn

Some Fejér type inequalities for strongly $(\mathcal{M}_\phi, \mathcal{M}_\psi)$ - convex functions

Nguyen Ngoc Hue*

Department of Technology and Science, Tay Nguyen University, Dak Lak, Vietnam

Received: 30/03/2022; Accepted: 07/06/2022; Published: 28/10/2022

ABSTRACT

In this paper, we propose and study a class of generalized convex functions, which are defined according to a pair of quasi-arithmetic means and called $(\mathcal{M}_\phi, \mathcal{M}_\psi)$ -convex functions, and establish various Fejér type inequalities for such a function class. These inequalities not merely provide a natural and intrinsic characterization of the $(\mathcal{M}_\phi, \mathcal{M}_\psi)$ -convex functions, but actually offer a generalization and refinement of some Hermite-Hadamard and Fejér type inequalities obtained in earlier studies for different kinds of strong convexity.

Keywords: *Strongly $(\mathcal{M}_\phi, \mathcal{M}_\psi)$ -convex functions, quasi-arithmetic mean, convexity, Hermite-Hadamard inequality, Fejér inequality.*

1. INTRODUCTION

In the field of mathematical inequalities, the well-known Hermite-Hadamard inequality for convex functions was first discovered by Hermite¹ in 1883 and independently discovered 10 years later by Hadamard.² This inequality says that if $f : [a, b] \rightarrow \mathbb{R}$ is a convex function then

$$f\left(\frac{a+b}{2}\right) \leq \frac{1}{b-a} \int_a^b f(x)dx \leq \frac{f(a)+f(b)}{2}. \quad (1)$$

A weighted generalization of Hermite-Hadamard inequality was developed by Fejér:³ If $f : [a, b] \rightarrow \mathbb{R}$ is a convex function, $g : [a, b] \rightarrow [0, \infty)$ is an integrable function with $\int_a^b g(x)dx > 0$ and it is symmetric to $\frac{a+b}{2}$, i.e. $g(x) = g(a+b-x)$ for all $x \in [a, b]$, then

$$f\left(\frac{a+b}{2}\right) \leq \frac{\int_a^b f(x)g(x)dx}{\int_a^b g(x)dx} \leq \frac{f(a)+f(b)}{2}. \quad (2)$$

Since then, the inequalities (1) and (2) have been generalized, extended and improved in various ways and found interesting applications to convex analysis, optimization theory and nonlinear analysis. One of such ways is to establish new inequalities for various generalized convex functions (see e.g.,⁴⁻⁷). Among them, an important subclass of convex functions in the optimization theory is strongly convex functions. This class was developed by Polyak⁸ in 1966 for dealing with some related issues arisen from optimization theory.

Let c be a positive number. A function $f : [a, b] \rightarrow \mathbb{R}$ is called strongly convex with modulus c if

$$f(tx+(1-t)y) \leq tf(x)+(1-t)f(y)-ct(1-t)(x-y)^2$$

for all $x, y \in [a, b]$. One says that f is strongly mid-convex with modulus c if

$$f\left(\frac{x+y}{2}\right) \leq \frac{f(x)+f(y)}{2} - c\frac{(x-y)^2}{4} \quad (3)$$

for all $x, y \in [a, b]$.

In 2010, Merentes and Nikodem⁹ established a generalized version of Hermite-Hadamard inequality for strongly convex functions as follows: Let $f : [a, b] \rightarrow \mathbb{R}$ be a strongly convex function with modulus c . Then, the following inequality holds

$$\begin{aligned} f\left(\frac{a+b}{2}\right) + \frac{c}{12}(b-a)^2 &\leq \frac{1}{b-a} \int_a^b f(x)dx \\ &\leq \frac{f(a)+f(b)}{2} - \frac{c}{6}(b-a)^2. \end{aligned} \quad (4)$$

In 2012, Azocar¹⁰ et al. proposed a Fejér type inequality for strongly convex functions: Let $f : [a, b] \rightarrow \mathbb{R}$ be a strongly convex function with modulus c and $g : [a, b] \rightarrow [0, \infty)$ be an integrable function

*Corresponding author:

Email: nnhue@ttn.edu.vn

with $\int_a^b g(x)dx = 1$ and symmetric to $\frac{a+b}{2}$. Then,

$$\begin{aligned} & f\left(\frac{a+b}{2}\right) + c \left[\int_a^b x^2 g(x)dx - \left(\frac{a+b}{2}\right)^2 \right] \\ & \leq \int_a^b f(x)g(x)dx \quad (5) \\ & \leq \frac{f(a) + f(b)}{2} - c \left[\frac{a^2 + b^2}{2} - \int_a^b x^2 g(x)dx \right]. \end{aligned}$$

In recent years, some generalizations of inequality (5) have been established for strongly log-convex functions and strongly harmonic convex functions.^{11,12} Motivated by the achievements, we continue the research direction. Our contributions in this paper are that we first deeply investigate the class of generalized strongly convex functions regarding to a pair of quasi-arithmetic means and then derive some new Fejér-type inequalities. The derived inequalities are not only characterizations for generalized strongly convex continuous functions, but they also generalize inequalities that were recently derived in the papers.^{11,12}

The rest of this paper is organized as follows. In Section 2, we will introduce $(\mathcal{M}_\phi, \mathcal{M}_\psi)$ -convex functions, strongly $(\mathcal{M}_\phi, \mathcal{M}_\psi)$ -convex functions with positive modulus and refer related particular cases. The main results of this paper will be presented in Section 3. Finally, the paper closes with the conclusions in Section 4.

2. STRONGLY $(\mathcal{M}_\phi, \mathcal{M}_\psi)$ - CONVEX FUNCTIONS

Let I and J be the intervals of real numbers. Let $\phi : I \rightarrow \mathbb{R}$ and $\psi : J \rightarrow \mathbb{R}$ be continuous and strictly monotone functions. Using a pair of quasi-arithmetic means \mathcal{M}_ϕ and \mathcal{M}_ψ , with $\mathcal{M}_\phi(a, b; \alpha) = \phi^{-1}(\alpha\phi(a) + (1-\alpha)\phi(b))$ Aumann¹³ proposed the concept of $(\mathcal{M}_\phi, \mathcal{M}_\psi)$ -convex functions that is stated as follows.

Definition 1.¹³ A function $f : I \rightarrow J$ is said to be $(\mathcal{M}_\phi, \mathcal{M}_\psi)$ -convex if

$$f(\mathcal{M}_\phi(a, b; \alpha)) \leq \mathcal{M}_\psi(f(a), f(b); \alpha) \quad (6)$$

for all $a, b \in I$ and $\alpha \in [0, 1]$.

In the case that f fulfills the inequality (6) with $\phi(x) = x$, f is called \mathcal{M}_ψ -convex. If f satisfies the inequality (6) with $\phi(x) = x$ and $\psi(x) = x$, then the $(\mathcal{M}_\phi, \mathcal{M}_\psi)$ -convexity of f reduces to the usual convexity in the literature of convex analysis.

For a pair of quasi-arithmetic means \mathcal{M}_ϕ and \mathcal{M}_ψ , we define a class of generalized strongly convex functions as follows.

Definition 2. Let c be a positive number. A function $f : I \rightarrow J$ is called strongly $(\mathcal{M}_\phi, \mathcal{M}_\psi)$ -convex with modulus c if

$$\begin{aligned} f(\mathcal{M}_\phi(a, b; \alpha)) & \leq \psi^{-1} \left(\alpha\psi \circ f(a) + (1-\alpha)\psi \circ f(b) \right. \\ & \quad \left. - c\alpha(1-\alpha)(\phi(a) - \phi(b))^2 \right) \quad (7) \end{aligned}$$

for all $a, b \in I$ and $\alpha \in [0, 1]$. If the inequality (7) is reversed, we call that f is strongly $(\mathcal{M}_\phi, \mathcal{M}_\psi)$ -concave with modulus c .

Note that if ψ is increasing then $f : I \rightarrow J$ is strongly $(\mathcal{M}_\phi, \mathcal{M}_\psi)$ -convex with modulus c if and only if $\psi \circ f \circ \phi^{-1}$ is strongly convex function with modulus c on $\phi(I)$. If ψ is decreasing then $f : I \rightarrow J$ is strongly $(\mathcal{M}_\phi, \mathcal{M}_\psi)$ -convex with modulus c iff $\psi \circ f \circ \phi^{-1}$ is strongly concave with modulus c on $\phi(I)$.

We say that a function f is strongly \mathcal{M}_ψ -convex with modulus c if f satisfies the inequality (7) for $\phi(x) = x$. For particular forms of ϕ and ψ , we obtain the following concepts:

- *strongly convex functions* if we take $\phi(x) = x$ and $\psi(x) = x$:

$$\begin{aligned} & f(\alpha a + (1-\alpha)b) \\ & \leq \alpha f(a) + (1-\alpha)f(b) - c\alpha(1-\alpha)(a-b)^2 \end{aligned}$$

for all $a, b \in I$ and $\alpha \in [0, 1]$.

- *Strongly log-convex functions*¹⁴ if we take $\phi(x) = x$ and $\psi(x) = \ln x$:

$$\begin{aligned} & \ln f(\alpha a + (1-\alpha)b) \\ & \leq \alpha \ln f(a) + (1-\alpha) \ln f(b) - c\alpha(1-\alpha)(a-b)^2 \end{aligned}$$

for all $a, b \in I$ and $\alpha \in [0, 1]$.

- *Strongly exponentially convex functions*¹⁵ if we take $\phi(x) = x$ and $\psi(x) = e^x$:

$$\begin{aligned} & e^{f(\alpha a + (1-\alpha)b)} \\ & \leq \alpha e^{f(a)} + (1-\alpha)e^{f(b)} - c\alpha(1-\alpha)(a-b)^2 \end{aligned}$$

for all $a, b \in I$ and $\alpha \in [0, 1]$.

- *Strongly harmonic convex functions*¹¹ if we take $\phi(x) = 1/x$ and $\psi(x) = x$:

$$\begin{aligned} & f\left(\frac{ab}{\alpha a + (1-\alpha)b}\right) \\ & \leq \alpha f(a) + (1-\alpha)f(b) - c\alpha(1-\alpha)\left(\frac{a-b}{ab}\right)^2 \end{aligned}$$

for all $a, b \in I$ and $\alpha \in [0, 1]$.

- *Strongly harmonic log-convex functions*¹¹ if we take $\phi(x) = 1/x$ and $\psi(x) = \ln x$:

$$\begin{aligned} & f\left(\frac{ab}{\alpha a + (1-\alpha)b}\right) \\ & \leq f(a)^\alpha f(b)^{(1-\alpha)} - c\alpha(1-\alpha)\left(\frac{a-b}{ab}\right)^2 \end{aligned}$$

for all $a, b \in I$ and $\alpha \in [0, 1]$.

- Strongly p -convex functions if $\phi(x) = x^p$ and $\psi(x) = x$:

$$f([\alpha a^p + (1 - \alpha)b^p]^{1/p}) \leq \alpha f(a) + (1 - \alpha)f(b) - c\alpha(1 - \alpha)(a^p - b^p)^2$$

for all $a, b \in I$ and $\alpha \in [0, 1]$.

- Strongly geometrically convex functions if we take $\phi(x) = \ln x$ and $\psi(x) = \ln x$:

$$f(a^\alpha b^{(1-\alpha)}) \leq f(a)^\alpha f(b)^{(1-\alpha)} - c\alpha(1-\alpha) \ln^2 \left(\frac{a}{b}\right)$$

for all $a, b \in I$ and $\alpha \in [0, 1]$.

Lemma 3. ¹⁶

1. A function $f : I \rightarrow J$ is strongly convex with modulus c if and only if the function $g(x) = f(x) - cx^2$ is convex.
2. A function $f : I \rightarrow J$ is strongly midconvex with modulus c if and only if $g(x) = f(x) - cx^2$ is midconvex.

Due to Lemma 3 and Jensen's inequality¹⁷, one can verify that if f is continuous on I and strongly midconvex with modulus c then f is a strongly convex function with modulus c on I .

Lemma 4. A function f is strongly $(\mathcal{M}_\phi, \mathcal{M}_\psi)$ -convex with modulus c if and only if $g(x) := \psi \circ f \circ \phi^{-1}(x) - cx^2$ is strongly convex on $\phi(I)$.

Proof. We have f is strongly $(\mathcal{M}_\phi, \mathcal{M}_\psi)$ -convex with modulus c if and only if $\psi \circ f \circ \phi^{-1}$ is strongly convex with modulus c on $\phi(I)$. This achievement together with Lemma 3 yield $f : I \rightarrow J$ is strongly $(\mathcal{M}_\phi, \mathcal{M}_\psi)$ -convex with modulus c if and only if $g(x) := \psi \circ f \circ \phi^{-1}(x) - cx^2$ is convex on $\phi(I)$. \square

3. FEJÉR TYPE INEQUALITIES FOR STRONGLY $(\mathcal{M}_\phi, \mathcal{M}_\psi)$ -CONVEX FUNCTIONS

Throughout this paper, we assume that $f : I \rightarrow J$ is a strongly $(\mathcal{M}_\phi, \mathcal{M}_\psi)$ -convex function with modulus c ($c > 0$); $a, b \in I$, $a < b$; $\alpha \in (0, 1)$; $w_1, w_2 : [0, 1] \rightarrow [0, \infty)$ are integrable functions and satisfy the condition $\int_0^s w_1(t)dt > 0$ for all $s \in (0, 1]$, and $\int_s^1 w_2(t)dt > 0$ for all $s \in [0, 1)$. Denote

$$\mathcal{L}(t) = \mathcal{M}_\phi(a, \mathcal{M}_\phi(a, b; \alpha); t)$$

and

$$\mathcal{R}(t) = \mathcal{M}_\phi(b, \mathcal{M}_\phi(a, b; \alpha); t)$$

for $t \in [0, 1]$.

Theorem 5. Let $\mathcal{F}, \mathcal{G} : [0, 1] \rightarrow \mathbb{R}$ be two functions defined as

$$\mathcal{F}(t) = \psi^{-1} \left(\alpha(\psi \circ f \circ \mathcal{L}(t) - c[\phi \circ \mathcal{L}(t)]^2) + (1 - \alpha)(\psi \circ f \circ \mathcal{R}(t) - c[\phi \circ \mathcal{R}(t)]^2) \right)$$

and

$$\mathcal{G}(t) = t\mathcal{F}(1) + (1 - t)\mathcal{F}(0).$$

Then,

- (1) \mathcal{F} and \mathcal{G} are \mathcal{M}_ψ -convex, increasing on $[0, 1]$ and

$$\begin{aligned} \mathcal{F}(0) &= \mathcal{G}(0) \\ \mathcal{F}(t) &\leq \mathcal{G}(t), \quad t \in [0, 1], \\ \mathcal{F}(1) &= \mathcal{G}(1). \end{aligned} \tag{8}$$

- (2) For $s \in (0, 1]$, let

$$\mathcal{I}_1(s) = \psi^{-1} \left(\frac{\int_0^s \psi \circ \mathcal{F}(t)w_1(t)dt}{\int_0^s w_1(t)dt} \right)$$

and

$$\beta_1(s) = \frac{\int_0^s tw_1(t)dt}{\int_0^s w_1(t)dt}.$$

Then, $\mathcal{F} \circ \beta_1$, \mathcal{I}_1 and $\mathcal{G} \circ \beta_1$ are increasing on $(0, 1]$ and satisfy

$$\lim_{s \rightarrow 0^+} \mathcal{F} \circ \beta_1(s) = \lim_{s \rightarrow 0^+} \mathcal{I}_1(s) = \lim_{s \rightarrow 0^+} \mathcal{G} \circ \beta_1(s) = \mathcal{G}(0),$$

$$\mathcal{F} \circ \beta_1(s) \leq \mathcal{I}_1(s) \leq \mathcal{G} \circ \beta_1(s), \quad s \in (0, 1]. \tag{9}$$

- (3) Similarly, for $s \in [0, 1)$, we define

$$\mathcal{I}_2(s) = \psi^{-1} \left(\frac{\int_s^1 \psi \circ \mathcal{F}(t)w_2(t)dt}{\int_s^1 w_2(t)dt} \right)$$

and

$$\beta_2(s) = \frac{\int_s^1 tw_2(t)dt}{\int_s^1 w_2(t)dt}.$$

Then, $\mathcal{F} \circ \beta_2$, \mathcal{I}_2 and $\mathcal{G} \circ \beta_2$ are increasing on $[0, 1)$ and satisfy

$$\mathcal{F} \circ \beta_2(s) \leq \mathcal{I}_2(s) \leq \mathcal{G} \circ \beta_2(s), \quad s \in [0, 1), \tag{10}$$

$$\lim_{s \rightarrow 1^-} \mathcal{F} \circ \beta_2(s) = \lim_{s \rightarrow 1^-} \mathcal{I}_2(s) = \lim_{s \rightarrow 1^-} \mathcal{G} \circ \beta_2(s) = \mathcal{G}(1).$$

Moreover, if $w_1 = w_2$ then $\mathcal{I}_1(1) = \mathcal{I}_2(0)$.

In order to prove Theorem 5, we need to introduce the following auxiliary result.

Lemma 6. ⁵ Let $P : [0, 1] \rightarrow \mathbb{R}$ be increasing and continuous.

- (1) For $s \in (0, 1]$, define

$$P_1(s) = \frac{\int_0^s P(t)w_1(t)dt}{\int_0^s w_1(t)dt}.$$

Then, P_1 is increasing on $(0, 1]$ and

$$\lim_{s \rightarrow 0^+} P_1(s) = P(0) \leq P_1(s) \leq P(s), \quad s \in (0, 1].$$

(2) Similarly, for $s \in [0, 1)$, define

$$P_2(s) = \frac{\int_s^1 P(t)w_2(t)dt}{\int_s^1 w_2(t)dt}.$$

Then, P_2 is increasing on $[0, 1)$ and

$$P(s) \leq P_2(s) \leq P(1) = \lim_{s \rightarrow 1^-} P_2(s), \quad s \in [0, 1).$$

We are now in a position to provide the proof of Theorem 5.

Proof of Theorem 5. Since ψ is strictly monotone, we consider two possible cases of ψ : strictly increasing and strictly decreasing.

First, suppose that ψ is strictly increasing on J . Since ψ is continuous on J , the function ψ^{-1} is continuous and strictly increasing on $\psi(J)$.

1. In order to prove that \mathcal{F} is \mathcal{M}_ψ -convex on $[0, 1]$, it suffices to show that $\psi \circ \mathcal{F}$ is convex on $[0, 1]$. Indeed,

$$\begin{aligned} \psi \circ \mathcal{F}(t) &= \alpha (\psi \circ f \circ \phi^{-1}(A(t)) - c(A(t))^2) \\ &\quad + (1 - \alpha) (\psi \circ f \circ \phi^{-1}(B(t)) - c(B(t))^2), \end{aligned}$$

where

$$A(t) = t\phi(a) + (1 - t)(\alpha\phi(a) + (1 - \alpha)\phi(b)) \quad (11)$$

and

$$B(t) = t\phi(b) + (1 - t)(\alpha\phi(a) + (1 - \alpha)\phi(b)). \quad (12)$$

By Lemma 4, $\psi \circ f \circ \phi^{-1}(x) - cx^2$ is convex on $\phi([a, b])$. Moreover, since $A(t)$ and $B(t)$ are linear on $[0, 1]$, the function $\psi \circ \mathcal{F}$ is convex on $[0, 1]$. The \mathcal{M}_ψ -convexity of \mathcal{G} on $[0, 1]$ immediately follows from the definition of \mathcal{G} .

By simple computations, one can verify that

$$\begin{aligned} \mathcal{F}(0) &= \mathcal{G}(0) \\ &= \psi^{-1} \left(\psi \circ f(\mathcal{M}_\phi(a, b; \alpha)) \right. \\ &\quad \left. - c(\alpha\phi(a) + (1 - \alpha)\phi(b))^2 \right) \end{aligned} \quad (13)$$

and

$$\begin{aligned} \mathcal{F}(1) &= \mathcal{G}(1) \\ &= \psi^{-1} \left(\alpha\psi \circ f(a) + (1 - \alpha)\psi \circ f(b) \right. \\ &\quad \left. - c(\alpha\phi^2(a) + (1 - \alpha)\phi^2(b)) \right). \end{aligned} \quad (14)$$

Now, due to the convexity of $\psi \circ f \circ \phi^{-1}(x) - cx^2$, one gets

$$\begin{aligned} &\psi \circ f \circ \phi^{-1}(A(t)) - c(A(t))^2 \\ &\leq t(\psi \circ f(a) - c(\phi(a))^2) \\ &\quad + (1 - t)(\psi \circ f(\mathcal{M}_\phi(a, b; \alpha)) \\ &\quad - c(\alpha\phi(a) + (1 - \alpha)\phi(b))^2) \end{aligned}$$

and

$$\begin{aligned} &\psi \circ f \circ \phi^{-1}(B(t)) - c(B(t))^2 \\ &\leq t(\psi \circ f(b) - c(\phi(b))^2) \\ &\quad + (1 - t)(\psi \circ f(\mathcal{M}_\phi(a, b; \alpha)) \\ &\quad - c(\alpha\phi(a) + (1 - \alpha)\phi(b))^2). \end{aligned}$$

Thus,

$$\begin{aligned} \psi \circ \mathcal{F}(t) &\leq t\psi^{-1} \left(\alpha\psi \circ f(a) + (1 - \alpha)\psi \circ f(b) \right. \\ &\quad \left. - c(\alpha\phi^2(a) + (1 - \alpha)\phi^2(b)) \right) \\ &\quad + (1 - t)\psi^{-1} \left(\psi \circ f(\mathcal{M}_\phi(a, b; \alpha)) \right. \\ &\quad \left. - c(\alpha\phi(a) + (1 - \alpha)\phi(b))^2 \right) \\ &= \psi \circ \mathcal{G}(t). \end{aligned}$$

Since ψ^{-1} is increasing on $\psi(J)$,

$$\mathcal{F}(t) \leq \mathcal{G}(t), \quad t \in [0, 1],$$

the claims (8) hold.

Next, we prove that \mathcal{F} is increasing. Suppose that $0 < t < r \leq 1$. Due to the strongly $(\mathcal{M}_\phi, \mathcal{M}_\psi)$ -convexity of f and $\alpha A(t) + (1 - \alpha)B(t) = \alpha\phi(a) + (1 - \alpha)\phi(b)$, one has

$$\begin{aligned} \psi \circ \mathcal{F}(0) &= \psi \circ f \circ \phi^{-1}(\alpha\phi(a) + (1 - \alpha)\phi(b)) \\ &\quad - c(\alpha\phi(a) + (1 - \alpha)\phi(b))^2 \\ &= \psi \circ f \circ \phi^{-1}(\alpha A(t) + (1 - \alpha)B(t)) \\ &\quad - c(\alpha A(t) + (1 - \alpha)B(t))^2 \\ &\leq \alpha (\psi \circ f \circ \phi^{-1}(A(t)) - c(A(t))^2) \\ &\quad + (1 - \alpha) (\psi \circ f \circ \phi^{-1}(B(t)) - c(B(t))^2) \\ &= \psi \circ \mathcal{F}(t). \end{aligned}$$

On the other hand, since $\psi \circ \mathcal{F}$ is convex,

$$\frac{\psi \circ \mathcal{F}(r) - \psi \circ \mathcal{F}(t)}{r - t} \geq \frac{\psi \circ \mathcal{F}(t) - \psi \circ \mathcal{F}(0)}{t - 0}.$$

Thus,

$$\frac{\psi \circ \mathcal{F}(r) - \psi \circ \mathcal{F}(t)}{r - t} \geq \frac{\psi \circ \mathcal{F}(t) - \psi \circ \mathcal{F}(0)}{t - 0} \geq 0,$$

i.e. $\psi \circ \mathcal{F}$ is increasing on $[0, 1]$. Since ψ^{-1} is increasing on $\psi(J)$, \mathcal{F} is increasing on $[0, 1]$. Since

$$\psi \circ \mathcal{G}(t) = t[\mathcal{F}(1) - \mathcal{F}(0)] + \mathcal{F}(0)$$

and

$$\mathcal{F}(1) - \mathcal{F}(0) \geq 0,$$

one gets $\psi \circ \mathcal{G}$ is increasing on $[0, 1]$ and then \mathcal{G} is increasing on $[0, 1]$.

2. Applying Lemma 6 where $P = \psi \circ \mathcal{F}$, the function $\psi \circ \mathcal{I}_1$ is increasing on $(0, 1]$ and

$$\lim_{s \rightarrow 0^+} \psi \circ \mathcal{I}_1(s) = \psi \circ \mathcal{F}(0).$$

Since ψ^{-1} is strictly increasing and it is continuous on $\psi(J)$, the function \mathcal{I}_1 is increasing on $(0, 1]$ and

$$\lim_{s \rightarrow 0^+} \mathcal{I}_1(s) = \psi \circ \mathcal{F}(0).$$

Also, due to Lemma 6, the function β_1 is increasing on $(0, 1]$ and

$$\lim_{s \rightarrow 0^+} \beta_1(s) = 0 \leq \beta_1(s) \leq s, \quad s \in (0, 1].$$

Therefore, $\mathcal{F} \circ \beta_1$ and $\mathcal{G} \circ \beta_1$ are well-defined, increasing on $(0, 1]$ and

$$\lim_{s \rightarrow 0^+} \mathcal{F} \circ \beta_1(s) = \lim_{s \rightarrow 0^+} \mathcal{G} \circ \beta_1(s) = \mathcal{G}(0).$$

Next, we prove the inequalities in (9). Let us fix $s \in (0, 1]$. Applying Jensen's inequality⁷ to the convex function $\psi \circ \mathcal{F}$ on the interval $[0, s]$, we obtain

$$\psi \circ \mathcal{F} \left(\frac{\int_0^s t w_1(t) dt}{\int_0^s w_1(t) dt} \right) \leq \frac{\int_0^s \psi \circ \mathcal{F}(t) w_1(t) dt}{\int_0^s w_1(t) dt}.$$

It follows

$$\mathcal{F} \circ \beta_1(s) \leq \mathcal{I}_1(s).$$

Since $\mathcal{F}(t) \leq \mathcal{G}(t)$, $t \in [0, 1]$, we have

$$\begin{aligned} \frac{\int_0^s \psi \circ \mathcal{F}(t) w_1(t) dt}{\int_0^s w_1(t) dt} &\leq \frac{\int_0^s \psi \circ \mathcal{G}(t) w_1(t) dt}{\int_0^s w_1(t) dt} \\ &= \psi \circ \mathcal{G} \circ \beta_1(s). \end{aligned}$$

Since ψ^{-1} is increasing, one gets

$$\mathcal{I}_1(s) \leq \mathcal{G} \circ \beta_1(s).$$

3. Applying Lemma 6 with $P = \psi \circ \mathcal{F}$, we have that the function $\psi \circ \mathcal{I}_2$ is increasing on $[0, 1]$ and

$$\lim_{s \rightarrow 1^-} \psi \circ \mathcal{I}_2(s) = \psi \circ \mathcal{F}(1).$$

Since ψ^{-1} is strictly increasing and continuous on $\psi(J)$, \mathcal{I}_2 is increasing on $[0, 1]$ and

$$\lim_{s \rightarrow 1^-} \mathcal{I}_2(s) = \mathcal{F}(1).$$

Due to Lemma 6, β_2 is increasing $[0, 1]$ and

$$\lim_{s \rightarrow 1^-} \beta_2(s) = 1 \geq \beta_2(s) \geq s, \quad s \in [0, 1].$$

Thus, $\mathcal{F} \circ \beta_2$ and $\mathcal{G} \circ \beta_2$ is well-defined, increasing on $[0, 1]$ and

$$\lim_{s \rightarrow 1^-} \mathcal{F} \circ \beta_2(s) = \lim_{s \rightarrow 1^-} \mathcal{G} \circ \beta_2(s) = \mathcal{G}(1).$$

Now, we prove the inequalities (10). Fixing $s \in [0, 1]$ and applying Jensen's inequality⁷ to convex function $\psi \circ \mathcal{F}$ on $[s, 1]$, we obtain

$$\psi \circ \mathcal{F} \left(\frac{\int_s^1 t w_2(t) dt}{\int_s^1 w_2(t) dt} \right) \leq \frac{\int_s^1 \psi \circ \mathcal{F}(t) w_2(t) dt}{\int_s^1 w_2(t) dt}$$

and hence

$$\mathcal{F} \circ \beta_2(s) \leq \mathcal{I}_2(s).$$

Since $\mathcal{F}(t) \leq \mathcal{G}(t)$, $t \in [0, 1]$, it implies that

$$\begin{aligned} \frac{\int_s^1 \psi \circ \mathcal{F}(t) w_2(t) dt}{\int_s^1 w_2(t) dt} &\leq \frac{\int_s^1 \psi \circ \mathcal{G}(t) w_2(t) dt}{\int_s^1 w_2(t) dt} \\ &= \psi \circ \mathcal{G} \circ \beta_2(s). \end{aligned}$$

Since ψ^{-1} is increasing, one has

$$\mathcal{I}_2(s) \leq \mathcal{G} \circ \beta_2(s).$$

Moreover, if $w_1 = w_2$, due to the definitions of \mathcal{I}_1 and \mathcal{I}_2 , one gets $\mathcal{I}_1(1) = \mathcal{I}_2(0)$.

The proof is similar for the case that ψ is decreasing. □

Note that Theorem 5 is not only a consequence of strong $(\mathcal{M}_\phi, \mathcal{M}_\psi)$ -convexity, but it is also a characterization of strongly $(\mathcal{M}_\phi, \mathcal{M}_\psi)$ -convex continuous functions with modulus c .

Corollary 7. *Let $f : I \rightarrow J$ be a continuous function. The following statements are equivalent:*

- (1) f is a strongly $(\mathcal{M}_\phi, \mathcal{M}_\psi)$ -convex function with modulus c .
- (2) \mathcal{F} is increasing on $[0, 1]$ for all $a, b \in I, a < b$ and $\alpha = 1/2$.
- (3) \mathcal{I}_1 is increasing on $(0, 1]$ for all $a, b \in I, a < b, \alpha = 1/2$ and $w_1 = 1$.
- (4) For all $a, b \in I$ and $a < b$, we have

$$\begin{aligned} \psi \circ f(\mathcal{M}_\phi(a, b; \alpha)) - c(\alpha\phi(a) + (1 - \alpha)\phi(b))^2 \\ \leq \frac{1}{\phi(b) - \phi(a)} \int_a^b (\psi \circ f(x) - c\phi^2(x)) d\phi(x). \end{aligned}$$

- (5) \mathcal{I}_2 is increasing on $[0, 1]$ for all $a, b \in I, a < b, \alpha = 1/2$ and $w_2 = 1$.
- (6) For all $a, b \in I$ and $a < b$, we have

$$\begin{aligned} \frac{1}{\phi(b) - \phi(a)} \int_a^b (\psi \circ f(x) - c\phi^2(x)) d\phi(x) \\ \leq \alpha\psi \circ f(a) + (1 - \alpha)\psi \circ f(b) \\ - c(\alpha\phi^2(a) + (1 - \alpha)\phi^2(b)). \end{aligned}$$

- (7) \mathcal{G} is increasing on $[0, 1]$ for all $a, b \in I, a < b$ and $\alpha = 1/2$.

In order to prove Corollary 7, we need the following lemma.

Lemma 8 ⁽⁹⁾ Theorem 6). Let $I \subset \mathbb{R}$ be an interval and $f : I \rightarrow \mathbb{R}$ is a continuous function. Then, the following statements are equivalent.

- (1) f is strongly convex with modulus c .
- (2) For all $x, y \in I, x < y$, we have

$$f\left(\frac{x+y}{2}\right) + \frac{c}{12}(y-x)^2 \leq \frac{1}{y-x} \int_x^y f(t)dt.$$

- (3) For all $x, y \in I, x < y$, we have

$$\frac{1}{y-x} \int_x^y f(t)dt \leq \frac{f(x)+f(y)}{2} - \frac{c}{6}(y-x)^2.$$

Proof of Corollary 7. Due to Theorem 5, the implications (1) \Rightarrow (2) \Rightarrow (3) \Rightarrow (4), (1) \Rightarrow (5) \Rightarrow (6) và (1) \Rightarrow (7) hold. For the rest of proof, we prove the implications (4) \Rightarrow (1), (6) \Rightarrow (1) and (7) \Rightarrow (1). Without loss of generality, we assume that ψ is increasing. We need to prove that $\psi \circ f \circ \phi^{-1}$ is strongly convex on $\phi(I)$ provided that one of conditions (4), (6) và (7) holds. Since ϕ is continuous and strictly monotone on I , ϕ^{-1} is continuous and strictly monotone on $\phi(I)$. Now, the continuity of ψ, f and ϕ^{-1} imply that $\psi \circ f \circ \phi^{-1}$ is continuous on $\phi(I)$. Clearly, (7) implies that $\psi \circ f \circ \phi^{-1}$ is strongly midconvex on $\phi(I)$. Thus, $\psi \circ f \circ \phi^{-1}$ is strongly convex on $\phi(I)$. Finally, due to Corollary 8, if one of conditions (4) and (6) holds for the continuous function $\psi \circ f \circ \phi^{-1}$ on $\phi(I)$ then $\psi \circ f \circ \phi^{-1}$ is strongly convex on $\phi(I)$. \square

As a result of Theorem 5, one can derive new Fejér type inequalities for strongly $(\mathcal{M}_\phi, \mathcal{M}_\psi)$ -convex functions with modulus c by different choices of w_1 and w_2 . For examples, we take

$$w_j(t) = (1-\alpha)g_j \circ \mathcal{L}(t) + \alpha g_j \circ \mathcal{R}(t), \quad t \in [0, 1],$$

where $g_j : [a, b] \rightarrow [0, \infty)$, for $j = 1, 2$, is chosen such that

$$\frac{1-\alpha}{\alpha}g_1 \circ \mathcal{L}(t) = \frac{\alpha}{1-\alpha}g_1 \circ \mathcal{R}(t), \quad t \in [0, s] \quad (15)$$

and

$$\frac{1-\alpha}{\alpha}g_2 \circ \mathcal{L}(t) = \frac{\alpha}{1-\alpha}g_2 \circ \mathcal{R}(t), \quad t \in [s, 1]. \quad (16)$$

Note that for $\alpha = 1/2$ and $\phi(x) = x$, the assumptions (15) and (16) hold if g_1 and g_2 are symmetric about $(a+b)/2$.

Due to (15) and $\mathcal{L}(0) = \mathcal{R}(0)$, one can verify that

$$\begin{aligned} \int_0^s w_1(t)dt &= (1-\alpha) \int_0^s g_1 \circ \mathcal{L}(t)dt + \alpha \int_0^s g_1 \circ \mathcal{R}(t)dt \\ &= \frac{1}{\phi(b)-\phi(a)} \int_{\mathcal{L}(s)}^{\mathcal{R}(s)} g_1(x)d\phi(x) \end{aligned}$$

and

$$\begin{aligned} &\int_0^s \psi \circ \mathcal{F}(t)w_1(t)dt \\ &= (1-\alpha) \int_0^s (\psi \circ f \circ \mathcal{L}(t) - c[\phi \circ \mathcal{L}(t)]^2) g_1 \circ \mathcal{L}(t)dt \\ &\quad + \alpha \int_0^s (\psi \circ f \circ \mathcal{R}(t) - c[\phi \circ \mathcal{R}(t)]^2) g_1 \circ \mathcal{R}(t)dt \\ &= \frac{1}{\phi(b)-\phi(a)} \int_{\mathcal{L}(s)}^{\mathcal{R}(s)} (\psi \circ f(x) - c\phi^2(x)) g_1(x)d\phi(x) \end{aligned}$$

and hence

$$\mathcal{I}_1(s) = \psi^{-1} \left(\frac{\int_{\mathcal{L}(s)}^{\mathcal{R}(s)} (\psi \circ f(x) - c\phi^2(x)) g_1(x)d\phi(x)}{\int_{\mathcal{L}(s)}^{\mathcal{R}(s)} g_1(x)d\phi(x)} \right).$$

Similarly, since (16), $\mathcal{L}(1) = a$ and $\mathcal{R}(1) = b$,

$$\begin{aligned} \mathcal{I}_2(s) &= \psi^{-1} \left(\frac{\int_a^{\mathcal{L}(s)} (\psi \circ f(x) - c\phi^2(x)) g_2(x)d\phi(x)}{\int_a^{\mathcal{L}(s)} g_2(x)d\phi(x) + \int_{\mathcal{R}(s)}^b g_2(x)d\phi(x)} \right. \\ &\quad \left. + \frac{\int_{\mathcal{R}(s)}^b (\psi \circ f(x) - c\phi^2(x)) g_2(x)d\phi(x)}{\int_a^{\mathcal{L}(s)} g_2(x)d\phi(x) + \int_{\mathcal{R}(s)}^b g_2(x)d\phi(x)} \right). \end{aligned}$$

Together with Theorem 5, we obtain the following result.

Corollary 9. Let $g_1, g_2 : [a, b] \rightarrow [0, \infty)$ be integrable functions, where $\int_0^s g_1 \circ \mathcal{L}(t)dt > 0$ for all $s \in (0, 1)$ and $\int_s^1 g_2 \circ \mathcal{R}(t)dt > 0$ for all $s \in [0, 1)$ and satisfy (15), (16). Then,

- (i) For all $s \in (0, 1)$, we have

$$\begin{aligned} &\psi^{-1} \left(\psi \circ f(\mathcal{M}_\phi(a, b; \alpha)) - c(\alpha\phi(a) + (1-\alpha)\phi(b))^2 \right) \\ &\leq \mathcal{F} \left(\frac{\int_0^s t g_1 \circ \mathcal{L}(t)dt}{\int_0^s g_1 \circ \mathcal{L}(t)dt} \right) \\ &\leq \psi^{-1} \left(\frac{\int_{\mathcal{L}(s)}^{\mathcal{R}(s)} (\psi \circ f(x) - c\phi^2(x)) g_1(x)d\phi(x)}{\int_{\mathcal{L}(s)}^{\mathcal{R}(s)} g_1(x)d\phi(x)} \right) \\ &\leq \mathcal{G} \left(\frac{\int_0^s t g_1 \circ \mathcal{L}(t)dt}{\int_0^s g_1 \circ \mathcal{L}(t)dt} \right) \\ &\leq \psi^{-1} \left(\alpha\psi \circ f(a) + (1-\alpha)\psi \circ f(b) \right. \\ &\quad \left. - c(\alpha\phi^2(a) + (1-\alpha)\phi^2(b)) \right). \end{aligned} \quad (17)$$

(ii) For all $s \in [0, 1]$, we have

$$\begin{aligned} & \psi^{-1} \left(\psi \circ f(\mathcal{M}_\phi(a, b; \alpha)) - c(\alpha\phi(a) + (1 - \alpha)\phi(b))^2 \right) \\ & \mathcal{F} \left(\frac{\int_s^1 t g_2 \circ \mathcal{L}(t) dt}{\int_s^1 g_2 \circ \mathcal{L}(t) dt} \right) \\ & = \psi^{-1} \left(\frac{\int_a^{\mathcal{L}(s)} (\psi \circ f(x) - c\phi^2(x)) g_2(x) d\phi(x)}{\int_a^{\mathcal{L}(s)} g_2(x) d\phi(x) + \int_{\mathcal{R}(s)}^b g_2(x) d\phi(x)} \right. \\ & \quad \left. + \frac{\int_{\mathcal{R}(s)}^b (\psi \circ f(x) - c\phi^2(x)) g_2(x) d\phi(x)}{\int_a^{\mathcal{L}(s)} g_2(x) d\phi(x) + \int_{\mathcal{R}(s)}^b g_2(x) d\phi(x)} \right) \\ & \leq \mathcal{G} \left(\frac{\int_s^1 t g_2 \circ \mathcal{L}(t) dt}{\int_s^1 g_2 \circ \mathcal{L}(t) dt} \right) \\ & \leq \psi^{-1} \left(\alpha\psi \circ f(a) + (1 - \alpha)\psi \circ f(b) \right. \\ & \quad \left. - c(\alpha\phi^2(a) + (1 - \alpha)\phi^2(b)) \right). \end{aligned} \tag{18}$$

Remark 10. Corollary 9 actually generalizes some Hermite-Hadamard type inequalities that was recently established for strongly convex functions and generalized ones. We can list as below.

1. For $\alpha = 1/2$ and $\psi(x) = \phi(x) = x$, due to (17) we obtain an inequality that is sharper than Fejér (5) type inequality established by Azocar et al.¹⁰ Theorem 5 for strongly convex functions.
2. Let $\alpha = 1/2$, $g_1 = 1$ and $\psi(x) = \phi(x) = x$. Then, the inequality (17) implies

$$\begin{aligned} & f\left(\frac{a+b}{2}\right) + \frac{c}{12}(b-a)^2 \\ & \leq \frac{f\left(\frac{5a+3b}{8}\right) + f\left(\frac{3a+5b}{8}\right)}{2} + \frac{13c}{192}(b-a)^2 \\ & \leq \frac{2}{b-a} \int_{\frac{a+3b}{4}}^{\frac{3a+b}{4}} f(x) dx + \frac{c}{16}(b-a)^2 \\ & \leq \frac{f\left(\frac{3a+b}{4}\right) + f\left(\frac{a+3b}{4}\right)}{2} + \frac{c}{48}(b-a)^2 \\ & \leq \frac{1}{b-a} \int_a^b f(x) dx \\ & \leq \frac{1}{2} \left[\frac{f(a) + f(b)}{2} + f\left(\frac{a+b}{2}\right) \right] - \frac{c}{24}(b-a)^2 \\ & \leq \frac{f(a) + f(b)}{2} - \frac{c}{6}(b-a)^2, \end{aligned}$$

where $f : [a, b] \rightarrow \mathbb{R}$ is strongly convex with modulus c . This is a refinement of inequality (4).

3. Let $\alpha = 1/2$, $g_1 = 1$ and $\phi(x) = 1/x$, $\psi(x) = x$. Then, (17) reduces to the following inequality.¹¹

$$\begin{aligned} & f\left(\frac{2ab}{a+b}\right) + \frac{c}{12}\left(\frac{b-a}{ab}\right)^2 \\ & \leq \frac{f\left(\frac{8ab}{5a+3b}\right) + f\left(\frac{8ab}{3a+5b}\right)}{2} + \frac{13c}{192}\left(\frac{b-a}{ab}\right)^2 \\ & \leq \frac{(3a+b)(a+3b)}{8(b-a)} \int_{\frac{3a+b}{4}}^{\frac{a+3b}{4}} \frac{f(x)}{x^2} dx + \frac{c}{16}\left(\frac{b-a}{ab}\right)^2 \\ & \leq \frac{f\left(\frac{4ab}{a+3b}\right) + f\left(\frac{4ab}{3a+b}\right)}{2} + \frac{c}{48}\left(\frac{b-a}{ab}\right)^2 \\ & \leq \frac{ab}{b-a} \int_a^b \frac{f(x)}{x^2} dx \\ & \leq \frac{1}{2} \left(f\left(\frac{2ab}{a+b}\right) + \frac{f(a) + f(b)}{2} \right) - \frac{c}{24}\left(\frac{b-a}{ab}\right)^2 \\ & \leq \frac{f(a) + f(b)}{2} - \frac{c}{6}\left(\frac{b-a}{ab}\right)^2. \end{aligned}$$

The above inequality is a refinement of the inequality in¹¹ that was established by Noor et al. for strongly harmonic convex functions with modulus c .

4. Due to (17), we obtain a refinement of Hermite-Hadamard inequality for strongly log-convex functions¹² if $\alpha = \frac{1}{2}$, $g_1 = 1$ and $\phi(x) = x$, $\psi(x) = \ln x$:

$$\begin{aligned} & \exp\left(\ln f\left(\frac{a+b}{2}\right) + \frac{c}{12}(b-a)^2\right) \\ & \leq \exp\left(\frac{\ln f\left(\frac{5a+3b}{8}\right) + \ln f\left(\frac{3a+5b}{8}\right)}{2} + \frac{13c}{192}(b-a)^2\right) \\ & \leq \exp\left(\frac{2}{b-a} \int_{\frac{3a+b}{4}}^{\frac{a+3b}{4}} \ln f(x) dx + \frac{c}{16}(b-a)^2\right) \\ & \leq \exp\left(\frac{\ln f\left(\frac{3a+b}{4}\right) + \ln f\left(\frac{a+3b}{4}\right)}{2} + \frac{c}{48}(b-a)^2\right) \\ & \leq \exp\left(\frac{1}{b-a} \int_a^b \ln f(x) dx\right) \\ & \leq 1/2 \exp\left(\ln f\left(\frac{a+b}{2}\right) + \frac{c}{12}(b-a)^2\right) \\ & \quad + 1/2 \exp\left(\frac{\ln f(a) + \ln f(b)}{2} - \frac{c}{6}(b-a)^2\right) \\ & \leq \exp\left(\frac{\ln f(a) + \ln f(b)}{2} - \frac{c}{6}(b-a)^2\right). \end{aligned}$$

4. CONCLUSIONS

In the paper, we studied a class of generalized convex functions, which are defined according to a pair of quasi-arithmetic means, called $(\mathcal{M}_\phi, \mathcal{M}_\psi)$ -convex functions, and derived various Fejér type inequalities. These not merely provide a natural and intrinsic characterization of the $(\mathcal{M}_\phi, \mathcal{M}_\psi)$ -convex

functions, but actually offer generalizations and refinements of some Hermite-Hadamard and Fejér type inequalities obtained in earlier studies for different kinds of strong convexity.

REFERENCES

1. C. Hermite. Sur deux limites d'une intégrale dé finie, *Mathesis*, **1883**, 3, 82.
2. J. Hadamard. Étude sur les propriétés des fonctions entières et en particulier d'une fonction considérée par Riemann, *Journal des Mathématiques Pures et Appliquées*, **1893**, 58, 171-215.
3. L. Fejér. Über die Fourierreihen II, *Math. Naturwiss. Anz. Ungar. Akad. Wiss.*, **1906**, 24, 369-390.
4. S. S. Dragomir, C. E. M. Pearce. *Selected Topics on Hermite-Hadamard Inequalities and Applications*, RGMIA Monographs, Victoria University, 2002.
5. D. T. Duc, N. N. Hue, N. D. V. Nhan, V. K. Tuan. Convexity according to a pair of quasi-arithmetic means and inequalities, *Journal of Mathematical Analysis and Applications*, **2020**, 488, 124059.
6. C. P. Niculescu, L. E. Persson. *Convex Functions and their applications. A contemporary approach*, Springer, New York, 2006.
7. J. E. Pečarić, F. Proschan, Y. C. Tong. *Convex functions, partial orderings and statistical applications*, Academic Press, Boston, 1992.
8. B. T. Poljak. Existence theorems and convergence of minimizing sequences in extremum problems with restrictions, *Soviet Mathematics - Doklady*, **1966**, 7, 72-75.
9. N. Merentes, K. Nikodem. Remarks on strongly convex functions, *Aequationes Math*, **2010**, 80, 193-199.
10. A. Azocar, K. Nikodem, G. Roa. Fejér-type inequalities for strongly convex functions, *Annales Mathematicae Silesianae*, **2012**, 26, 43-54.
11. M. A. Noor, K. I. Noor, S. Iftikhar. Hermite-Hadamard inequalities for strongly harmonic convex functions, *Journal of Inequalities and Special Functions*, **2016**, 7, 99-113.
12. M. Z. Sarikaya and H. Yaldiz. On Hermite-Hadamard type inequalities for strongly log-convex functions, arXiv: 1203.2281v1 [math.FA], **2012**.
13. G. Aumann. Konvexe Funktionen und die Induktion bei Ungleichungen zwischen Mittelwerten, *Sitzungsber., Bayer. Akad. Wiss., Math.-Naturwiss. Kl.*, **1933**, 403-415.
14. M. A. Noor, K. I. Noor. Strongly log-Convex Functions, *Information Sciences Letters*, **2021**, 10, 33-38.
15. M. A. Noor and K. I. Noor. Strongly exponentially convex functions, *UPB Scientific Bulletin, Series A: Applied Mathematics And Physics*, **2019**, 81, 75-84.
16. K. Nikodem, Zs. Pales. Characterizations of inner product spaces by strongly convex functions, *Banach Journal of Mathematical Analysis*, **2011**, 5, 83-87.
17. J. L. W. V. Jensen. Sur les fonctions convexes et les inegalités entre les valeurs moyennes, *Acta Mathematica*, **1906**, 30, 175-193.
18. A. Azócar, J. Giménez, K. Nikodem, J. L. Sanchez. On strongly midconvex functions, *Opuscula Mathematica*, **2021**, 31, 15-26.

Đánh giá tổng quan tế bào nhiên liệu vi sinh: Những tiến bộ gần đây về cơ chất

Đinh Kha Lil^{1,*}, Imee Saladaga Padillo²

¹Khoa Khoa học Tự nhiên, Trường Đại học Cần Thơ, Việt Nam

²Khoa Công nghệ, Đại học bang Eastern Visayas, Phi-líp-pin

Ngày nhận bài: 25/06/2022; Ngày nhận đăng: 18/10/2022; Ngày xuất bản: 28/10/2022

TÓM TẮT

Trong hai thập kỷ qua, pin nhiên liệu vi sinh vật (Microbial fuel cells - MFCs) đã được chú ý vì chúng có thể chuyển đổi trực tiếp năng lượng hóa học từ các hợp chất hữu cơ để tạo ra điện sinh học. Với việc sử dụng MFC, năng lượng sinh khối có thể được thu trực tiếp dưới dạng điện năng, đây là năng lượng sạch, phổ biến và tiện lợi nhất. Do đó, MFC được xem là một phương pháp đầy hứa hẹn khác để khai thác năng lượng bền vững trong sinh khối. Có nhiều cơ chất đã được nghiên cứu để sử dụng làm nguồn cấp nguyên liệu sử dụng trong MFC. Chúng bao gồm nhiều loại nước thải nhân tạo, nước thải thực và sinh khối lignocellulosic. Trong số các yếu tố ảnh hưởng đến hiệu suất của MFCs: thiết kế, vật liệu điện cực, cơ chất, màng trao đổi, vi sinh vật hoạt động điện, pH, nhiệt độ vận hành,... Cơ chất là thách thức quan trọng nhất trong công nghệ MFCs, đòi hỏi sự ổn định lâu dài. Việc sử dụng cơ chất không ổn định ảnh hưởng trực tiếp đến hiệu suất của MFC. Tương tự, ảnh hưởng của các chất lên cộng đồng vi sinh vật cũng được thảo luận. Bài tổng quan này cập nhật những tiến bộ gần đây trong việc cải tiến công nghệ MFC để tăng cường hiệu suất phát điện, đặc biệt là các cơ chất khác nhau được dùng trong MFC cho đến nay cũng như các cơ chất tiềm năng trong tương lai.

Từ khóa: Cơ chất, mật độ năng lượng, pin nhiên liệu vi sinh, xử lý nước thải.

*Tác giả liên hệ chính.

Email: lildk93@gmail.com

A review of the general microbial fuel cell: Recent advances in substrates

Dinh Kha Lil^{1,*}, Imee Saladaga Padillo²

¹College of Natural Sciences, Can Tho University, Vietnam

²College of Engineering, Eastern Visayas State University, Philippines

Received: 25/06/2022; Accepted: 18/10/2022; Published: 28/10/2022

ABSTRACT

Over the past two decades, microbial fuel cells (MFCs) have gained attention because they can directly convert chemical energy from organic compounds to bioelectricity. Using MFCs, biomass energy can be directly harvested in the form of electricity, which is the most convenient, widely available, and clean energy. Therefore, MFCs are considered to be another promising way to harness sustainable energy in biomass and add a new dimension to the biomass energy industry. Many substrates have been studied for microbial nourishment. These include a variety of artificial and natural wastewater and lignocellulosic biomass. Among factors essential for long-term stability in MFCs, the substrate is the most challenging. Studies have shown that an unstable substrate directly harms the performance of MFCs. This review discusses the effect of substrates on the microbial community. Furthermore, it provides updates on recent advances in improving MFC technology, particularly the different substrates discovered in MFCs to date, power generation efficiency, and potential substrates in the future.

Keywords: *Microbial fuel cell, substrate, wastewater treatment, power density.*

1. INTRODUCTION

Due to the unsustainable nature and harmful environmental impacts of fossil fuels, attention to renewable energy has increased.¹ Renewable energy has become an important alternative to fossil fuels since it produces useful energy without being depleted. In addition, water shortage is one of the critical global issues. According to climate change forecasts, this problem will be even more severe in the future.² The increase in water demand has led to an increase in the amount of wastewater generated. At the same time, there is an urgent need for renewable energy due to the rapid depletion of fossil fuels and growing concern about climate change.³ Many countries worldwide are looking for alternative resources

such as biomass as a more reliable, sustainable, and environmentally beneficial resource to reduce the need for fossil fuels. To date, biomass can be converted into different types of energy products such as heat, gas, fuel, and electricity.³ MFCs are a type of power generation device that uses bacteria as biological catalysts to generate electricity by oxidizing organic matter from the wastewater through respiration.⁴ It has considerable potential for applications in wastewater treatment,⁵ electrical equipment,⁶ and biosensors.⁷ Recently, reactors with a scale of several hundred liters have been designed.⁸ The move to bring this technology from the laboratory scale to the current pilot scale brought it closer to practical application.

*Corresponding author.

Email: lildk93@gmail.com

MFCs function through bacterial activities, resulting in electron production from these substrates. To produce power, these electrons are transferred from the negative anode to the positive cathode through a conductive material and a load or resistor (Figure 1).

For a system to be categorized as an MFC, its substrate must be replenished continuously or intermittently; otherwise, it is considered a bio-battery. Electron mediators or shuttles transfer electrons to the anode⁹ through electron transfers

directly associated with the membrane or through nanowires formed by bacteria,¹⁰ or possibly through some other unexplored ways. Chemical mediators, such as neutral red or anthraquinone-2,6-disulfonate can be used in MFCs to facilitate electricity generation by bacteria that cannot use the electrode without aid.¹¹ Suppose the system has no added exogenous mediators. In that case, the MFC is considered “mediator-less” even if the electron transfer mechanism may be unknown.¹²

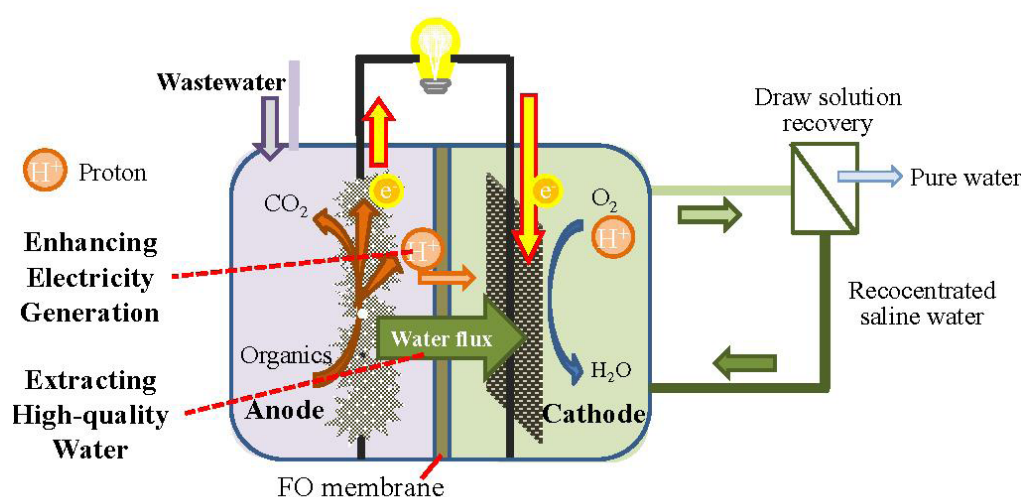


Figure 1. Structure diagram of a microbial fuel cell.¹³

Research is increasing on MFCs constructed with various materials and configurations. The operating conditions also differ in temperature, pH, electron acceptor, operating time, surface areas of electrodes, and reactor size. Studies report potentials using different reference states and occasionally only using a single resistor (load). These and sometimes the lack of essential data, such as resistance internal to the system, or power densities obtained from polarization curves using differing methods, have created a challenge in interpreting and comparing results among studies.¹⁴

MFC has been an interesting topic for more than 20 years now not only because of its electricity generation but also because it is an environmentally friendly wastewater treatment technology.¹⁵ Many types of wastewater today

contain various toxic wastes, making them expensive to treat before being discharged into the environment. Previous studies have demonstrated the ability of MFCs to treat contaminated wastewater containing metals, food, and urine, even producing drinking water post-treatment.¹⁶⁻¹⁷ MFCs have coexisted with biological filter tanks in wastewater treatment to enhance pollution control and improve treatment capacity.¹⁸ Most treatment methods aim to remove organic compounds that reduce chemical oxygen demand (COD), azo dyes,¹⁹ and heavy metal waste.²⁰ The aeration system in wastewater treatment is reported to consume more than 54% of the electricity required in the treatment process, while the MFCs use anaerobic bacteria for the wastewater treatment process, which indicates a potential for energy saving of

MFCs.¹⁹ In addition, MFCs used as biosensors are expected to be one of the promising applications of MFC-derived technology. Such biosensors have been studied to measure various parameters, including COD, volatile fatty acids, dissolved oxygen (DO), biochemical oxygen demand (BOD), toxic substances and microbial activity.²¹ This helps to reduce the time and cost required to measure toxicity in water.

Recent advancement in the application of power generation capabilities includes using MFCs to power a small computer (158 mW) directly and continuously without any management equipment or power source.²² The performance enhancement of MFC is accomplished through many aspects, such as electrode material and surface, electrochemically active bacteria (EAB), substrate, and load resistance.

2. DESIGN OF MFCs REACTOR

Many types of MFC designs have been researched and developed. Each design has its advantages and disadvantages and is suitable for specific uses. Various factors are considered in designing MFCs. The size, shape, and configuration of reactors widely differ and are wholly decided upon by the designer. There is no existing recommended standard design yet. The MFC's overall performance is significantly affected by reactor configurations, including the volume, oxygen supply, area of the membrane, and spacing between electrodes. Among the studied structures, double chamber H-type MFC is typically used because of its ion exchange membrane, facilitating proton diffusion and limiting the crossover of substrate and oxygen.²³ It is up to the designer to decide the project's aims and plan the design accordingly. Presently, the available reactor designs are horseshoe-shaped, cylindrical, cubed, dual- and single-chamber, and H-type. Some are made of glass, while others are made up of a variety of plastic materials.

Also, sizes range widely, with reactor volumes of a few square millimeters and others of up to a square meter, ranging from microliters to thousands of liters. The fuel cell design is an important element in the MFC/microbial electrolysis cell (MEC). Single-chamber cells have been created from a two-chamber design to eliminate the membrane.²⁴ Furthermore, single-chamber MFCs have shown promising results; however, dual-chamber is still widely studied. Dual-chamber cells are easier to construct than single-chamber reactors. A simple MFC device can either be dual- or single-chambered, based on the anode and cathode chamber assembly. Several MFC design and structure adaptations have been made from these two typical designs.¹⁶

H-shaped fuel cells commonly consist of two bottles connected by a tube containing a separator, usually a cation exchange membrane (CEM) such as Nafion,¹¹ or Ultrex,²⁵ or a plain salt bridge (Figure 2).²⁶ The vital consideration for this design is selecting a membrane that allows proton transfer between the chambers but hinders the cathode chamber's substrate or electron acceptor (usually oxygen) from crossing. Using a glass tube heated and bent to a U-shape is a cost-effective method to connect the bottles. Agar and salt are used as a CEM in the U-shaped glass tube and are inserted through the bottles' lids (Figure 2). However, it was observed that MFCs using salt bridge generates low power because of high internal resistance.

H-shaped MFC devices are generally accepted for basic parameter research. An example is testing the power produced using new materials or new microbes developing from some compound decomposition. However, this MFC type typically generates low power densities. The relative surface area of the cathode to that of anode²⁷ and the membrane surface²⁸ affect the power generation.

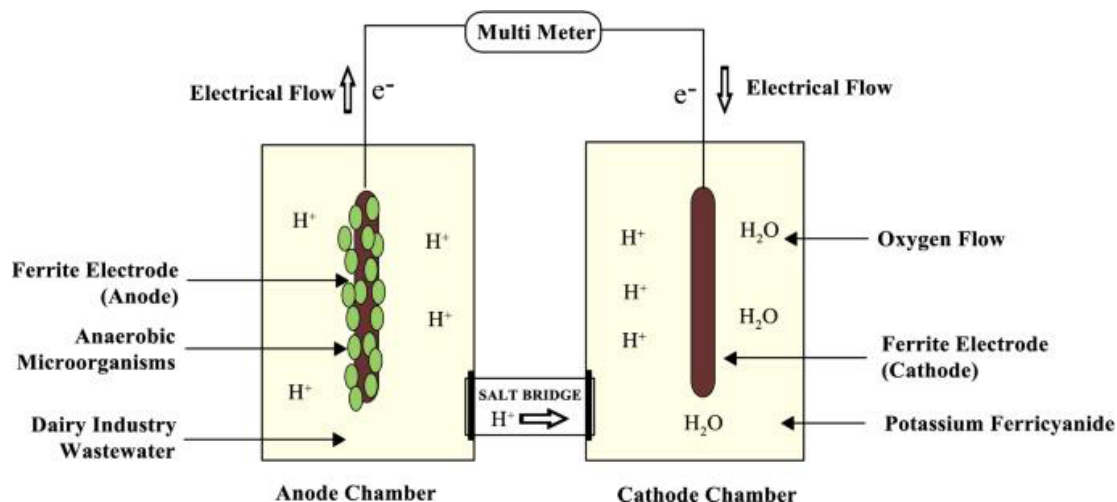


Figure 2. MFC types device with a salt bridge (pointed by arrow) which is easily assembled.²⁹

Limitations to the power densities generated in these systems are typically due to considerable internal resistance and losses from the electrodes. Therefore, to compare systems' power production, it is logical to evaluate using equally sized anodes, cathodes, and membranes.²⁸ Ferricyanide, the cathodic electron acceptor, improves power generation because of the high concentrations of electron acceptors. In an H-shaped reactor using Nafion as CEM, compared to a Pt-catalyst and dissolved oxygen in the cathode, ferricyanide increased the power produced by 1.5 to 1.8 times.²⁸ MFCs with the highest power densities and low internal resistances that have been published so far reported the use of ferricyanide in the cathode chamber.⁹ Even though this chemical is excellent

as a catholyte for system performance, it is not sustainable to use since it is not chemically regenerated. Therefore, ferricyanide use is restricted to basic laboratory research only. Several studies have also explored using cathode directly in contact with air (Figure 3A, B), either with or without a membrane.³⁰ In one study, a separator based on kaolin clay and a cathode made of graphite were connected to combine the separator and cathode structure.³¹ MFCs using air cathodes improved power densities significantly compared to MFCs with aqueous cathodes. The most straightforward configuration involves placing the anode and cathode on either side of a tube, sealing the anode against a flat plate, and exposing the cathode to air on one side and water on the other (Figure 3A).

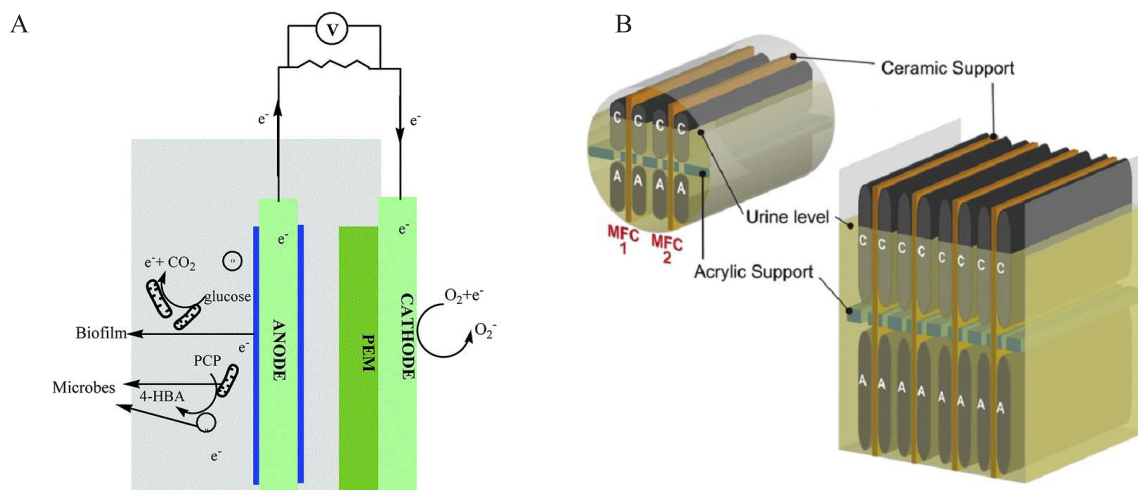
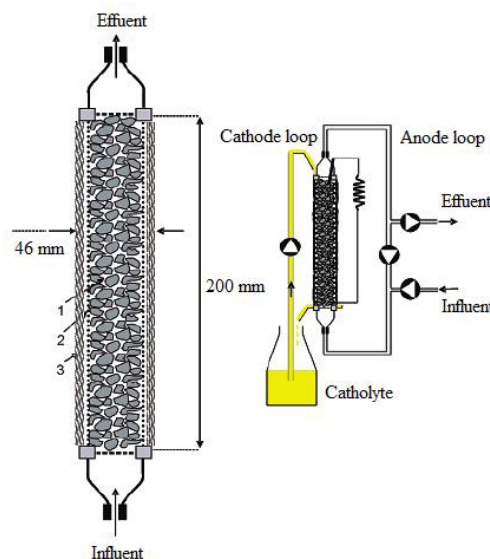


Figure 3. MFC types in studies: (A) single-chamber, simple “tube” arrangement of air-cathode³²; (B) stacked MFC, with one out of two ceramic supports removed.³³

A



B

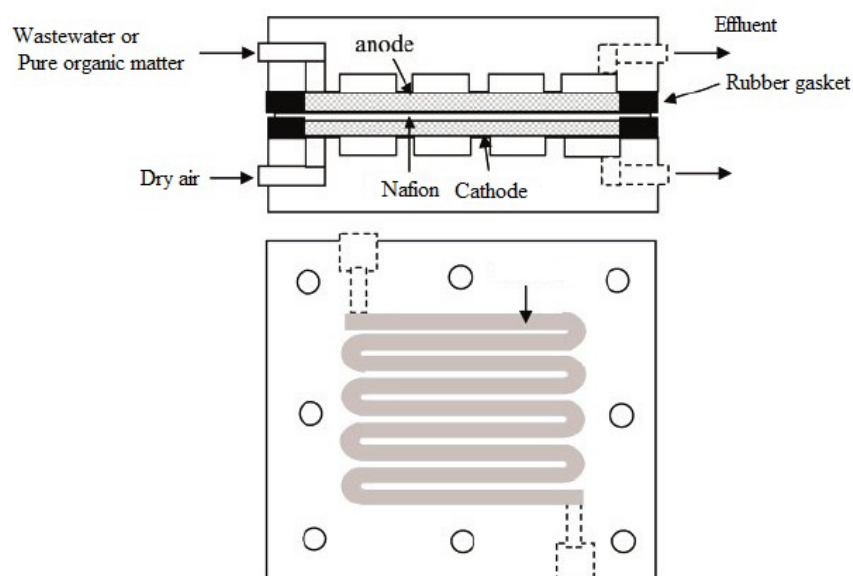


Figure 4. MFC operated continuously: (A) upward flowing, tubular type MFC with inner graphite bed anode and outer cathode;³⁴ (B) flat plate design where a serpentine pattern for fluid flow.³⁵

A membrane's purpose in an air-cathode device is to prevent water leakage through the cathode. However, it also decreases oxygen diffusion into the anode chamber. The bacterial oxygen demand in the anode chamber can lower Coulombic efficiency, which is the fraction of electrons recovered over the maximum number of electrons that can possibly be recovered.³⁰ Although hydrostatic pressure on the cathode will cause water leaks, this can be minimized

using coatings, such as polytetrafluoroethylene (PTFE), outside the cathode. These coatings allow the diffusion of oxygen but limit the bulk loss of water.³⁶

The systems mentioned so far are batch-operated devices. Several other basic designs also exist that provide continuous flow through the anode chamber. Some designs include an outer cylindrical reactor and a concentric inner cathode tube.³⁷ Some are the other way around

having an internal cylindrical anode filled with granular media and an outer cathode (Figure 4A).³⁴ Another design variation is an upward-flowing fixed-bed biofilm reactor, with fluid flowing continuously through permeable anodes to a membrane that separates the anode from the cathode chamber.³⁸ System designs resembling hydrogen fuel cells have been employed, where a CEM is placed between the cathode and anode (Figure 4B). Stacking systems as a series of flat plates or linking together in series can increase overall system voltage (Figure 3B).³³

Sediment MFCs have been developed. These are created by putting an electrode inside marine sediment abundant in sulfides and organic substances, and the other electrode is placed in the overlying oxic water. With these, electricity is produced sufficiently to provide power to some marine devices.³⁹ Graphite disks¹¹ and platinum mesh electrodes³⁹ have been used as electrodes. “Bottlebrush” cathodes have a high surface area and are corrosive-resistant. Therefore, these find applications for seawater batteries and are promising for long-term operation.⁴⁰ H-tube dual-chamber systems have also been applied to sediment MFCs to study bacterial communities.¹¹ Modifications have also been done to produce hydrogen. Using a slight external potential in the MFC, the potential produced at the anode by the bacteria was assisted, making cathodic hydrogen generation possible.⁴¹ These are called bioelectrochemical assisted microbial reactors (BEAMRs) or bio-catalyzed electrolysis systems and are not considered as real fuel cells since they are operated to generate not electricity, but hydrogen. Having a second chamber for hydrogen gas capture would make it possible to develop various designs for hydrogen generation.

3. ELECTROACTIVE BIOFILMS

Electroactive biofilms (EAB) have been identified in many natural ecosystems such as soils, sediments, seawater, or freshwater and in samples collected from a wide range of different microbially-rich environments (sewage sludge,

activated sludge, or industrial and domestic effluents). The microbes transfer the electrons to the electrode through various electron transfer mechanisms. However, the electron transfer mechanism plays a vital role in maximizing the microbe to electrode interaction and helps provide an understanding of how such systems operate in the MFC.⁴² Researchers have proposed three extracellular electron transfer (EET) mechanisms.⁴³ Depending on the mechanisms involved, the distances of EET may vary greatly, from the nanometer-scale in the case of electron transfer across the cell envelope to lengths exceeding one centimeter for cable bacteria.⁴⁴

3.1. Direct electron transfer

The first transfer mechanism uses direct electron transfer (DET) between electron carriers in the bacteria and the solid electron acceptors.⁴⁵ The mechanism is carried out by the presence of outer membrane cytochromes that can interact directly with the solid surface to carry out respiration.⁴⁶ DET can occur through direct physical contact between the cell and an electrode without the involvement of any diffusible redox compounds. This is achieved if the microbe contains redox-active proteins on the outer surface of the cell membrane or cell envelope, e.g., cytochromes,⁴⁷ flavoproteins,⁴⁸ or multi-copper proteins,⁴⁹ which allow transport of electrons between the inside of the cell and an external environment. According to studies reported so far, three different mechanisms accomplishing this type of electrical connection have been proposed⁵⁰: (i) ET through electrically conductive pili,⁵¹ (ii) ET between redox proteins bound to the outer cell surfaces,⁵² or (iii) ET through abiotic conductive materials.⁵³

3.2. Mediated electron transfer

The second transfer mechanism employs an electron shuttle between bacteria and electrodes. The mediated electron transfer (MET) has redox mediators involved in shuttling electrons between bacteria and electrodes.⁴⁶ MET takes place by the presence of redox-active mediating

compounds, which shuttle electrons between an external donor/acceptor and a microorganism. Some compounds shown to be effective electron shuttles including both inorganic and organic compounds have been identified potassium ferricyanide,⁵⁴ flavin mononucleotide,⁵⁵ neutral red,⁵⁶ phenazines, phenoxazines, phenothiazines, and quinones,⁵⁷ 9,10-anthraquinone-2,6-disulfonic acid disodium salt, safranin O, resazurin, methylene blue, and humic acids.⁵⁸ As multiple prior studies have proven that bacteria excrete various primary and secondary metabolites, which may be involved in EET as diffusible mediators.⁵⁹ Thus, these disadvantages lead to the general relinquishment of this approach. Because MET uses natural electron shuttles and DET mechanisms, it is generally established that artificial mediators are no longer significant.⁶⁰

3.3. Indirect electron transfer

The third type of mechanism is indirect electron transfer (IET), which is based on the electrochemical synthesis of a wide range of microbial electron donors and acceptors. Here, the compounds used as electron donors or acceptors undergo irreversible redox processes, creating new compounds such as hydrogen or formic acid. Additionally, electroactive (metabolic) substances can be secreted by microorganisms and transfer electrons between the microbes and electrodes.⁴⁴

4. FACTORS AFFECTING THE ACTIVITY OF MFCs

4.1. Electrode materials

An important goal of the anode chamber in the MFC is to serve as an electron receiver for the electric current generation. An effective anode material is electrically conductive, biocompatible, free from corrosion and fouling over time, inexpensive, and with a high surface area.⁶¹ The electrode materials greatly influence the performance of the MFC.⁶² Carbon materials are used as electrodes in MFC because they are non-corrosive, highly biocompatible, and

exhibit some distinctive surface characteristics of electrode materials. Modification of the electrode material has been shown to be an effective way to improve the performance of the MFC.⁶³

Many studies have shown that electrodes with nanoparticle modification are more efficient than simple electrodes. This change in the physical and chemical properties of the electrode helps the microorganism better bind and transfer electrons. The efficiency of MFC can be increased through the improvement of bacterial adhesion and electron transfer with the modification of the electrode surface.⁶⁴ The biofilm attached to the electrode is an essential element of electrochemical bioreaction.⁶⁵ The growth and development of biofilms on the MFC electrodes, especially on the anode electrode, will help organic matter oxidation and transfer electrons to the cathode.⁶⁶ The anode electrode of the MFC must contain a stable and homogeneous bioreactor for enhanced energy generation.⁶⁷

In summary, the electrode properties and the correlation between electrode, substrate, and bacteria are the main factors affecting the performance of MFC. It can be seen that the development of MFC technology is a diverse combination of specialties such as biochemistry, electrochemistry, mechanical engineering, and materials science.

4.2. Proton exchange system

In a dual-chamber design, the anode and the cathode compartments are separated by an ion-selective membrane, allowing proton transfer from the anode to the cathode and preventing oxygen diffusion in the anode chamber from the cathode compartment. The membrane in the MFCs plays an important role in MFC performance. The most commonly used materials for PEM affect the internal resistance and concentration of the polarisation loss of the system and influences the power output of the MFCs. There are several significant types of ion exchange membranes used in MFC systems: anion exchange membranes (AEM), cation

exchange membranes (CEM), and polarized membranes (PBM).⁶⁸

The bioreactor architecture, material type, and reactor geometry determine the device's performance and cost. Studies aim to find the optimal combination of materials and design that will result in high performance, low cost, and multiple functions to establish a standard for convenient and economically feasible scaling up. One such effort is using CEM such as Nafion derived from the existing technology on hydrogen PEMFC⁶⁹ or treatment systems on water using membranes.³⁸ Since Nafion is expensive, most research is concentrated on possible alternatives, including investigations on materials such as nylon and glass fibers, j-cloth, biodegradable plastic bags, and ceramics.⁶⁹ Several waste materials, such as laboratory gloves and natural rubber, have also been tested.⁷⁰ Results show that these materials offer benefits in terms of membrane fouling.

MFC operation was studied using similar metals in different solutions or different metals in similar solutions when liquid electrolytes are employed in the anode and cathode, as long as the cathode is not exposed to open air. Ions are contained in liquid solutions, which creates the need for an ion-exchange membrane. Therefore, in theory, a membrane is not a necessity for MFCs,³⁰ given that the anode and cathode are either dissimilar (electrochemically separated) or identical but placed at a distance apart to avoid short-circuit.

Membrane-less MFC was therefore developed.⁷¹ While this eliminates the need for high-cost membranes and fouling problems, the downside involves oxygen diffusion, which creates adverse competition with the anode on the available electrons. Most MFCs have been designed to have rigid, inert structural materials for housing anode and cathode half-cells, regardless of the presence of membranes. Currently, studies have emerged using 3-D

printing in the fabrication of MFCs.⁷² 3-D printing of MFC bioreactors also has the advantage of creating complete reactors. As a result, these products can be employed in various applications and environments.⁷³

The challenge of electrode spacing can be addressed by material type. Porosity, strength, chemical inertness, and longevity are the factors that may address this challenge while hindering oxygen penetration. The materials that have been studied so far are canvas,⁷¹ photocopy paper,⁷⁴ microporous filtration membranes,⁷⁵ and nylon infused membrane.⁷⁶

4.3. pH

MFCs are very susceptible to the influence of external pH on their ability to generate renewable energy and remove contaminants. When the external pH changes, many physiological changes occur, including changes in ion concentration, proton shutdown, microbial cell pH, and biofilm formation at the anode electrode. pH value plays a vital role in the growth of microorganisms, and it is necessary to consider the right pH conditions for the microorganisms to achieve maximum performance. The bacteria responsible for generating electricity in the MFC were more active at pH 6 to 8 in the anode chamber and at neutral or slightly higher pH in the cathode chamber. The activities of the bacteria decrease due to the low pH in the anolyte, which has a tremendous effect on the biofilm formation and power output of the MFC. The main effect of pH on the electrolyte influences bacterial metabolism and the cathodic oxygen reduction reaction rate.⁷⁷

4.4. Temperature

Temperature affects microbial metabolism, mass displacement, and thermodynamics, leading to an effect on MFC performance. Orellana et al.⁷⁸ reports that MFCs operate stability at the temperature range of 25°C to 30°C. MFCs operating at higher temperatures have an advantageous performance and better substrate

removal. This is because the temperature contributes to the initial biofilm formation, augmentation of the bacterial metabolism, and membrane permeability.⁷⁹ The optimum temperature for mesophilic microbes ranges from 35°C to 40°C. Warmer temperatures generally positively affect power generation, CE, and COD removal.⁸⁰ MFCs operating at higher temperatures have a performance advantage and substrate removal. This is because of the temperature contributes to the initial biofilm formation, augmentation of the bacterial metabolism, and membrane permeability.⁸¹ These results indicate that temperature plays an important role in shaping microbial communities of the anode biofilms and the cell's internal resistance in MFCs through changes in species evenness.⁸²

4.5. Substrate

The substrate is considered one of the essential biological factors related to the power efficiency in MFCs.⁸³ Organic substrates range from simple to complex, and their mixtures can be used as a nutrient source by electrically active bacteria for power generation in MFCs. Studies reported that substrates for MFCs range from simple (i.e., glucose, acetate, sucrose, etc.) to complex (i.e., amino proteins, acids, etc.).⁸⁴⁻⁸⁵ Aside from those, some wastewater such as seafood industrial wastewater,⁸⁶ petroleum recycling wastewater,⁸⁷ bamboo fermentation effluent,⁸⁸ were used as a complex substrate in MFC. In most cases, the ultimate purpose of wastewater use is to remove the pollutants present in the wastewater before releasing them into the environment. Different researchers used varying units to represent MFC performance. A unit most often used is called power density, which can signify an amount of power (time rate of energy transfer) per unit area of the anode electrode surface (mW/m^2) or the power density per volume of the cell (mW/m^3). This review discusses the most commonly used substrates with the corresponding MFC performance.

5. RESEARCH ON SUBSTRATES AND THEIR EFFECT ON MFCs PERFORMANCES

5.1. Acetate

In most of the research on MFC, acetate has been the most widely used substrate type for electricity generation. As a simple substrate, acetate is rich in carbon which electroactive microorganisms can easily metabolize. Ions are present in acetic acid that tends to prompt electroactive microbes. Notably, acetate is the final product of various metabolic pathways for higher-order carbon sources.⁸⁹ As a simple compound, acetate is easier to degrade in MFCs.⁹⁰ Liu et al.⁹¹ observed that the acetate-fed single-chamber MFC obtained a power generation of $506 \text{ mW}/\text{m}^2$, $800 \text{ mg}/\text{L}$, which was approximately 66% higher than the power produced by an MFC with butyrate ($305 \text{ mW}/\text{m}^2$, $1000 \text{ mg}/\text{L}$). Liu et al.⁸³ observed that the MFC fed by acetate substrate and acetate-acclimatized microbial consortia obtained more than twice higher power generation with half optimal external load resistance compared to MFC with protein-rich wastewater as substrate. However, a wide range of microbial community compositions was observed in the anode biofilm for the protein-enriched wastewater compared to the acetate substrate. Chae et al.⁹² evaluated the power generation of four diverse substrates where the acetate-fed MFC obtained the maximum power generation with CE of 72.3% while the other substrate-operated MFC achieved the lower power generation with butyrate (43.0%), propionate (36.0%) and glucose (15.0%). Dinh et al.⁹⁰ reported that a power density of $593.4 \text{ mW}/\text{m}^2$ was produced from acetate at the concentration of 10 mM. An MFC using a mixture of acetate and lactate substrates at 30 mM yielded a power density of $956.75 \text{ mW}/\text{m}^2$.

5.2. Glucose

Another common substrate used in MFC is glucose. The presence of glucose in wastewater sludge enhances the conductivity property of the MFC.

Generally, MFC using glucose as substrate achieves low power generation by lower electron transfer (CE) efficiency between electroactive bacteria and electrode. This is due to methanogenic and fermentative bacteria that are unrelated to electricity production in the MFC system that readily consume glucose.⁹³ Therefore, a combination of simple and complex substrates is recommended to be used in MFCs.⁹²

5.3. Synthetic wastewater

Various synthetic or chemical wastewater with known compositions have been used in MFCs as the conductivity, pH, and other parameters are easily controlled. Mohan et al.⁹⁴ operated MFCs fed with various loadings of synthetic wastewater to obtain an ideal loading rate.

A few media used during bacterial growth contain large quantities of redox mediators, including high-intensity wastewater composed of reduced species of sulfur and cysteine that can serve as an abiotic donor of electrons and improve power output for a brief period.⁹⁵ However, this does not adequately reflect the system's performance. One solution utilizes a minimum salt solution containing only one electron donor, like glucose or acetate. Sun et al.⁹⁶ used synthetic wastewater prepared fresh by dissolving glucose in tap water until the COD concentration was about 300 mg/L. The power density was 112.36 mW/m². The COD removal efficiency was about 60%, and the effluent COD was about 100 mg/L. Rodrigo et al.⁹⁷ studied the production of electricity and the oxidation of the pollutants contained in a synthetic wastewater fed with glucose and peptone of soybean as carbon sources. Waste-fed MFC that is slowly biodegradable generates higher energy. It is most likely because of the formation of intermediates that favor the production of electricity.

5.4. Brewery effluent

Brewery effluent is generally nontoxic and characterized by high COD and total nitrogen content in the presence of higher organic

contents, mainly consisting of protein and starch components.⁹⁸ Wang et al.⁹⁹ reported the power generation efficiency from brewery wastewater in the non-diaphragm MFC with a maximum power density of 483 mW/m² at 20°C. The test results show that MFC can generate electricity from high-intensity wastewater with COD concentrations ranging from 400 to 1,400 mg/L. Brewery wastewater is a preferred substrate in MFC because the strength is low and also because the organic matter is derived from food, thus resulting in low inhibitory compound concentrations, such as ammonia contained in animal wastewater.¹⁰⁰

5.5. Dye wastewater

Azo dyes are abundant in the textile and dyeing industries. The presence of high concentrations of dyes will have severe environmental effects, such as blocking the passage of oxygen and light into the water, which will seriously affect aquatic life.¹⁰¹ Therefore, removing dyes from these effluents before discharge into the environment is necessary. Some processing technology, such as physical, chemical, and electrochemical treatments, are being effectuated before discharging into the land.¹⁰² Recently, MFC technologies have converted chemical energy directly to electricity through a biological pathway.¹⁰³ Qiu et al.¹⁰⁴ used a novel combined process of constructed wetland-microbial fuel cell and three dimensional biofilm electrode reactor to treat reactive brilliant red X-3B dye wastewater. The results showed that the decolorization rate of the combination process was over 96%, and the COD removal rates ranging from 78.9% to 90.8% were achieved. Fatima et al.¹⁰⁵ designed and optimized for efficient treatment of recalcitrant textile wastewater. A maximum power density of 120 mW/m² was obtained under optimized conditions. As a result, the MFC's color removal and COD reduction were up to 81 and 58%. Consequently, treating wastewater containing azo dye and wastewater containing organic matter that is easily bio-degraded simultaneously

can be performed by combining the two different types of wastewater in MFC that can improve both cost and energy.¹⁰⁶ The downside of this is that significant development is still needed in finding a dense bacterial community suitable for dyes mixed with simple carbon sources to provide a realistic solution in the wastewater treatment of MFCs.

5.6. Lignocellulosic biomass

Lignocellulosic biomass is abundantly available in nature, mainly generated from agricultural waste, and considered a promising and cost-effective feedstock for energy production.¹⁰⁷

Due to their new availability and reproducibility, lignocellulosic compounds derived from agricultural by-products are favorable raw materials for low-cost electricity generation.¹⁰⁸ However, microorganisms in the MFC cannot use its lignocellulosic biomass for energy production. It must be broken down into monosaccharides or other reducing agents.⁸⁹

Until now, much biomass, including forest detritus in a forested wetland,¹⁰⁹ kitchen waste,¹¹⁰ chitin,¹¹¹ cow dung,¹¹² orange peel waste biomass,¹¹³ wheat straw,¹¹⁴ algae grown,¹¹⁵ rice straw,¹¹⁶ potato wastes,¹¹⁷ hydrothermal liquefied cornstalk biomass,¹¹⁸ food waste,¹¹⁹ lemon peel biomass,⁷⁹ has been exploited as fuel sources for bioenergy production in MFCs.

Dai et al.⁸⁸ used wastewater from biohydrogen fermentation as a potential substrate. The wastewater used is reported to contain end-product metabolites (acetic acid, lactic acid, and butyric acid), which constitute a rich source of substrates for bacteria. This is a type of wastewater with a stable composition, rich in nutrients and low in toxic components. Hou et al.¹¹⁰ reported that anaerobically digested kitchen waste produced a power density of 6255 mW/m³, biomass concentration which was 325 mg/L, and COD removal efficiency of 43.59% when *Golenkinia* SDEC-16 was cultivated in the single chamber MFC. Miran et al.¹¹³ demonstrated

bioelectricity production from orange peel waste without chemical pretreatment or adding extra mediators. The maximum power density was 358.8 ± 15.6 mW/m². Liu et al.¹¹⁸ has shown the continuous production of electricity from cornstalk biomass after hydrothermal liquefaction treatment. A maximum power density of 680 mW/m³. About 80% of COD and TOC were effectively removed. In the study of Li et al.,¹¹⁹ electricity recovery was achieved with efficient organic biodegradation in the MFC using canteen-based food waste as substrates. A maximum power density of 5.6 W/m³ and an average output voltage of 0.51V was obtained.

Biomass quality is often determined by its inherent properties such as moisture content, bulk density, yield, size and shape, which affect its bioconversion and ability to bioelectricity production in MFC.¹²⁰ Most of the raw biomass or biomass derived from organic waste can be used as a substrate for MFC, implying that MFC is widely adaptable for energy harvesting from biomass.

6. APPLICATIONS OF MFC

Using MFC technology is very attractive because waste can be reduced and converted into energy, reducing waste disposal costs and increasing economic efficiency. This technology has led to many important applications, such as bioelectricity production, wastewater treatment, metal removal/recovery, biohydrogen production, biosensors, etc.

6.1. Wastewater treatment with bioelectricity production

Wastewater treatment and bioelectricity generation have become MFC's most heavily researched areas. Food processing wastewater, domestic wastewater, sewage sludge, and many other types of wastewater are rich in organic matter and can provide a wide range of microorganisms used in MFC. Furthermore, wastewater containing heavy metals and other harmful pollutants has also been used as a

substrate in MFC to reduce pollution.¹²¹ They can remove COD up to 90% and Coulombic efficiency up to 80%.¹²² Mehmood et al. reported that this is an effective and highly cost-effective method to remove nitrogen and organic matter from leachate, biological treatment.¹²³ The traditional wastewater treatment methods have many limitations, such as energy consumption for the aeration of wastewater and generation of harmful emissions to the environment.¹²⁴ MFC technology is used to treat wastewater with a completely different method because of its ability to capture energy.¹²⁵ Also, MFC could be an efficient method of electricity generation. Du Z. and et al. reported that MFC has potential applications for waste treatment and energy generation in spaceships.¹²⁶ Wang et al. reported a maximum power of 6.0 W/m^3 , with the current being $1.9 \pm 0.4 \text{ mA}$ and high biomass retention.¹²² Rojas-Flores et al. reported having a peak voltage and current of $1.127 \pm 0.096 \text{ V}$ and $(1.130 \pm 0.018 \text{ mA})$. The maximum power density was $3.155 \pm 0.24 \text{ W/cm}^2$ at 374.4 mA/cm^2 current density was achieved using blueberry waste as substrate.¹²⁷

6.2. Biosensors

MFCs used as biosensors have attracted increasing attention because of their simplicity and robustness in various applications. One such sensor measures the amount of hydrogen peroxide produced and the lack of oxygen, having the advantages of being easily fabricated and assembling small-sized systems.¹²⁸ MFC-based biosensors are reported to be much more stable and durable than traditional BOD biosensors.¹²⁹ MFC-based biosensors are alternative dissolved oxygen (DO) measurement strategy. They are based on the fundamental principle that is based on cathode behavior. Wang et al. used a mini autonomous MFC-based for monitoring hexavalent chromium in wastewater.¹³⁰ Also, the potential of remediating toxicants, such as phenols, formaldehyde, and petroleum compounds, is another application of MFC.¹³¹⁻¹³²

6.3. Biohydrogen production

Hydrogen may be produced in MFCs, such as secondary fuels, instead of electricity. To generate hydrogen gas in a typical MFC, the anodic potential must be increased with a supplemental voltage of about 0.23V or more to overcome this thermodynamic barrier. The oxygen in the cathode chamber should also be enhanced.¹²⁵ MFCs provide simultaneous wastewater remediation along with hydrogen generation has proven to be a sustainable process for energy production.¹³³ Chae et al. demonstrated a solar-powered microbial electrolysis cell for hydrogen production. Their work demonstrated that solar energy could be coupled into an MFC device and provide a critical driving force for the bioelectrochemical reaction.¹³⁴ The production of hydrogen by MFC is an environmentally friendly method compared to glucose fermentation.¹³⁵

7. CONCLUSION

Power generation through an MFC using quality substrates oxidized by bacterial species offers a promising technology for the future. In previous studies, simple substrates such as lactate and acetate were widely used; however, in recent years, many available substrates have been used as anode chamber nutrients to utilize waste biomass and their treatment. The production of electricity from renewable waste biomass using MFC techniques has been considered a major development compared to traditional non-renewable biofuels. It is expected that the MFC technology will be designed to adapt a variety of substrates to make it a sustainable source of bioenergy.

The power generation efficiency of the systems is still very low, which prevents them from being widely used and limits their practical applications. It has been discovered that power density and combined efficiency can be increased through the appropriate selection of microorganisms, modes of operation, suitable materials for construction, and improved design

of MFCs. In addition, the large-scale application of MFCs is limited by its high cost and low wastewater buffering capacity. Therefore, more technological advances are needed, especially in the design of low-cost materials. The use of available substrates, especially wastewater, creates complexity in MFCs due to their high organic loads and inhibitory agents. Establishing a diverse and efficient microbial community is necessary to utilize the wastewater substrates efficiently and improve system performance. Combining MFC with conventional wastewater treatment technologies may be the best possible alternative for this technology.

This review discusses substrates such as acetate, brewery water, bamboo fermentation wastewater, inorganic substances, and azo coolants, which are harmful to the environment and organisms. New functions can be explored through power generation through MFC as substrate. Until now, a variety of substrates have been used in MFC for high efficiency/performance. Even so, the important factors that limits the practical use of MFCs need to be worked out and addressed, such as power output reduction, in order to expand regulation. These factors contribute to the difficulty of commercializing MFC, so more efforts are needed to provide a viable technology that can be effectively applied to commercialize MFC technology.

Optimal and cost-effective design for scaled-up versions of laboratory-scale reactors is one of the most challenging issues in commercializing MFCs. In the case of COD removal and power generation, laboratory-scale MFCs have shown outstanding results. However, many aspects must be addressed in order for it to be scalable for practical applications, including the separator configuration, mechanical strength, electrode cost, and its low output power. Since most microbial electrochemical processes are based on redox reactions, various elements, such as electrodes, could be improved to enhance their performance. Using well-surfaced electrodes

that promote microbial affinity can improve the performance of MFCs.

MFC performance has been illustrated when it comes to removing contaminants. The key to fully implementing MFCs in the field is to improve long-term operational stability. Most of the current MFC research was performed in the laboratory. Therefore, more scaled-up MFC research is needed to better understand how large-scale MFC systems operate and to enhance power production while maintaining economic feasibility. This is essential in the commercial adoption of this technology.

REFERENCES

1. M. Kumar. Social, economic, and environmental impacts of renewable energy resources, *Wind Solar Hybrid Renewable Energy System*, IntechOpen, 2020.
2. N. Mancosu, R. L. Snyder, G. Kyriakakis, D. Spano. Water scarcity and future challenges for food production, *Water*, **2015**, 7(3), 975-992.
3. J. M. Moradian, Z. Fang, Y.-C. Yong. Recent advances on biomass-fueled microbial fuel cell, *Bioresources and Bioprocessing*, **2021**, 8(1), 1-13.
4. K. Obileke, H. Onyeaka, E. L. Meyer, N. Nwokolo. Microbial fuel cells, a renewable energy technology for bio-electricity generation: A mini-review, *Electrochemistry Communications*, **2021**, 107003.
5. W. F. Liu, S. A. Cheng. Microbial fuel cells for energy production from wastewaters: the way toward practical application, *Journal of Zhejiang University Science A*, **2014**, 15(11), 841-861.
6. D. G. A. Avilés, O. F. N. Barrionuevo, O. F. S. Olmedo, B. D. C. Piñan, D. A. A. Briones, R. A. B. Soria. Application of a direct current circuit to pick up and to store bioelectricity produced by microbial fuel cells, *Revista Colombiana de Química*, **2019**, 48(3), 26-35.
7. J. Z. Sun, G. P. Kingori, R. W. Si, D. D. Zhai, Z. H. Liao, D. Z. Sun, T. Zheng, Y. C. Yong. Microbial fuel cell-based biosensors for

- environmental monitoring: A review, *Water Science and Technology*, **2015**, 71(6), 801-809.
8. H. Hiegemann, T. Littfinski, S. Krimmler, M. Lübken, D. Klein, K. G. Schmelz, K. Ooms, D. Pant, M. Wichern. Performance and inorganic fouling of a submersible 255 L prototype microbial fuel cell module during continuous long-term operation with real municipal wastewater under practical conditions, *Bioresource Technology*, **2019**, 294, 122227.
 9. K. Rabaey, N. Boon, S. D. Siciliano, M. Verhaege, W. Verstraete. Biofuel cells select for microbial consortia that self-mediate electron transfer, *Applied and Environmental Microbiology*, **2004**, 70(9), 5373-5382.
 10. D. R. Bond, D. R. Lovley. Electricity production by *Geobacter sulfurreducens* attached to electrodes, *Applied and Environmental Microbiology*, **2003**, 69(3), 1548-1555.
 11. D. R. Bond, D. E. Holmes, L. M. Tender, D. R. Lovley. Electrode-reducing microorganisms that harvest energy from marine sediments, *Science*, **2002**, 295(5554), 483-485.
 12. B. E. Logan. Peer reviewed: extracting hydrogen and electricity from renewable resources, *Environmental Science & Technology*, **2004**, 38(9), 160A-167A.
 13. Y. Lu, M. Qin, H. Yuan, I. M. Abu-Reesh, Z. He. When bioelectrochemical systems meet forward osmosis: accomplishing wastewater treatment and reuse through synergy, *Water*, **2015**, 7(1), 38-50.
 14. W. V. K. Rabaey. Microbial fuel cells: novel biotechnology for energy generation. *Trends in Biotechnology*, **2005**, 23 (291-298).
 15. M. Schechter, A. Schechter, S. Rozenfeld, E. Efrat, R. Cahan. Anode biofilm, *Technology and Application of Microbial Fuel Cells*, **2014**, 57.
 16. D. Pant, G. V. Bogaert, L. Diels, K. Vanbroekhoven. A review of the substrates used in microbial fuel cells (MFCs) for sustainable energy production, *Bioresource Technology*, **2010**, 101(6), 1533-1543.
 17. T. Catal, A. Kul, V. E. Atalay, H. Bermek, S. Ozilhan, N. Tarhan. Efficacy of microbial fuel cells for sensing of cocaine metabolites in urine-based wastewater, *Journal of Power Sources*, **2019**, 414, 1-7.
 18. A. J. Mohammed, Z. Z. Ismail. Slaughterhouse wastewater biotreatment associated with bioelectricity generation and nitrogen recovery in hybrid system of microbial fuel cell with aerobic and anoxic bioreactors, *Ecological Engineering*, **2018**, 125, 119-130.
 19. A. G. Capodaglio, G. Olsson. Energy issues in sustainable urban wastewater management: Use, demand reduction and recovery in the urban water cycle, *Sustainability*, **2020**, 12(1), 266.
 20. A. S. Mathuriya, J. Yakhmi. Microbial fuel cells to recover heavy metals, *Environmental Chemistry Letters*, **2014**, 12(4), 483-494.
 21. Y. Cui, B. Lai, X. Tang. Microbial fuel cell-based biosensors, *Biosensors*, **2019**, 9(3), 92.
 22. X. A. Walter, J. Greenman, I. A. Ieropoulos. Microbial fuel cells directly powering a microcomputer, *Journal of Power Sources*, **2020**, 446, 227328.
 23. S. Kondaveeti, J. Lee, R. Kakarla, H. S. Kim, B. Min. Low-cost separators for enhanced power production and field application of microbial fuel cells (MFCs), *Electrochimica Acta*, **2014**, 132, 434-440.
 24. D. Call, B. E. Logan. Hydrogen production in a single chamber microbial electrolysis cell lacking a membrane, *Environmental Science & Technology*, **2008**, 42(9), 3401-3406.
 25. K. Rabaey, G. Lissens, S. D. Siciliano, W. Verstraete. A microbial fuel cell capable of converting glucose to electricity at high rate and efficiency, *Biotechnology Letters*, **2003**, 25(18), 1531-1535.
 26. B. Min, S. Cheng, B. E. Logan. Electricity generation using membrane and salt bridge microbial fuel cells, *Water Research*, **2005**, 39(9), 1675-1686.
 27. S. Oh, B. Min, B. E. Logan. Cathode performance as a factor in electricity generation in microbial fuel cells, *Environmental Science & Technology*, **2004**, 38(18), 4900-4904.

28. S.-E. Oh, B. E. Logan. Proton exchange membrane and electrode surface areas as factors that affect power generation in microbial fuel cells, *Applied Microbiology and Biotechnology*, **2006**, 70(2), 162-169.
29. D. Sivakumar. Wastewater treatment and bioelectricity production in microbial fuel cell: salt bridge configurations, *International Journal of Environmental Science and Technology*, **2021**, 18(6), 1379-1394.
30. H. Liu, B. E. Logan. Electricity generation using an air-cathode single chamber microbial fuel cell in the presence and absence of a proton exchange membrane, *Environmental Science & Technology*, **2004**, 38(14), 4040-4046.
31. D. H. Park, J. G. Zeikus. Improved fuel cell and electrode designs for producing electricity from microbial degradation, *Biotechnology and Bioengineering*, **2003**, 81(3), 348-355.
32. N. Khan, M. D. Khan, A. S. Nizami, M. Rehan, A. Shaida, A. Ahmad, M. Z. Khan. Energy generation through bioelectrochemical degradation of pentachlorophenol in microbial fuel cell, *RSC Advances*, **2018**, 8(37), 20726-20736.
33. X. A. Walter, I. Gajda, S. Forbes, J. Winfield, J. Greenman, I. Ieropoulos. Scaling-up of a novel, simplified MFC stack based on a self-stratifying urine column, *Biotechnology for Biofuels*, **2016**, 9(1), 1-11.
34. K. Rabaey, P. Clauwaert, P. Aelterman, W. Verstraete. Tubular microbial fuel cells for efficient electricity generation, *Environmental Science & Technology*, **2005**, 39(20), 8077-8082.
35. B. Min, B. E. Logan. Continuous electricity generation from domestic wastewater and organic substrates in a flat plate microbial fuel cell, *Environmental Science & Technology*, **2004**, 38(21), 5809-5814.
36. S. Cheng, H. Liu, B. E. Logan. Increased performance of single-chamber microbial fuel cells using an improved cathode structure, *Electrochemistry Communications*, **2006**, 8(3), 489-494.
37. H. Liu, R. Ramnarayanan, B. E. Logan. Production of electricity during wastewater treatment using a single chamber microbial fuel cell, *Environmental Science & Technology*, **2004**, 38(7), 2281-2285.
38. Z. He, S. D. Minteer, L. T. Angenent. Electricity generation from artificial wastewater using an upflow microbial fuel cell, *Environmental Science & Technology*, **2005**, 39(14), 5262-5267.
39. L. M. Tender, C. E. Reimers, H. A. Stecher, D. E. Holmes, D. R. Bond, D. A. Lowy, K. Pilobello, S. J. Fertig, D. R. Lovley. Harnessing microbially generated power on the seafloor, *Nature Biotechnology*, **2002**, 20(8), 821-825.
40. Ø. Hasvold, H. Henriksen, E. Melv, G. Citi, B. Ø. Johansen, T. Kjørnigsen, R. Galetti. Sea-water battery for subsea control systems, *Journal of Power Sources*, **1997**, 65(1-2), 253-261.
41. A. J. Hutchinson, J. C. Tokash, B. E. Logan. Analysis of carbon fiber brush loading in anodes on startup and performance of microbial fuel cells, *Journal of Power Sources*, **2011**, 196(22), 9213-9219.
42. T. H. Lan, W. M. Yan, T. Sangeetha, Y. T. Ou, C. T. Wang, Y. C. Yang. 2D Numerical physical model settings for three electron transfer pathways in microbial fuel cells, *Sensors and Materials*, **2017**, 29(7), 1055-1060.
43. G. Pankratova, L. Hederstedt, L. Gorton. Extracellular electron transfer features of Gram-positive bacteria, *Analytica Chimica Acta*, **2019**, 1076, 32-47.
44. A. Sydow, T. Krieg, F. Mayer, J. Schrader, D. Holtmann. Electroactive bacteria - molecular mechanisms and genetic tools, *Applied Microbiology and Biotechnology*, **2014**, 98(20), 8481-8495.
45. C. I. Torres, A. K. Marcus, H.-S. Lee, P. Parameswaran, R. Krajmalnik-Brown, B. E. Rittmann. A kinetic perspective on extracellular electron transfer by anode-respiring bacteria, *FEMS Microbiology Reviews*, **2010**, 34(1), 3-17.
46. B. E. Logan. Exoelectrogenic bacteria that power microbial fuel cells, *Nature Reviews Microbiology*, **2009**, 7(5), 375-381.

47. H. K. Carlson, A. T. Iavarone, A. Gorur, B. S. Yeo, R. Tran, R. A. Melnyk, R. A. Mathies, M. Auer, J. D. Coates. Surface multiheme c-type cytochromes from *Thermincola potens* and implications for respiratory metal reduction by Gram-positive bacteria, *Proceedings of the National Academy of Sciences*, **2012**, *109*(5), 1702-1707.
48. S. H. Light, L. Su, R. Rivera-Lugo, J. A. Cornejo, A. Louie, A. T. Iavarone, C. M. Ajo-Franklin, D. A. Portnoy. A flavin-based extracellular electron transfer mechanism in diverse Gram-positive bacteria, *Nature*, **2018**, *562*(7725), 140-144.
49. D. E. Holmes, T. Mester, R. A. O'Neil, L. A. Perpetua, M. J. Larrahondo, R. Glaven, M. L. Sharma, J. E. Ward, K. P. Nevin, D. R. Lovley. Genes for two multicopper proteins required for Fe (III) oxide reduction in *Geobacter sulfurreducens* have different expression patterns both in the subsurface and on energy-harvesting electrodes, *Microbiology*, **2008**, *154*(5), 1422-1435.
50. D. R. Lovley. Syntrophy goes electric: direct interspecies electron transfer, *Annual Review of Microbiology*, **2017**, *71*, 643-664.
51. A. E. Rotaru, P. M. Shrestha, F. Liu, M. Shrestha, D. Shrestha, M. Embree, K. Zengler, C. Wardman, K. P. Nevin, D. R. Lovley. A new model for electron flow during anaerobic digestion: direct interspecies electron transfer to *Methanosaeta* for the reduction of carbon dioxide to methane, *Energy & Environmental Science*, **2014**, *7*(1), 408-415.
52. P. T. Ha, S. R. Lindemann, L. Shi, A. C. Dohnalkova, J. K. Fredrickson, M. T. Madigan, H. Beyenal. Syntrophic anaerobic photosynthesis via direct interspecies electron transfer, *Nature Communications*, **2017**, *8*(1), 1-7.
53. J. Tang, L. Zhuang, J. Ma, Z. Tang, Z. Yu, S. Zhou. Secondary mineralization of ferrihydrite affects microbial methanogenesis in *Geobacter-Methanosarcina* cocultures, *Applied and Environmental Microbiology*, **2016**, *82*(19), 5869-5877.
54. K. Hasan, S. A. Patil, K. Górecki, D. Leech, C. Hägerhäll, L. Gorton. Electrochemical communication between heterotrophically grown *Rhodobacter capsulatus* with electrodes mediated by an osmium redox polymer, *Bioelectrochemistry*, **2013**, *93*, 30-36.
55. Y. Lee, S. Bae, C. Moon, W. Lee. Flavin mononucleotide mediated microbial fuel cell in the presence of *Shewanella putrefaciens* CN32 and iron-bearing mineral, *Biotechnology and Bioprocess Engineering*, **2015**, *20*(5), 894-900.
56. T. D. Harrington, V. N. Tran, A. Mohamed, R. Renslow, S. Biria, L. Orfe, D. R. Call, H. Beyenal. The mechanism of neutral red-mediated microbial electrosynthesis in *Escherichia coli*: menaquinone reduction, *Bioresource Technology*, **2015**, *192*, 689-695.
57. P. K. Koochana, A. Mohanty, B. Subhadarshane, S. Satpati, R. Naskar, A. Dixit, R. K. Behera. Phenothiazines and phenoxazines: as electron transfer mediators for ferritin iron release, *Dalton Transactions*, **2019**, *48*(10), 3314-3326.
58. C. J. Sund, S. McMasters, S. R. Crittenden, L. E. Harrell, J. J. Sumner. Effect of electron mediators on current generation and fermentation in a microbial fuel cell, *Applied Microbiology and Biotechnology*, **2007**, *76*(3), 561-568.
59. U. Schröder. Anodic electron transfer mechanisms in microbial fuel cells and their energy efficiency, *Physical Chemistry Chemical Physics*, **2007**, *9*(21), 2619-2629.
60. S. C. Barton, J. Gallaway, P. Atanassov. Enzymatic biofuel cells for implantable and microscale devices, *Chemical Reviews*, **2004**, *104*(10), 4867-4886.
61. A. A. Yaqoob, M. N. M. Ibrahim, S. Rodríguez-Couto. Development and modification of materials to build cost-effective anodes for microbial fuel cells (MFCs): An overview, *Biochemical Engineering Journal*, **2020**, 107779.
62. S. Kalathil, S. Patil, D. Pant. Microbial fuel cells: electrode materials, *Encyclopedia of Interfacial Chemistry*, **2018**, 13459-13466.
63. M. Zhou, M. Chi, J. Luo, H. He, T. Jin. An overview of electrode materials in microbial fuel cells, *Journal of Power Sources*, **2011**, *196*(10), 4427-4435.

64. P. Choudhury, U. S. P. Uday, T. K. Bandyopadhyay, R. N. Ray, B. Bhunia. Performance improvement of microbial fuel cell (MFC) using suitable electrode and Bioengineered organisms: A review, *Bioengineered*, **2017**, 8(5), 471-487.
65. M. N. Gatti, R. H. Milocco. A biofilm model of microbial fuel cells for engineering applications, *International Journal of Energy and Environmental Engineering*, **2017**, 8(4), 303-315.
66. T. H. Lan, C. T. Wang, T. Sangeetha, Y. C. Yang, A. Garg. Constructed mathematical model for nanowire electron transfer in microbial fuel cells, *Journal of Power Sources*, **2018**, 402, 483-488.
67. L. Wang, C. Yang, T. Sangeetha, Z. He, Z. Guo, G. Lei, A. Wang, W. Liu. Methane production in a bioelectrochemistry integrated anaerobic reactor with layered nickel foam electrodes, *Bioresource Technology*, **2020**, 123657.
68. M. Rahimnejad, G. Bakeri, G. Najafpour, M. Ghasemi, S.-E. Oh. A review on the effect of proton exchange membranes in microbial fuel cells, *Biofuel Research Journal*, **2014**, 1(1), 7-15.
69. J. X. Leong, W. R. W. Daud, M. Ghasemi, K. B. Liew, M. Ismail. Ion exchange membranes as separators in microbial fuel cells for bioenergy conversion: a comprehensive review, *Renewable and Sustainable Energy Reviews*, **2013**, 28, 575-587.
70. J. Winfield, L. D. Chambers, J. Rossiter, J. Greenman, I. Ieropoulos. Towards disposable microbial fuel cells: natural rubber glove membranes, *International Journal of Hydrogen Energy*, **2014**, 39(36), 21803-21810.
71. L. Zhuang, S. Zhou, Y. Wang, C. Liu, S. Geng. Membrane-less cloth cathode assembly (CCA) for scalable microbial fuel cells, *Biosensors and Bioelectronics*, **2009**, 24(12), 3652-3656.
72. I. Ieropoulos, J. Greenman, C. Melhuish, I. Horsfield. In *EcoBot-III-A Robot with Guts*, ALIFE, Proceeding of the Alife XII Conference, Odense, Denmark, 2010.
73. H. Philamore, J. Rossiter, P. Walters, J. Winfield, I. Ieropoulos. Cast and 3D printed ion exchange membranes for monolithic microbial fuel cell fabrication, *Journal of Power Sources*, **2015**, 289, 91-99.
74. J. Winfield, L. D. Chambers, J. Rossiter, J. Greenman, I. Ieropoulos. Urine-activated origami microbial fuel cells to signal proof of life, *Journal of Materials Chemistry A*, **2015**, 3(13), 7058-7065.
75. Y. Zuo, S. Cheng, D. Call, B. E. Logan. Tubular membrane cathodes for scalable power generation in microbial fuel cells, *Environmental Science & Technology*, **2007**, 41(9), 3347-3353.
76. F. Hernández-Fernández, A. P. de los Ríos, F. Mateo-Ramírez, C. Godínez, L. Lozano-Blanco, J. Moreno, F. Tomás-Alonso. New application of supported ionic liquids membranes as proton exchange membranes in microbial fuel cell for waste water treatment, *Chemical Engineering Journal*, **2015**, 279, 115-119.
77. M. H. Kim, I. J. Iwuchukwu, Y. Wang, D. Shin, J. Sanseverino, P. Frymier. An analysis of the performance of an anaerobic dual anode-chambered microbial fuel cell, *Journal of Power Sources*, **2011**, 196(4), 1909-1914.
78. R. Orellana, J. J. Leavitt, L. R. Comolli, R. Csencsits, N. Janot, K. A. Flanagan, A. S. Gray, C. Leang, M. Izallalen, T. Mester. U (VI) reduction by diverse outer surface c-type cytochromes of *Geobacter sulfurreducens*, *Applied and Environmental Microbiology*, **2013**, 79(20), 6369-6374.
79. W. Miran, M. Nawaz, J. Jang, D. S. Lee. Sustainable electricity generation by biodegradation of low-cost lemon peel biomass in a dual chamber microbial fuel cell, *International Biodeterioration & Biodegradation*, **2016**, 106, 75-79.
80. I. Bohn, L. Björnsson, B. Mattiasson. Effect of temperature decrease on the microbial population and process performance of a mesophilic anaerobic bioreactor, *Environmental Technology*, **2007**, 28(8), 943-952.
81. N. T. Phung, J. Lee, K. H. Kang, I. S. Chang, G. M. Gadd, B. H. Kim. Analysis of microbial diversity in oligotrophic microbial fuel cells using 16S rDNA sequences, *FEMS Microbiology Letters*, **2004**, 233(1), 77-82.

82. X. Mei, D. Xing, Y. Yang, Q. Liu, H. Zhou, C. Guo, N. Ren. Adaptation of microbial community of the anode biofilm in microbial fuel cells to temperature, *Bioelectrochemistry*, **2017**, *117*, 29-33.
83. Z. Liu, J. Liu, S. Zhang, Z. Su. Study of operational performance and electrical response on mediator-less microbial fuel cells fed with carbon-and protein-rich substrates, *Biochemical Engineering Journal*, **2009**, *45*(3), 185-191.
84. M. Tariq, J. Wang, Z. A. Bhatti, M. Bilal, A. J. Malik, M. S. Akhter, Q. Mahmood, S. Hussain, A. Ghfar, M. M. Al-Anazy. Bioenergy potential of albumin, acetic acid, sucrose, and blood in microbial fuel cells treating synthetic wastewater, *Processes*, **2021**, *9*(8), 1289.
85. M. A. Islam, A. Karim, F. Ameen. Effect of substrates on the performance of microbial fuel cell for sustainable energy production, *In Progressive Thermochemical Biorefining Technologies*, CRC Press, 2021, 161-176.
86. M. T. Jamal, A. Pugazhendhi, R. B. Jeyakumar. Application of halophiles in air cathode MFC for seafood industrial wastewater treatment and energy production under high saline condition, *Environmental Technology & Innovation*, **2020**, *20*, 101119.
87. S. Seveda, I. M. Abu-Reesh. Improved petroleum refinery wastewater treatment and seawater desalination performance by combining osmotic microbial fuel cell and up-flow microbial desalination cell, *Environmental technology*, **2019**, *40*(7), 888-895.
88. H. N. Dai, T.-A. D. Nguyen, L.-P. M. LE, M. V. Tran, T.-H. Lan, C.-T. Wang. Power generation of *Shewanella oneidensis* MR-1 microbial fuel cells in bamboo fermentation effluent, *International Journal of Hydrogen Energy*, **2021**, *46*(31), 16612-16621.
89. A. A. Yaqoob, A. Serrà, M. N. M. Ibrahim, A. S. Yaakop. Self-assembled oil palm biomass-derived modified graphene oxide anode: An efficient medium for energy transportation and bioremediating Cd (II) via microbial fuel cells, *Arabian Journal of Chemistry*, **2021**, *14*(5), 103121.
90. K. L. Dinh, C. T. Wang, H. N. Dai, V. M. Tran, M. L. P. Le, I. A. Saladaga, Y. A. Lin. Lactate and acetate applied in dual-chamber microbial fuel cells with domestic wastewater, *International Journal of Energy Research*, **2021**, *45*(7), 10655-10666.
91. H. Liu, S. Cheng, B. E. Logan. Production of electricity from acetate or butyrate using a single-chamber microbial fuel cell, *Environmental Science & Technology*, **2005**, *39*(2), 658-662.
92. K. J. Chae, M. J. Choi, J. W. Lee, K. Y. Kim, I. S. Kim. Effect of different substrates on the performance, bacterial diversity, and bacterial viability in microbial fuel cells, *Bioresource Technology*, **2009**, *100*(14), 3518-3525.
93. H. S. Lee, P. Parameswaran, A. Kato-Marcus, C. I. Torres, B. E. Rittmann. Evaluation of energy-conversion efficiencies in microbial fuel cells (MFCs) utilizing fermentable and non-fermentable substrates, *Water research*, **2008**, *42*(6-7), 1501-1510.
94. S. V. Mohan, G. Mohanakrishna, B. P. Reddy, R. Saravanan, P. Sarma. Bioelectricity generation from chemical wastewater treatment in mediatorless (anode) microbial fuel cell (MFC) using selectively enriched hydrogen producing mixed culture under acidophilic microenvironment, *Biochemical Engineering Journal*, **2008**, *39*(1), 121-130.
95. S. S. Kumar, V. Kumar, R. Kumar, S. K. Malyan, A. Pugazhendhi. Microbial fuel cells as a sustainable platform technology for bioenergy, biosensing, environmental monitoring, and other low power device applications, *Fuel*, **2019**, *255*, 115682.
96. Y. Sun, J. Zuo, L. Cui, Q. Deng, Y. Dang. Diversity of microbes and potential exoelectrogenic bacteria on anode surface in microbial fuel cells, *The Journal of General and Applied Microbiology*, **2010**, *56*(1), 19-29.
97. M. A. Rodrigo, P. Cañizares, H. García, J. J. Linares, J. Lobato. Study of the acclimation stage and of the effect of the biodegradability on the performance of a microbial fuel cell. *Bioresource Technology*, **2009**, *100*(20), 4704-4710.

98. G. P. Roveroto, J. C. Teles, G. A. Vuitik, J. S. d. S. Batista, A. C. Barana. Craft brewery wastewater treatment: a fixed-bed single-batch reactor with intermittent aeration to remove COD and TN, *Brazilian Archives of Biology and Technology*, **2021**, 64.
99. X. Wang, Y. Feng, H. Lee. Electricity production from beer brewery wastewater using single chamber microbial fuel cell, *Water Science and Technology*, **2008**, 57(7), 1117-1121.
100. W. Miran, M. Nawaz, A. Kadam, S. Shin, J. Heo, J. Jang, D. S. Lee. Microbial community structure in a dual chamber microbial fuel cell fed with brewery waste for azo dye degradation and electricity generation, *Environmental Science and Pollution Research*, **2015**, 22(17), 13477-13485.
101. S. Khalid, F. Alvi, M. Fatima, M. Aslam, S. Riaz, R. Farooq, Y. Zhang. Dye degradation and electricity generation using microbial fuel cell with graphene oxide modified anode, *Materials Letters*, **2018**, 220, 272-276.
102. H. B. Slama, A. C. Bouket, Z. Pourhassan, F. N. Alenezi, A. Silini, H. Cherif-Silini, T. Oszako, L. Luptakova, P. Golinska, L. Belbahri,. Diversity of synthetic dyes from textile industries, discharge impacts and treatment methods, *Applied Sciences*, **2021**, 11(14), 6255.
103. L. Zhang, J. Wang, G. Fu, Z. Zhang. Simultaneous electricity generation and nitrogen and carbon removal in single-chamber microbial fuel cell for high-salinity wastewater treatment, *Journal of Cleaner Production*, **2020**, 276, 123203.
104. D. Qiu, S. Liu. In *Degradation of azo dye wastewater by the combination process of 3D BER and CW-MFC*, IOP Conference Series: Earth and Environmental Science, IOP Publishing, 2021, 012017.
105. M. Fatima, Y. Kiros, R. Farooq, and R.W. Lindström. Low-cost single chamber MFC integrated with novel lignin-based carbon fiber felt bioanode for treatment of recalcitrant azo dye, *Frontiers in Energy Research*, **2021**, 9, 260.
106. X. Cao, H. Wang, X.-q. Li, Z. Fang, X.-n. Li. Enhanced degradation of azo dye by a stacked microbial fuel cell-biofilm electrode reactor coupled system, *Bioresource Technology*, **2017**, 227, 273-278.
107. D. Sharma, A. Saini. *Lignocellulosic Ethanol production from a biorefinery perspective*, Springer, 2020.
108. A. A. Yaqoob, M. N. M. Ibrahim, A. S. Yaakop, A. Ahmad. Application of microbial fuel cells energized by oil palm trunk sap (OPTS) to remove the toxic metal from synthetic wastewater with generation of electricity, *Applied Nanoscience*, **2021**, 11(6), 1949-1961.
109. J. Dai, J. J. Wang, A. T. Chow, WW. H. Conner. Electrical energy production from forest detritus in a forested wetland using microbial fuel cells, *Gcb Bioenergy*, **2015**, 7(2), 244-252.
110. Q. Hou, C. Nie, H. Pei, W. Hu, L. Jiang, Z. Yang. The effect of algae species on the bioelectricity and biodiesel generation through open-air cathode microbial fuel cell with kitchen waste anaerobically digested effluent as substrate, *Bioresource Technology*, **2016**, 218, 902-908.
111. S.-W. Li, R. J. Zeng, G.-P. Sheng. An excellent anaerobic respiration mode for chitin degradation by *Shewanella oneidensis* MR-1 in microbial fuel cells, *Biochemical Engineering Journal*, **2017**, 118, 20-24.
112. S. Kumar, H. D. Kumar, K. G. Babu. A study on the electricity generation from the cow dung using microbial fuel cell, *Journal of Biochemical Technology*, **2012**, 3(4).
113. W. Miran, M. Nawaz, J. Jang, D. S. Lee. Conversion of orange peel waste biomass to bioelectricity using a mediator-less microbial fuel cell, *Science of the Total Environment*, **2016**, 547, 197-205.
114. T. S. Song, D. B. Wang, S. Han, X. Y. Wu, C. C. Zhou. Influence of biomass addition on electricity harvesting from solid phase microbial fuel cells, *International Journal of Hydrogen Energy*, **2014**, 39(2), 1056-1062.
115. I. Gajda, J. Greenman, C. Melhuish, I. Ieropoulos. Self-sustainable electricity production from algae grown in a microbial fuel cell system, *Biomass and Bioenergy*, **2015**, 82, 87-93.
116. S. H. Hassan, S. M. G. El-Rab, M. Rahimnejad, M. Ghasemi, J. H. Joo, Y. Sik-Ok, I. S. Kim, S.

- E. Oh. Electricity generation from rice straw using a microbial fuel cell, *International Journal of Hydrogen Energy*, **2014**, 39(17), 9490-9496.
117. H. Du, F. Li, K. Huang, W. Li, C. Feng. Potato waste treatment by microbial fuel cell. Evaluation based on electricity generation, organic matter removal and microbial structure, *Environment Protection Engineering*, **2017**, 43(1).
118. Z. Liu, Y. He, R. Shen, Z. Zhu, X. H. Xing, B. Li, Y. Zhang. Performance and microbial community of carbon nanotube fixed-bed microbial fuel cell continuously fed with hydrothermal liquefied cornstalk biomass, *Bioresource Technology*, **2015**, 185, 294-301.
119. H. Li, Y. Tian, W. Zuo, J. Zhang, X. Pan, L. Li, X. Su. Electricity generation from food wastes and characteristics of organic matters in microbial fuel cell, *Bioresource Technology*, **2016**, 205, 104-110.
120. A. Tursi. A review on biomass: importance, chemistry, classification, and conversion, *Biofuel Research Journal*, **2019**, 6(2), 962-979.
121. C. Abourached, T. Catal, H. Liu. Efficacy of single-chamber microbial fuel cells for removal of cadmium and zinc with simultaneous electricity production, *Water Research*, **2014**, 51, 228-233.
122. Y. P. Wang, X. W. Liu, W. W. Li, F. Li, Y. K. Wang, G. P. Sheng, R. J. Zeng, H. Q. Yu. A microbial fuel cell-membrane bioreactor integrated system for cost-effective wastewater treatment, *Applied Energy*, **2012**, 98, 230-235.
123. M. Mehmood, E. Adetutu, D. Nedwell, A. Ball. In situ microbial treatment of landfill leachate using aerated lagoons, *Bioresource technology*, **2009**, 100(10), 2741-2744.
124. Y. Wei, R. T. V. Houten, A. R. Borger, D. H. Eikelboom, Y. Fan. Minimization of excess sludge production for biological wastewater treatment, *Water Research*, **2003**, 37(18), 4453-4467.
125. B. E. Logan. *Microbial fuel cells*, John Wiley & Sons, 2008.
126. Z. Du, H. Li, T. Gu. A state of the art review on microbial fuel cells: a promising technology for wastewater treatment and bioenergy, *Biotechnology Advances*, **2007**, 25(5), 464-482.
127. S. Rojas-Flores, S. M. Benites, D. L. Cruz-Noriega, L. Cabanillas-Chirinos, F. Valdiviezo-Dominguez, M. A. Quezada Álvarez, V. Vega-Ybañez, L. Angelats-Silva. Bioelectricity Production from Blueberry Waste, *Processes*, **2021**, 9(8), 1301.
128. M. Gerritsen, J. Jansen, J. Lutterman. Performance of subcutaneously implanted glucose sensors for continuous monitoring, *The Netherlands Journal of Medicine*, **1999**, 54(4), 167-179.
129. B. H. Kim, I. S. Chang, G. C. Gil, H. S. Park, H. J. Kim. Novel BOD (biological oxygen demand) sensor using mediator-less microbial fuel cell, *Biotechnology Letters*, **2003**, 25(7), 541-545.
130. C. T. Wang, A. T. Ubando, V. Katiyar, T. T. Li, Y. A. Lin, A. B. Culaba, J. H. Jang. Feasibility study on a mini autonomous biosensor based on microbial fuel cell for monitoring hexavalent chromium in wastewater, *International Journal of Energy Research*, **2021**, 45(4), 6293-6302.
131. H. Luo, G. Liu, R. Zhang, S. Jin. Phenol degradation in microbial fuel cells, *Chemical Engineering Journal*, **2009**, 147(2-3), 259-264.
132. W. Yang, X. Wei, A. Fraiwan, C. G. Coogan, H. Lee, S. Choi. Fast and sensitive water quality assessment: a μL -scale microbial fuel cell-based biosensor integrated with an air-bubble trap and electrochemical sensing functionality, *Sensors and Actuators B: Chemical*, **2016**, 226, 191-195.
133. A. Saravanan, S. Karishma, P. S. Kumar, P. Yaashikaa, S. Jeevanantham, B. Gayathri. Microbial electrolysis cells and microbial fuel cells for biohydrogen production: current advances and emerging challenges, *Biomass Conversion and Biorefinery*, **2020**, 1-21.
134. K. J. Chae, M.-J. Choi, K. Y. Kim, F. F. Ajayi, I. S. Chang, I. S. Kim. A solar-powered microbial electrolysis cell with a platinum catalyst-free cathode to produce hydrogen, *Environmental Science & Technology*, **2009**, 43(24), 9525-9530.
135. S. Nanda, R. Rana, Y. Zheng, J. A. Kozinski, A. K. Dalai. Insights on pathways for hydrogen generation from ethanol, *Sustainable Energy & Fuels*, **2017**, 1(6), 1232-1245.

Nghiên cứu tính chất trương nước của vật liệu siêu hấp thụ trên cơ sở poly(vinyl alcohol)/lignin/chitosan

Bùi Thị Thảo Nguyễn*, Nguyễn Nhị Trự, Huỳnh Quang Phú,
Nguyễn Huy Hân, Trần Anh Hào

Đại học Bách Khoa – Đại học Quốc gia Thành phố Hồ Chí Minh, Việt Nam

Ngày nhận bài: 01/09/2022; Ngày nhận đăng: 27/10/2022; Ngày xuất bản: 28/10/2022

TÓM TẮT

Màng hydrogel trên cơ sở poly(vinyl alcohol), lignin và chitosan (PLCG) được tổng hợp với chất tạo liên kết ngang glyoxal. Hỗn hợp PLCG được chuẩn bị bằng phương pháp đổ khuôn, sau đó hydrogel hình thành bằng phản ứng đóng rắn ở nhiệt độ 80 °C trên khuôn petri trong một khoảng thời gian nhất định. Mẫu hydrogel sau đó được phân tích và khảo sát tính chất bằng kính hiển vi điện tử quét (SEM), quang phổ hồng ngoại Fourier (FTIR), nhiễu xạ tia X, và thí nghiệm trương nở. Kết quả đo độ trương nở cho thấy màng PLCG hydrogel có khả năng trương nước vượt trội lên đến 797% sau 24 giờ thử nghiệm ngâm trong nước cất ở 25 °C và đạt độ trương nước tối đa đến 826% khi so với khối lượng khô của mẫu. Quan sát ảnh SEM cho thấy, bề mặt hydrogel có nhiều cấu trúc xốp làm tăng khả năng hấp thụ. Với những đặc tính nổi bật, màng PLCG hydrogel được coi là vật liệu tổng hợp thân thiện môi trường, không độc hại, có tính trương nước tốt.

Từ khóa: *Màng hydrogel, hấp thụ nước, chitosan, lignin, poly(vinyl alcohol).*

**Tác giả liên hệ chính.*

Email: btnguyen@hcmut.edu.vn

Study on swelling properties of the super-absorbent hydrogel film based on poly(vinyl alcohol)/lignin/chitosan

Bui Thi Thao Nguyen*, Nguyen Nhi Tru, Huynh Quang Phu,
Nguyen Huy Han, Tran Anh Hao

Ho Chi Minh City University of Technology - Vietnam National University Ho Chi Minh City, Vietnam

Received: 01/09/2022; Accepted: 27/10/2022; Published: 28/10/2022

ABSTRACT

The composite hydrogel film based on poly(vinyl alcohol), lignin, and chitosan (PLCG) was synthesized with glyoxal crosslinker. PLCG mixture was prepared by hydrothermal method, then the film was formed by casting method on a petri dish and crosslinked at 80 °C within some periods. Well-prepared samples were analyzed with Scanning Electron Microscopy (SEM), Fourier Transform Infrared Spectroscopy (FTIR), X-Ray Diffraction (XRD), and swelling behavior. The obtained results of the water swelling measurements show that the PLCG hydrogel film had outstanding water swelling ability up to 797% after 24 hours of immersion test in neutral distilled water at 25 °C and obtained maximum swelling ratio to 826% compared to the dried sample. The surface has many porous structures that increase the adsorption capacity as revealed by SEM images. With outstanding properties, PLCG hydrogel film is considered as environmentally friendly and non-toxic material with good water-swelling materials.

Keywords: *Hydrogel film, chitosan, lignin, poly(vinyl alcohol), water swelling.*

1. INTRODUCTION

Nowadays, hydrogels attract the interests of most scientists due to their biomedical application with remarkable characteristics. Hydrogel biomaterial therapy containing active ingredients that promote regeneration is a new trend for effective prevention and treatment of wounds. They can create an environment with appropriate conditions to support the regeneration cells and promote skin regeneration, such as absorbing purulent drainage from the wound to reduce infection, functioning as a barrier against microbial invasion and easily removed without causing pain.¹ They could be applied as wound dressing, wound healing agent, scaffolds, contact lenses and drug-releasing.

In the present studies, PVA, chitosan and lignin are typical substances for hydrogel

synthesis with excellent properties such as water swelling capacity, high hydrophilicity, and biocompatibility of PVA^{2,3} along with superior properties such as antioxidant character, antibacterial, good biocompatibility of chitosan and lignin.³⁻⁶

Some studies have shown that hydrogel from PVA-chitosan has a broad potential in biomedical applications. Liang Quan Peng et al. have synthesized hydrogels with a ratio of PVA/Chitosan by freeze-thaw cycles method. The film has good mechanical properties, and it also shows stable physical and chemical properties with porosity and over 90% water content, no cytotoxicity and was able to promote cell proliferation. The research achieved the best cartilage healing.⁷ Hitesh Chopra et al. have prepared chitosan/polyvinyl alcohol

*Corresponding author.

Email: btnguyen@hcmut.edu.vn

(PVA)-based honey hydrogel films which were developed by a solvent-casting method for potential wound healing application. Membrane with excellent swelling, absorbency, and mechanical properties are ideal for therapeutic and wound healing applications.⁸

Despite the outstanding biocompatibility and antibacterial properties of PVA-chitosan composite hydrogel, its applicability as a wound dressing is constrained by its lack of mechanical strength. Lignin is being considered as a solution to add to PVA-Chitosan composite to improve the product's mechanical properties. In addition, lignin also possesses some additional properties, such as antioxidant, adsorbent UV receptor, and nanoscale antibacterial agent,^{9,10} which improves the wound protection effect.

This research focuses on studying the properties of PLCG hydrogel films based on polyvinyl alcohol, chitosan, and lignin with glyoxal crosslinker, utilizing numerous analytical methods including Scanning Electron Microscopy (SEM), Fourier Transform Infrared Spectroscopy (FTIR) and conducting swelling test to measure water absorbing ability.

2. MATERIALS AND METHODS

2.1. Materials

PVA - $(CH_2CH-OH)_n$ has Mw ~ 205000g/mol was purchased from Sigma Aldrich, Germany. Chitosan has Mw ~ 5000 g/mol was purchased from China. Lignin has Mw ~ 2330 ÷ 21500 g/mol from Nacalai Tesque. Deionized water is used for all the formulations that were prepared in the lab.

2.2. Methods

2.2.1. Preparation of PVA/lignin/chitosan mixture (PLC mixture)

PVA solution: 1 g of PVA is dissolved in 40 mL of distilled water, the solution was stirred continuously for 2 hours at room temperature. After the PVA was dissolved, the solution was heated to 80°C and remained stable for about 15 min.

PVA/lignin mixture: Weigh 0,2 g of lignin and add lignin into PVA solution. After the lignin was used up, continue stirring the solution for 2 hours at 80 °C to homogenize the mixture.

Chitosan solution: Use 0,5 g Chitosan to dissolve with 25 mL of 2% acetic acid solution, let the mixture soak in the acetic acid 2% at room temperature for 24 hours, then use stirring device to stir the solution at 60 °C for 1 hour.

Mix the PVA/lignin mixture and chitosan solution, using a stirring device to speed up the homogenization process, stirring at 40 °C for 2 hours, then increase the solution temperature to 60 °C and keep stirring to obtain a PLC homogenized mixture. After that, the PLC mixture will be crosslinked by glyoxal.

2.2.2. Crosslinking PLCG hydrogel film

Slowly add 1,4 g glyoxal (drop by drop) to the PLC mixture, stirring for 30 minutes at 60 °C. Pour the mixture into the mold to heat at 80 °C to form the crosslinking between the chemicals with the timelines: 30, 60 and 90 minutes. The samples were labelled as PLCG_30, PLCG_60, PLCG_90, shown in Table 1.

Table 1. Notation of the samples

Sample	Glyoxal/PVA ratio	Crosslinked reaction time (minutes)
PLCG_30	1,4 / 1	30
PLCG_60	1,4 / 1	60
PLCG_90	1,4 / 1	90

2.2.3. Swelling behavior of PVA/lignin/chitosan/glyoxal (PLCG) hydrogels

Prepare a 10 mm x 10 mm PVA/lignin/chitosan hydrogel film. Then, the residual glyoxal and lignin components in the sample were removed by immersing the film in distilled water until the film reached constant weight. Finally, the film was again dried to constant weight W_e . W_e is used in the calculation of gel fraction and swelling ratio.⁸

• Swelling ratio (SR%): Measuring the ability to absorb solution (usually water) by immersing. The formula is shown below:

$$SR\% = \frac{W_s - W_e}{W_e} \times 100 \quad (1)$$

After soaking the analytical sample for a specific period, remove the sample from the water and weigh the analyzed sample to get W_s .

When the sample reaches the equilibrium point (cannot absorb more water), the ESR% saturation point is obtained. The calculation formula for ESR% is similar to SR%.

• Gel fraction (GF%): Measuring the efficiency of the crosslinking reaction by immersing, usually the better the gel ratio results, the lower the water swelling results. The formula is shown below:

$$GF\% = \frac{W_{d2}}{W_{d1}} \times 100 \quad (2)$$

For the gel fraction measurement, the sample will be soaked for 48 hours, then the weight of the sample will be weighed and noted as W_{d2} . W_{d1} is the mass of the sample that was dried before testing.

2.2.4. FTIR

FTIR spectra of PLCG hydrogel samples was measured in transmittance mode at room temperature by Frontier FT-IR/NIR instrument model at Center of Scientific Equipment & Biological, Chemical and Physical Analysis - Institute of Applied Materials Science, Ho Chi Minh City, Vietnam. The number of scans is 20 and the resolution is 4 cm^{-1} . The scan range is 4000 - 450 cm^{-1} , the scan speed is 0,2 mm/s.

2.2.5. SEM

Sample surface structure was observed with Hitachi S-4800 High Resolution SEM system

at SHTPLAB, Research Laboratories of Saigon HI-TECH Park, HCM City, Vietnam. Hydrogel film samples after drying at 60 °C for 2 h under normal conditions were kept in a desiccator for 12 h, then taken for SEM, FTIR and other analytical methods.

3. RESULTS AND DISCUSSION

3.1. FTIR spectra

In the FTIR spectrum of chitosan (Figure 1a), it could be seen that the absorption peak at 3607 cm^{-1} was specific for -OH group.¹¹ The peak at 3075 cm^{-1} was characterized for -NH₂ vibration. The peak 281 cm^{-1} reflected for the -CH₂ group of stretching oscillations caused by the pyranose ring.¹² The absorption peak 1679 cm^{-1} referred for the prolonged C=O group (amides). The 1005 cm^{-1} peak was associated with the C-H bond.¹³

The peaks of PVA at 3282, 2922, 1716, 1374, 1085, and 833 cm^{-1} (Fig. 1d) were associated with O-H, -CH₂, C=O, C-H, C-O and C-C groups vibration.¹⁴ In the PVA/lignin/glyoxal (Fig. 1c), because of the interaction between PVA and lignin, a redshift appeared from 3282 cm^{-1} to 3311 cm^{-1} for hydroxyl group.¹⁵

In the Figure 1b, the peak at 3458 cm^{-1} was for the O-H group, which was contributed from PVA, chitosan and lignin components of the PLCG hydrogel.¹⁶⁻¹⁷ The appearance 1060 cm^{-1} peak, as previously reported,⁷ was associated with vibration of C-O-C-O-C linkage, demonstrating that there was a cross-linking between chitosan and glyoxal.¹⁶ The hydrogel became a network because of the reaction between glyoxal and -OH groups in chitosan,¹² PVA,¹⁴ and lignin.¹⁸

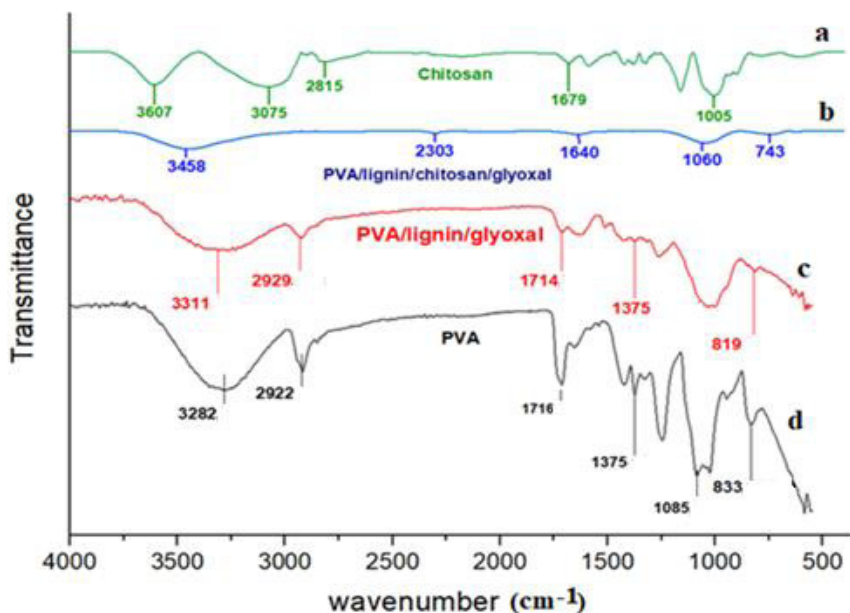


Figure 1. FTIR of Chitosan (a), PLCG_30 sample (b), PLG (c) and PVA (d).

3.2. SEM Image

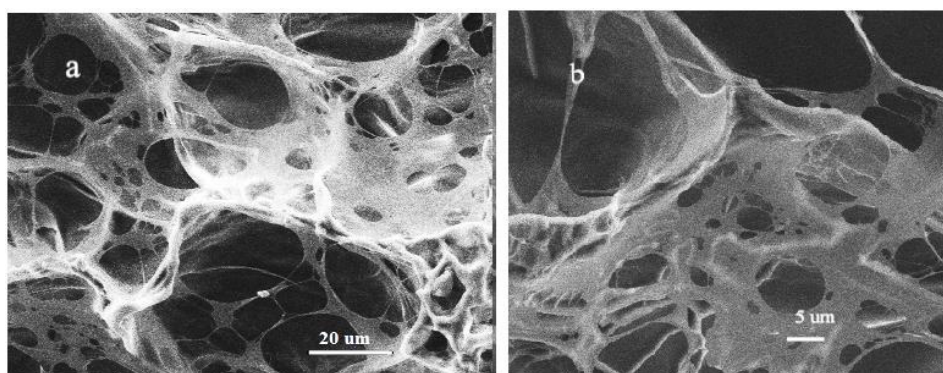


Figure 2. SEM images (a, b) of PLCG_30 hydrogel sample.

From the SEM image (Figure 6), the surface of the sample had many pores, and the density of holes is dense. In order to create porous screen materials, it was necessary to have additional curing agents, specifically glyoxal here.

The cross-linking between polymers in 3-dimensional space help them connect to each other to form a continuous network and appeared porous holes distributed from the inside to the outside of the material. This was consistent with the good water swelling properties of the sample.

3.3. XRD

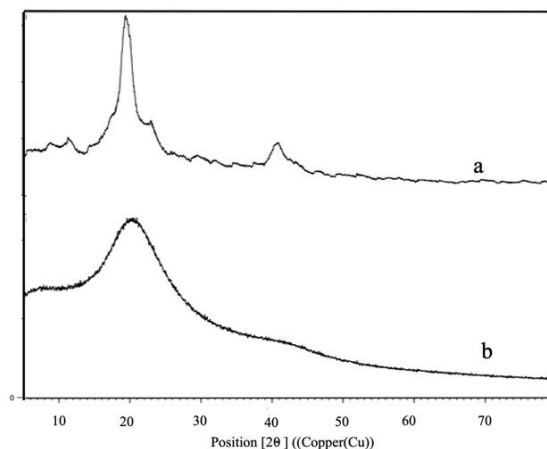


Figure 3. XRD of PVA (a) and PLCG_30 (b).

It could be seen on the XRD pattern of the PVA sample (Figure 3a) that there were two characteristic diffraction peaks located in the 2θ region at $19 - 20^\circ$ and $40 - 41^\circ$, which were typical for the semi-crystalline nature of the PVA film.¹⁹ This semi-crystalline structure of PVA was caused by intramolecular and intermolecular hydrogen bonds. The XRD image of PLCG_30 (Figure 3b) still showed the characteristic crystal peaks of PVA, but somewhat weaker with blunted and less sharp peaks. This indicated that the polar groups in lignin and chitosan linked with the hydroxyl groups of PVA and combined with glyoxal, resulting in an increased amorphous structure of the polymer complex compared to PVA sample.

3.4 Swelling behavior investigation

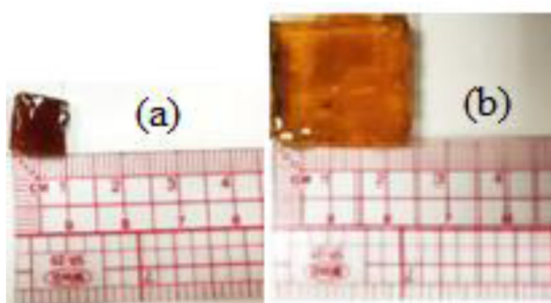


Figure 4. The size of the film before and after swelling test.

After the hydrogel test, the hydrogel films tended to absorb water and expanded the film structure, as seen in Figure 4 (a, b). The film got more translucent and changed color from dark brown to light brown. Additionally, the films' entire dimensions had increased.

Based on Figures 5 and 6, the hydrogel films had excellent water absorption speed and capacity. During the first six hours, the PLCG films absorbed a lot of water, about 80% of the water absorption compared to the equilibrium point. The sample PLCG_30 obtained about 797% after 24 hours of soaking in neutral distilled water at 25°C and up to maximum value about 826%, a rise of about 8-9 times the initial weight, which possessed the highest water absorbing ability. It could be seen that the equilibrium points of water swelling generally

decreased with increasing crosslinking time, which was 677% for PLCG_60 and 530% for PLCG_90.

The hydrogel films absorbed less water as the crosslinking time increased, which could be explained that the -OH group of PVA structure, one of the water-absorbing components of the film, reacted with the crosslinking agent during the crosslinking agent - glyoxal. The crosslinking reaction strengthened the film structure and made it more difficult to expand when absorbing water, which reduced water absorption.

According to Figure 7, the gel ratio gradually increased from sample PLCG_30 to PLCG_90, and overall, all samples produced gel fraction more than 80%, a good result which was drawn from the excellent crosslinking reaction forming hydrogel network in investigated samples, PLCG_30, PLCG_60, and PLCG_90. The gel fraction referred to the number of cross-links connecting the polymers in the hydrogel.²⁰

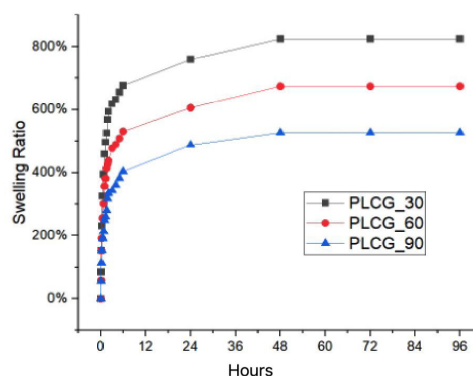


Figure 5. Swelling Ratio test of the hydrogel PLCG films.

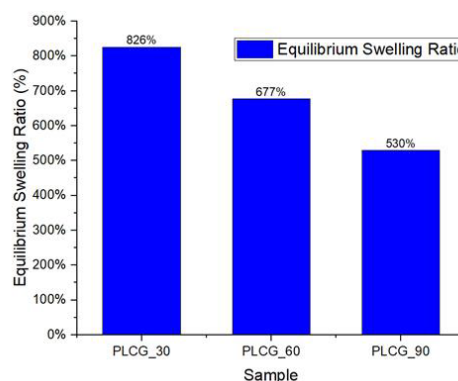


Figure 6. Equilibrium swelling ratio (ESR%) of 3 hydrogel samples.

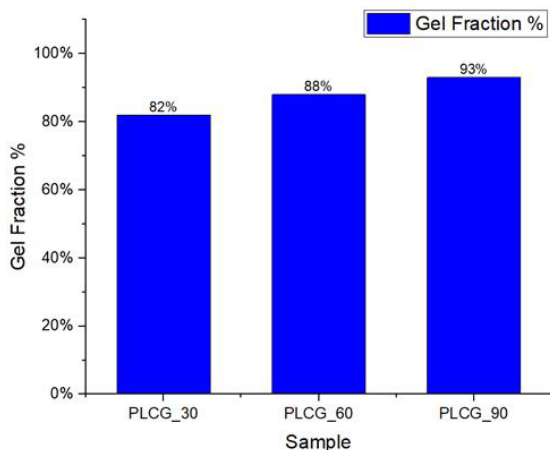


Figure 7. Gel fraction (GF%) of hydrogel samples

4. CONCLUSION

PLCG hydrogel films were prepared, and their characteristics were investigated using techniques including FTIR, SEM, XRD and swelling measurement. The swelling results showed that the hydrogel film sample had a very good swelling capacity and PLCG_30 hydrogel sample obtained maximum value to 826% in distilled water (pH = 7) at room temperature. In addition, the gel ratios of hydrogel samples gave good results about 80%, showing very good effectiveness of crosslinking reactions in creating matrix in hydrogel. The FTIR and SEM results could explain the good water swelling ability of the composite hydrogel films through the existence of the -OH groups of the composite and the surface pore structures of the hydrogel films. The measurements' results indicated that PLCG hydrogel films with remarkable water swelling had the potential for a wide range of actual application.

REFERENCES

1. P. N. Le, C. K. Huynh & N. Q. Tran. Advances in thermosensitive polymer-grafted platforms for biomedical applications, *Materials Science and Engineering: C*, **2018**, *92*, 1016-1030.
2. S. Kubo & J. F. Kadla. The Formation of strong intermolecular interactions in immiscible blends of poly(vinyl alcohol) (PVA) and lignin, *Biomacromolecules*, **2003**, *4*, 561-567.
3. G. Crini & P. M. Badot. Application of chitosan, a natural amino polysaccharide, for dye removal from aqueous solutions by adsorption processes using batch studies: A review of recent literature, *Progress in Polymer Science*, **2008**, *33*(4), 399-447.
4. M. N. V. Ravi Kumar. A review of chitin and chitosan applications, *Reactive & Functional Polymers*, **2000**, *46*, 1-27.
5. M. Rinaudo. Chitin and chitosan: Properties and applications, *Progress in Polymer Science*, **2006**, *31*(7), 603-632.
6. J. Chedly, S. Soares, A. Montebault, Y. V. Boxberg, M. V. Ravaille, C. Mouffle, M. N. Benassy, J. Taxi, L. David & F. Nothias. Physical chitosan microhydrogels as scaffolds for spinal cord injury restoration and axon regeneration, *Biomaterials*, **2017**, *138*, 91-107.
7. L. Peng, Y. Zhou, W. Lu, W. Zhu, Y. Li, K. Chen, G. Zhang, J. Xu, Z. Deng & D. Wang. Characterization of a novel polyvinyl alcohol/chitosan porous hydrogel combined with bone marrow mesenchymal stem cells and its application in articular cartilage repair, *BMC Musculoskelet Disord*, **2019**, *20*(1), 257-265.
8. H. Chopra, S. Bibi, S. Kumar, M. S. Khan, P. Kumar & I. Singh. Preparation and evaluation of Chitosan/PVA based Hydrogel films loaded with honey for wound healing application, *Gels*, **2022**, *8*(2), 111-120.
9. D. Kai, M. J. Tan, P. L. Chee, Y. K. Chua, Y. L. Yap & X. J. Loh. Towards lignin-based functional materials in a sustainable world, *Green Chemistry*, **2016**, *18*(5), 1175-1200.
10. V. K. Thakur, M. K. Thakur, P. Raghavan & M. R. Kessler. Progress in green polymer composites from lignin for multifunctional applications: A review, *ACS Sustainable Chemistry & Engineering*, **2014**, *2*(5), 1072-1092.
11. B. Krishnaveni & R. Ragunathan. Extraction and characterization of chitin and chitosan from *F. solani* CBNR BKRR, synthesis of their Bionanocomposites and study of their productive application, *Journal of Pharmaceutical Sciences and Research*, **2015**, *7*(4), 197-205.

12. Q. Yang, F. Dou, B. Liang & Q. Shen. Studies of cross-linking reaction on chitosan fiber with glyoxal, *Carbohydrate Polymers*, **2005**, *59*, 205–210.
13. J. A. Sirviö, M. Visanko & H. Liimatainen. Synthesis of imidazolium-crosslinked chitosan aerogel and its prospect as a dye removing adsorbent, *The Royal Society of Chemistry*, **2016**, *6*, 56544-56548.
14. Y. Zhang, P. C. Zhu & D. Edgren. Crosslinking reaction of Poly(Vinyl Alcohol) with Glyoxal, *Journal of Polymer Research*, **2009**, *17*, 725–730.
15. P. Posoknistakul, C. Tangkrakul, P. Chaosuanphae, S. Deepentham, W. Techasawong, N. Phonphirunrot, S. Bairak, C. Sakdaronnarong & N. Laosiripojana. Fabrication and characterization of lignin particles and their ultraviolet protection ability in PVA composite film, *American Chemical Society Omega*, **2020**, *5*(33), 20976–20982.
16. Y. Zhang, M. Jiang, Y. Zhang, Q. Cao, X. Wang, Y. Han, G. Sun, Y. Lia & J. Zhou. Novel lignin–chitosan–PVA composite hydrogel for wound dressing, *Materials Science & Engineering C*, **2019**, *104*, 110002.
17. K. W. Choo, Y. C. Ching, C. H. Chuah, J. Sabariah, & N. S. Liou. Preparation and characterization of polyvinyl alcohol-chitosan composite films reinforced with cellulose nanofiber, *Materials*, **2016**, *9*, 644.
18. S. Chaleawlerl-umpon & C. Liedel. More sustainable energy storage: lignin based electrodes with glyoxal crosslinking, *Journal of Materials Chemistry A*, **2017**, *5*, 24344-24352.
19. S. B. Aziz, O. Gh. Abdullah, S. A. Hussein & H. M. Ahmed. Effect of PVA blending on structural and Ion transport properties of CS:AgNt-based Polymer electrolyte membrane, *Polymers*, **2017**, *9*, 622.
20. M. T. S. Alcântara, A. J. C. Brant, D. R. Giannini, J. O. C. P. Pessoa, A. B. Andrade, H. G. Riella & A. B. Lugão. Influence of dissolution processing of PVA blends on the characteristics of their Hydrogels synthesized by radiation-Part I: Gel fraction, swelling, and mechanical properties, *Radiation Physics and Chemistry*, **2012**, *81*(9), 1465–1470.

MỤC LỤC

1. Quá trình điện cực bằng dòng một chiều (DC) cao áp với plasma điện hóa và các ứng dụng công nghệ
Nguyễn Đức Hùng 5
2. Đánh giá về việc sử dụng các tính toán hóa học lượng tử trong phát triển các cảm biến huỳnh quang
Nguyễn Khoa Hiền, Phan Thị Diễm Trân, Mai Văn Bầy, Phạm Cẩm Nam, và Dương Tuấn Quang..... 21
3. Định tuyến động cho video streaming VBR thích nghi HTTP dựa trên mạng điều khiển bằng phần mềm
Phạm Hồng Thịnh, Hồ Văn Phi..... 41
4. Bất đẳng thức kiểu Morrey cho các hàm có giá trị trung bình bằng 0
Nguyễn Văn Thành, Nguyễn Hữu Thuận, Nguyễn Đặng Thanh Giang, Đỗ Phương Oanh, Nguyễn Thị Hà Tiên, Đoàn Khánh Duy 49
5. Vật liệu huỳnh quang không pha tạp phát xạ ánh sáng toàn phổ ứng dụng trong đèn LED trắng
Võ Thị Phú, Tạ Thị Minh Luân, Đào Xuân Việt, Đặng Thị Tố Nữ, Nguyễn Minh Thông, Nguyễn Thị Tùng Loan, Lê Thị Thảo Viễn..... 55
6. Ứng dụng WebGIS trong quản lý thông tin giá đất trên địa bàn thành phố Tuy Hòa, tỉnh Phú Yên
Trương Quang Hiến, Ngô Anh Tú, Phan Văn Thơ, Bùi Thị Diệu Hiền..... 65
7. Tập tính ăn và lượng vi nhựa ăn vào của một số loài cá bống phân bố ở đầm Thị Nại, tỉnh Bình Định
Trình Thị Thúy Hằng, Võ Văn Chí..... 77
8. Một số bất đẳng thức kiểu Fejér cho hàm $(\mathcal{M}_\phi, \mathcal{M}_\psi)$ - lồi mạnh
Nguyễn Ngọc Huệ 87
9. Đánh giá tổng quan tế bào nhiên liệu vi sinh: Những tiến bộ gần đây về cơ chất
Đinh Kha Lil, Imee Saladaga Padillo..... 97
10. Nghiên cứu tính chất trương nước của vật liệu siêu hấp thụ trên cơ sở poly (vinyl alcohol)/ lignin/chitosan
Bùi Thị Thảo Nguyên, Nguyễn Nhị Trự, Huỳnh Quang Phú, Nguyễn Huy Hân, Trần Anh Hào 119

